M. Sc. Marine Environmental Sciences

Master Thesis

Clock gene oscillation in the copepod *Calanus finmarchicus* in the Arctic: the effect of latitude and season

Submitted by Lukas Hüppe

First Supervisor: Prof. Dr. Bettina Meyer

Second Supervisor: Dr. Kim Last

Oldenburg, 27.11.2019

Abstract

Life evolved under the permanent influence of environmental cycles, the most prominent being the daily light/dark cycle, caused by the earth's rotation about its axis. As a consequence almost all organisms have developed biological clocks that allow them to anticipate cyclic changes in the environment and thus to adjust their behavior and physiology accordingly. A biological clock has also been identified in the copepod *Calanus finmarchicus*, where it is thought to underpin diel and seasonal rhythms in behavior and physiology. *C. finmarchicus* plays a central role in sustaining the food webs of the North Atlantic and Subarctic regions, however, climate change induced latitudinal range shifts have introduced *C. finmarchicus* into the Arctic region, where it experiences extreme light conditions, with almost constant light throughout the Summer months and constant darkness in Winter. Therefore, this thesis centers on the question whether the *C. finmarchichus* clock stays functional throughout the High Arctic Summer, when diel fluctuations in light reach a minimum.

Net based 24 h samplings have been conducted at two stations along a latitudinal gradient from the southern Barents Sea (74.5 °N, 30 °E) to the Nansen Basin (82.56 °N, 30.85 °E) north of Svalbard, within 9 days of the Summer Solstice 2018. Further, temporal expression patterns of clock genes have been analyzed and the behavioral activity of individual *C. finmarchicus* has been assessed in onboard laboratory experiments. Results from gene expression analysis show significant rhythmic oscillations in a number of core clock genes in wild caught *C. finmarchicus*, suggesting a functional and synchronized endogenous clock during periods of minimal fluctuations in light intensity. Further, a period shortening could be observed in several clock genes at the northern station associated with lower diel oscillations in light properties. Results from behavioral experiments indicate overall low rhythmic behavioral activity during Summer in the High Arctic. The findings from this study are further discussed in the context of seasonal timing, concluding that the circadian clock likely stays functional throughout the whole active phase at high latitudes, including periods of Midnight Sun. This may further point out the importance of the circadian clock as a tool to track the progression of the season and help to time seasonal events, which is of fundamental importance for *C. finmarchicus* to survive in the extreme conditions of the Arctic.

Table of Content

List of Figures

List of Tables

List of Abbreviations

16s	*16s rRNA*
C	Circadian
Chl a	Chlorophyll a
clk (CLK)	*clock*
cry1 (CRY1)	*cryptochrome 1*
cry2 (CRY2)	*cryptochrome 2*
cwo (CWO)	*clockwork orange*
cyc (CYC)	*cycle*
dbt(2) (DBT)	*doubletime (2)*
DVM	Diel vertical migration
ef1	*elongation factor 1-α*
LAM	Locomotor Activity Monitor
mRNA	messenger RNA
NCC	Norwegian Coastal Current
PAR	Photosynthetically active radiation
Pdp1ε (PDP1ε)	*PAR domain protein 1ε*
per(1) (PER)	*period (1)*
POC	Particulate organic carbon
PSU	Practical salinity unit
rna-poly	*RNA polymerase*
tim (TIM)	*timeless*
U	Ultradian
vri (VRI)	*vrille*
WSC	West Spitzbergen Current

Abbreviations in *italic* indicate genes with their respective protein products in brackets

1 Introduction

The introductory part of this thesis is composed of four sections. In the first section I like to outline the general context and purpose of this study. The three following parts comprise a general description of the ecology of *Calanus finmarchicus*, as well as an introduction into the system of biological clocks and specifically the molecular mechanisms of the circadian clock machinery.

1.1 General context and purpose of the study

Biological clocks are a ubiquitous ancient and adaptive mechanism enabling organisms to anticipate environmental cycles and to regulate biological processes accordingly. Thus, they increase the fitness of the animal in its biotope (Emerson, Bradshaw, & Holzapfel, 2008). The identification of putative clock genes of *C. finmarchicus* by Christie et al. (2013a) has initiated first studies on the involvement of an endogenous timing system in diel and seasonal rhythms of this ecologically important zooplankter. Resulting studies were able to show that *C. finmarchicus* possesses a functional circadian clock (Häfker, 2018). Further, investigations of a *C. finmarchicus* population in a Scottish sea loch strongly suggest the involvement of an endogenous clock in the timing of both diel (DVM; Häfker et al., 2017) and seasonal events (e.g. timing of diapause; Häfker et al., 2018).

The Arctic region is characterized by strong seasonal fluctuations in photoperiod leading to constant illumination during Midnight Sun and constant darkness during Polar Night. As the circadian clock widely depends on light/dark cycles, the capacity of the mechanism to oscillate and its consequences for organisms in such environments remain uncertain. Moreover, climate change induced latitudinal range shifts introduce species like *C. finmarchicus* to higher latitudes (Reygondeau & Beaugrand, 2011). The impact of such extreme photoperiods on non-endemic endogenous timing systems is unknown, and the northward expansion of organisms at high latitudes may be limited by the adaptive capacity of its clock to extreme photoperiods (Saikkonen et al., 2012). Previous investigations of the circadian clock in copepods from a high latitude Fjord (78 ˚N) at the end of the Summer showed that *C. finmarchicus* is able to maintain clock

rhythmicity under very long photoperiods (Häfker, Teschke, Hüppe, & Meyer, 2018). However, during the time of sampling (end of the Midnight Sun period), a clear diel oscillation in light intensity was visible, which was strong enough to evoke diel rhythmic behavior and provide clock entrainment. Findings regarding diel rhythmic behavior during the high Arctic Midnight Sun are contrasting. There is evidence that rhythmic DVM ceases during the period of minimal changes in light level (e.g. around the summer solstice) at high latitudes (Blachowiak-Samolyk et al., 2006; Wallace et al., 2010) or becomes desynchronized (Cottier, Tarling, Wold, & Falk-Petersen, 2006). However, other studies found DVM to persist during periods of Midnight Sun (Dale & Kaartvedt, 2000; Fortier, 2001).

Regarding the contrasting findings of behavioral rhythmic activity in zooplankton during high Arctic Midnight Sun, the question arises of whether clock gene rhythmicity is maintained throughout this period or whether the clock stops "ticking" and resumes rhythmicity as soon as the organism experiences a distinct change in light level again, e.g. by the end of the summer.

Therefore, this study aims to investigate the effect of the Midnight Sun period on diel clock gene expression patterns and behavior of *C. finmarchicus* from high Arctic latitudes. To achieve that, 24 h time series of CV stage *C. finmarchicus* have been sampled at two stations over a latitudinal gradient (74.5 – 82.5˚N), close to the time of summer solstice, for subsequent gene expression analyses. Further, onboard screening of individual behavior of *C. finmarchicus* under different photoperiods in a laboratory set up has been conducted to investigate the behavioral patterns of *C. finmarchicus* from the field.

By shining light on both molecular and behavioral processes during the period of Midnight Sun in the Arctic, this study may help to increase the understanding of the functioning of the *C. finmarchicus* clock machinery and clock-controlled processes. Furthermore, to our knowledge this work presents the first ever insights into clock gene expression patterns at high Arctic latitudes (82.5 ˚N) within days of the summer solstice where changes in light intensity are at a minimum.

1.2 Ecology of *Calanus finmarchicus*

Calanus finmarchicus (Gunnerus, 1770) is an herbivorous zooplankter that is central to the marine ecosystems of the North Atlantic and sub-Arctic and within its range of distribution it often dominates zooplankton communities in terms of biomass (Conover, 1988; Falk-Petersen, Pavlov, Timofeev, & Sargent, 2007; Hirche & Kosobokova, 2007). As an herbivore, *C. finmarchicus* grazes on phytoplankton in the upper water layers and converts the low energy carbohydrates from primary producers into energy rich wax esters (Falk-Petersen, Mayzaud, Kattner, & Sargent, 2009). Its occurrence in large biomasses and its high energy content makes *C. finmarchicus* an important prey for various higher trophic levels, ranging from predatory amphipods (Kraft, Berge, Varpe, & Falk-Petersen, 2013), over commercially important fish species (Beaugrand & Kirby, 2010; Dalpadado, Ellertsen, Melle, & Dommasnes, 2000; Sundby, 2000) up to seabirds (Steen, Vogedes, Broms, Falk-Petersen, & Berge, 2007) and baleen whales (Baumgartner, Cole, Campbell, Teegarden, & Durbin, 2003). Together with its congeners *Calanus glacialis* and *Calanus hyperboreus*, *C. finmarchicus* forms the so called "*Calanus* complex", which sustains highly productive marine ecosystems from temperate regions of the North Atlantic to the high latitude regions of the Arctic Ocean, by channeling energy from the level of primary productivity to higher trophic levels (Falk-Petersen et al., 2009, 2007). *C. finmarchicus* displays two centers of distribution with highest standing stocks, one being located in the Labrador Sea and another one in the Norwegian Sea (Heath et al., 2004), however, the latter is thought to be the main center of reproduction (Melle et al., 2014). From the Norwegian Sea, the spatial distribution of *C. finmarchicus*

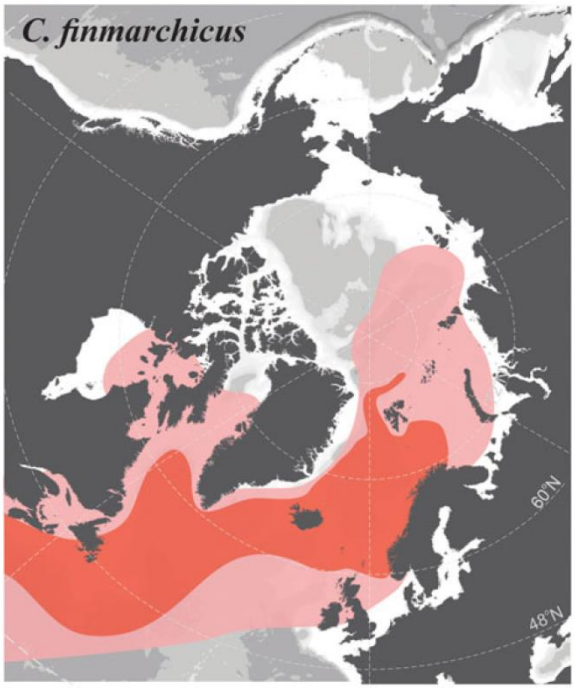

Figure 1: Geographic distribution of Calanus finmarchicus. The dark-shaded color shows the core distribution area where reproduction is known to occur, light-shaded color indicates the total area of reported occurrence.
Source: Choquet et al. 2017

mainly follows the flow of Atlantic water masses (Fig. 1), which advect parts of the population onto the Barents Sea shelf south of Spitsbergen, as well as along the west coast of Spitsbergen and into the Arctic Ocean (Choquet et al., 2017; Reygondeau & Beaugrand, 2011). Besides the fact, that parts of the *C. finmarchicus* population advected into Arctic regions manage to successfully overwinter and reproduce there (e.g. in the Southern Barents Sea or Kongsfjorden; Kvile, Fiksen, Prokopchuk, & Opdal, 2017; Walkusz et al., 2009), the advection of a new cohort from the Norwegian Sea each spring is still fundamental to sustain populations of *C. finmarchicus* at higher latitudes (Hirche & Kosobokova, 2007; Skaret, Dalpadado, Hjøllo, Skogen, & Strand, 2014; Torgersen & Huse, 2005). However, in recent decades the Arctic faced the most rapid warming on the planet resulting in substantial sea ice loss and increased inflow of warm Atlantic water, especially in the European Arctic (Årthun, Eldevik, Smedsrud, Skagseth, & Ingvaldsen, 2012; Carmack et al., 2015), which initiated a transformation from a cold, fresh Arctic Water dominated system to a warm, saline Atlantic water dominated system (Lind, Ingvaldsen, & Furevik, 2018), which has been referred to as the 'Atlantification' of the Arctic. With increasing temperatures, a northward shift in the distribution of *C. finmarchicus* has already been observed over the past decades (Reygondeau & Beaugrand, 2011). An ongoing warming and Atlantification of the southern Arctic Ocean is predicted to favor the establishment of *C. finmarchicus* in these regions and could be detrimental for its cold water adapted congeners *C. glacialis* and *C. hyperboreus,* with unknown consequences for *Calanus* population dynamics and higher trophic levels (Falk-Petersen et al., 2007; Hirche & Kosobokova, 2007).

The life cycle of *C. finmarchicus* is strongly influenced by diel and seasonal rhythms. On the daily scale, *C. finmarchicus* performs diel vertical migration (DVM), a highly synchronized vertical movement in the water column, known to be the biggest migration in terms of biomass on earth (Hays, 2003). The behavioral pattern is closely linked to the daily light dark cycle and is thought to have evolved as a trait off between predation pressure and the need to feed. As a consequence, the normal DVM pattern is characterized by an ascent in the early night to feed on phytoplankton in the surface layer and a descent to deeper and thus darker water layers in the early morning to hide from visual predators. This mass migration of zooplankton species has important

implications for both ecological interactions (Hays, 2003) as well as biogeochemical cycles (Archibald, Siegel, & Doney, 2019; Aumont, Maury, Lefort, & Bopp, 2018; Darnis et al., 2017). Especially the influence of DVM on carbon sequestration in deeper layers of the ocean has become evident once more in recent studies. By taking up carbon while feeding in the surface layers and subsequently migrating towards deeper layers, where respiration and defecation continues, an active transport of carbon to the deep layers of the ocean occurs, which has been estimated to be in the range of 13 to 58 % of the particulate organic carbon (POC) flux by sinking particles (Archibald et al., 2019; Aumont et al., 2018). Thus, DVM of marine zooplankton plays also a major role in the carbon cycle.

On the seasonal scale, each year *C. finmarchicus* passes through a complex life cycle, with an active phase of reproduction and development in the Spring / Summer months and an inactive phase (diapause) during winter, which is finely tuned to changes in its environment. The new life cycle begins in late winter / early spring when CV stage copepods terminate diapause in deeper waters and resume active development into adults and subsequent maturation (Baumgartner & Tarrant, 2017; Hirche, 1996a). Development is followed by sexual maturation and egg production in *C. finmarchicus* females and after fertilization, females migrate to the surface layer to spawn the eggs into the water column (Harris et al., 2000; Niehoff et al., 1999). Hatched from eggs, *C. finmarchicus* subsequently passes through six naupliar stages (NI - NVI) followed by six copepodite stages (CI - CVI), with the last stage being adult males and females (Hirche, 1996b). The whole process of *C. finmarchicus* reproduction and development is strongly dependent on and fueled by the spring phytoplankton bloom (e.g. Falk-Petersen et al., 2009; Niehoff & Hirche, 2000; Tande & Slagstad, 1982). In favorable conditions, e.g. in temperate regions with a pronounced and extended spring phytoplankton bloom, *C. finmarchicus* may complete up to three generations within one year (Durbin, Garrahan, & Casas, 2000). However, at higher latitudes only one generation per year is produced (Melle et al., 2014; Walkusz et al., 2009). In this case, copepods develop until the CV stage, where they accumulate large amounts of energy rich lipids and thereafter migrate to deeper layers to initiate a phase of diapause, characterized by arrested development and overall reduced metabolic activity to bridge the time of unfavorable conditions during the winter months (Hirche, 1996a;

Ingvarsdóttir, Houlihan, Heath, & Hay, 1999). Thus, with one generation per year, CV is the stage that experiences all seasons, while the other stages only experience spring / summer.

While the adaptive significance of these diel and seasonal rhythms seems obvious, the underlying mechanisms that create those rhythms still remain unclear.

1.3 Biological clocks

Life evolved under the permanent influence of environmental cycles - such as daily, seasonal or tidal cycles - that are caused by the rotational movements of the sun-earth-moon system. These cycles may lead to drastic changes in light, temperature or food availability. As a consequence, almost all organisms on earth, ranging from bacteria to humans, have adapted to these cyclic environmental changes by developing their own sense of time (Aschoff, 1954; Tessmar-Raible, Raible, & Arboleda, 2011). Rather than solely reacting to the external stimuli, they have developed endogenous biological clocks that allow them to anticipate cyclic changes in the environment and thus to adjust their behavior and physiology accordingly (Dunlap & Loros, 2016; Goldman et al., 2004; Kuhlman, Mackey, & Duffy, 2007; Tessmar-Raible, Raible, & Arboleda, 2011). Moreover, internal clocks allow organisms a temporal organization of biological processes (internal advantage; Panda et al., 2002). Endogenous rhythms are characterized by certain properties, being their ability to function in the absence of external time cues (*free run*), they can be tuned (*entrained*) by so called *Zeitgebers* to stay in synchrony with the environment and they are stable against changes in temperature (*temperature compensated*). Further, the molecular clock machinery can be split into three major parts: A central oscillator that produces the endogenous rhythm, input pathways that allow synchronization of the oscillator with the environment, and output pathways that pass the rhythmic information on to physiological and behavioral processes (Allada & Chung, 2010; Kuhlman et al., 2017; Yerushalmi & Green, 2009). Finally, endogenous clocks are assumed to be present in each cell of the organism.

1.4 The molecular machinery of the circadian clock

While extensive research has been done on biological clocks in terrestrial model organisms, knowledge on biological clocks in marine organisms is scarce (Tessmar-Raible et al., 2011). The best studied molecular timing system is the *circadian clock*, an endogenous system that produces a ~24 h rhythm. The molecular mechanisms of all eukaryotic clocks studied so far is based on the principle of transcriptional/posttranslational negative feedback loops of clock genes and their respective protein products and one of the most extensively studied molecular clock machineries is the one of the fruit fly *Drosophila melanogaster*, which is used as a model in the following mechanistic description of the circadian clock.

The endogenous oscillations are produced by three interlocking feedback loops (Fig. 2): the first loop consists of the clock genes *period (per)*, *timeless (tim)*, *clock (clk)* and *cycle (cyc)* and the protein products of the latter, CLK and CYC, form a heterodimer that allows them to bind to promoter regions (so called *E-boxes*) of *per* and *tim* to activate their transcription late in the day (Tomioka & Matsumoto, 2010). During early evening, peak messenger RNA (mRNA) levels of *per* and *tim* are reached, however, peak

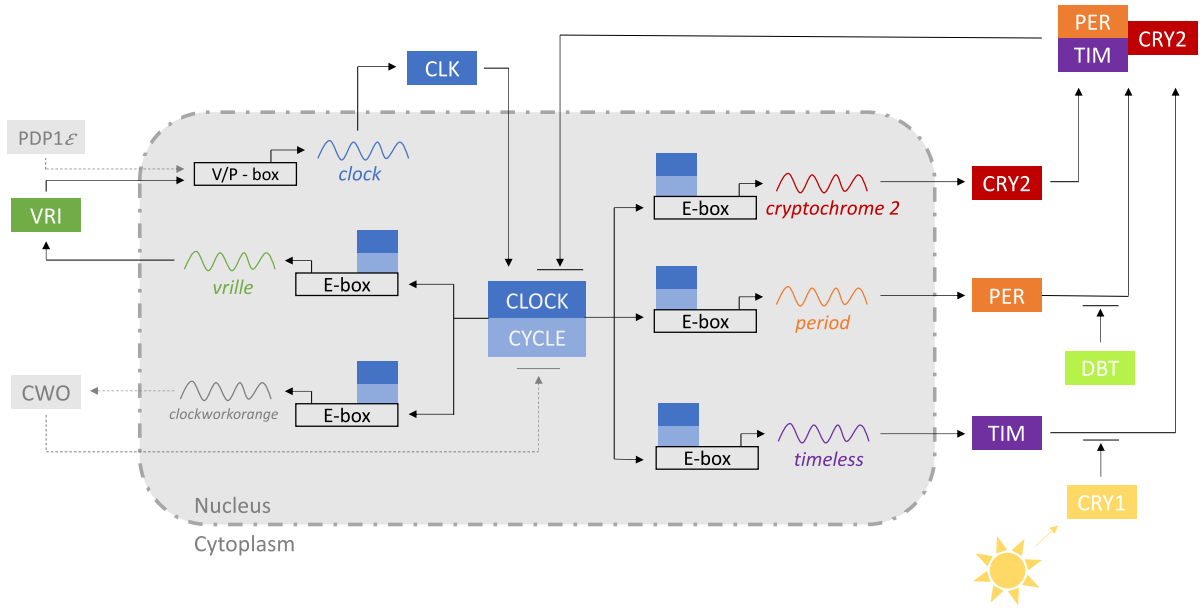

Figure 2: Schematic representation of main molecular components of the circadian clock. The scheme shows the three central feedback loops known from the Drosophila circadian system. In addition, cry2 is shown, which is lacking in the Drosophila system, but is present in other model organisms, like the monarch butterfly, and which has also been identified in C. finmarchicus. Components of genes investigated in this study are colored, additional central components that have not been investigated here are shown in grey.
The Figure has been adapted from Tomioka & Matsumoto, 2010.

concentrations of their protein products (PER and TIM) only occur later in the night due to posttranslational degradation processes (Bae & Edery, 2006; Mackey, 2007). Similar to CLK and CYC, PER and TIM form heterodimers which allows them to enter the nucleus, where they inhibit the transcriptional activity of CLK and CYC, thereby repressing their own transcription. Eventually, decreasing PER and TIM levels lead to the relaxation of the inhibiting function on CLK and CYC, which allows CLK and CYC to promote the transcription of *per* and *tim* again, starting a new cycle. In parallel to the activation of *per* and *tim*, the CLK/CYC heterodimer acts in a second feedback loop by activating the transcription of *vrille* (*vri*) and *PAR domain protein 1ε* (*Pdp1ε*). After rapid accumulation of VRI protein in the cytoplasm and subsequent translocation to the nucleus, VRI inhibits the transcription of *clk*, which leads to decreasing *clk* mRNA levels during the night. The role of *Pdp1ε* is not fully clear yet, but is has been thought to act contrary to the inhibitory activity of the VRI protein on *clk*, by activating *clk* transcription. Expression of *vri* and *Pdp1ε* is reduced again through inhibition of CLK/CYC by the PER/TIM heterodimer described in the first feedback loop, representing a connection between the loops. A third loop is formed by the cyclic transcription of *clockwork orange* (*cwo*), which regulates its own transcription as its protein product CWO inhibits the transcriptional activity of the CLK/CYC heterodimer at the E-box region of *cwo*. In *Drosophila*, this loop increases the amplitude of the endogenous rhythm and thus seems to be responsible to retain a robust oscillation (Tomioka & Matsumoto, 2015). While the feedback loops between clock genes and their protein products create endogenous oscillations, posttranslational modifications of the clock proteins are thought to be crucial processes to tune the oscillations to a period of ~24 h (Bae & Edery, 2006). A key component in posttranslational modifications is the protein product of the clock associated gene *doubletime* (*dbt*), called DBT. DBT phosphorylates the PER protein and thereby induces its degradation. This process delays the accumulation of PER and consequently the inhibitory action of PER/TIM on CLK/CYC, thereby playing a major role in period definition (Bae & Edery, 2006; Mackey, 2007).

Given the fact that the endogenously produced rhythm oscillates with a period of about, but not exactly, 24 h, to stay in phase the clock needs to be synchronized with the environment. In this course, the most reliable and widely used *Zeitgeber* is light (Aschoff, 1954). In *Drosophila*, the blue light photoreceptor CRYPTOCHROME 1 (CRY1) is known

to act as an input pathway to synchronize the clock to the light / dark alternations of the environment (Mackey, 2007; Tomioka & Matsumoto, 2015). In this course, daylight induces the degradative action of CRY1 acting on TIM. As this process happens in parallel to PER degradation through ongoing phosphorylation by DBT, it plays in important role in releasing the inhibitory activity of the PER/TIM heterodimer on CLK/CYC, which allows the start of a new cycle in the first feedback loop (Mackey, 2007). However, also factors like temperature or food availability were shown to be suitable as *Zeitgebers* in other organisms (Rensing & Ruoff, 2002; Tataroglu et al., 2015; Vera et al., 2013).

Despite of the common principle of transcriptional/posttranslational feedback loops, the molecular mechanisms may differ to a varying extent between species, e.g. regarding some genes that are involved in the molecular machinery (Doherty & Kay, 2010; Jay C Dunlap, 1999; Mackey, 2007). Thus, alternative clock models have been established, e.g. for mammals, the monarch butterfly, honeybees etc. (Bloch, 2010; Reppert, 2007; Takahashi, 2017). In *Calanus finmarchicus*, the identification of putative clock genes in the *de novo* transcriptome of *C. finmarchicus* by Christie et al. (2013a) has initiated first molecular studies of the circadian clock in this species. Results suggested that the organization of the copepod circadian system is an ancestral one, close to that of insects like the monarch butterfly *Danaus plexippus.* This assumption has been supported by temporal clock genes expression results (Häfker et al., 2017). This implies the presence of the mammalian type *cry2* gene, whose protein product CRY2 acts as a transcriptional repressor with PER and TIM, forming an PER/TIM/CRY2 heterotrimer (Merlin, Gegear, & Reppert, 2009).

Besides the timing of diel rhythms, the circadian clock is thought to play a role in the timing of seasonal events (Goto, 2013). Here, different models exist that describe e.g. the involvement of the circadian clock mechanism in the measurement of daylength and thereby tracking the progression of the season, or the evolution of a so-called circannual clock, a separate mechanism designed to time seasonal events (Bradshaw & Holzapfel, 2007; Goldman et al., 2004; Goto, 2013; Lincoln, 2019).

2 Material and Methods

Sampling for this work has been conducted during Cruise JR17006 of the "RRS James Clark Ross" in June and July 2018 and subsequent analysis have been performed in the laboratory facilities of the Alfred Wegener Institute, Helmholtz Centre for Polar and Marine Research in Bremerhaven. Molecular analysis have been used to assess the diel oscillation of *C. finmarchicus* clock genes during Midnight Sun at two locations, along a latitudinal gradient from the southern Barents Sea to the Arctic Ocean. In parallel, the individual copepod behavior over time has been assessed at each station, over four days under five different photoperiods, using modified *TriKinetics Drosophila activity monitors*. All experiments and analyzes have been performed on CV stage copepods.

2.1 Study site characteristics

Animals for both genetic and behavioral studies were sampled at two stations along a latitudinal gradient, from the Nansen Basin (JR85; 82.56 °N, 30.85 °E) northeast of Svalbard to the southern Barents Sea (B13; 74.5 °N, 30 °E; Fig. 3 A). Both stations show pronounced differences in their bathymetric profile as well as their hydrographic conditions. Station JR85 is located off the shelf northeast of Svalbard in the Nansen Basin, with a water depth of about 3700 m. The northern Barents Sea as well as the regions off the shelf are mainly influenced by cold Arctic Water masses, that flow southwestward onto the shelf and meet the Atlantic water masses at the Polar Front. However, parts of warmer Atlantic water is flowing along the west coast of Spitzbergen (Svalbard) as the West Spitsbergen Current (WSC), which eventually bends into the Arctic Ocean flowing along the shelf margin, where it can submerge under resident Arctic Water masses. In the western Part of the Barents Sea, the position of the Polar Front is well described as it follows mainly bathymetrical features in this area (Loeng, 1991), at the investigated longitude of 30 °E, it is located at a latitude of about 77 °N. In contrast, station B13 (74.5 °N) is located on the Barents Shelf with a relatively shallow water depth of about 360 m. The southern Barents Sea is mainly influenced by the inflow of relatively warm Atlantic Water originating from the Norwegian Coastal Current (NCC, Loeng, 1991).

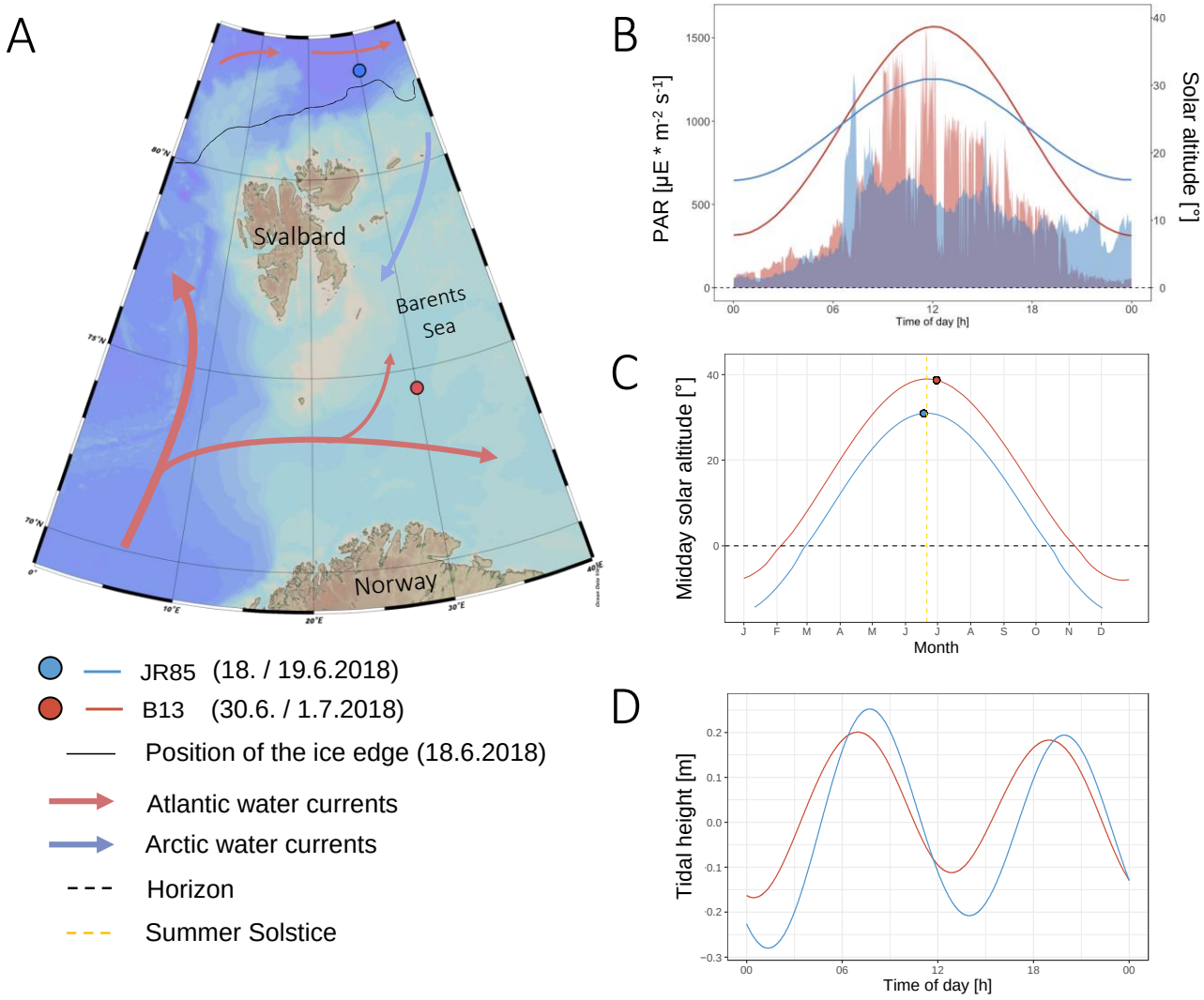

Figure 3: Physical characteristics of the study site. A) Map of the sampling area with sampled stations JR85 (blue circle) and B13 (red circle). The position of the ice edge is shown for the day of sampling at JR85 (18.06.2018, black line). The schematic current system of the Barents Sea region is shown with red arrows (Atlantic Water) and blue arrows (Arctic Water), after (Loeng, 1991). B) Diel fluctuations in PAR (area plot in the background) and model derived solar altitude (lines) for the respective day of sampling at both stations JR85 (18.06.2018, blue line) and B13 (30.06.2018, red line). The dashed black line marks the the horizon's altitude C) Model derived solar altitude at 12:00 throughout the year 2018 at both stations.. The dashed yellow line marks the day of summer solstice (21st of June). The blue and red dots mark the day of sampling for the respective station. D) Model derived tidal height over the course of the first day of sampling at the respective station.
Map created with Ocean Data View (Schlitzer, 2015).

Being located at high latitudes, the Barents Sea region and with it the sampled stations are further subjected to strong seasonal fluctuations in a range of environmental parameters, the most prominent being differences in light, specifically day length (photoperiod). Whereas in winter, constant darkness dominates the high latitudes (i.e. sun stays below the horizon, Fig. 3 C), in summer the sun never sets below the horizon. However, the sun's altitude above the horizon shows diel oscillations with a peak around

midday (Fig. 3 B), that persist throughout the summer months (Wallace et al., 2010). The fluctuations in solar altitude are also notable in diel patterns of light intensity (Fig 3 B), and even if local weather patterns might be able to diminish those diel oscillations temporarily, it potentially remains a reliable diel cue throughout the period of constant light. In addition, these diel fluctuations decrease towards the summer solstice (21st of June, see yellow line in Fig. 3 C) and increase again thereafter, making the summer solstice the day of the year with the least fluctuations in solar altitude and thus light intensity between midday and midnight. Moreover, the higher the latitude, the smaller are the fluctuations between midday and midnight.

Sampling for this study has been conducted in close proximity (within 9 days) to the summer solstice and thus within a period where diel fluctuations in light were minimal. Within diel and seasonal dynamics in the light environment, latitudinal differences are notable, with weaker diel fluctuations at higher latitudes (JR85) and stronger diel fluctuations in solar altitude at lower latitudes (B13; Fig. 3 B). Time series of photosynthetically active radiation (PAR, Fig. 3 B) have been taken by PQS1 PAR sensors (Kipp & Zonen, Netherlands) from the ship's meteorological platform. The PAR data were backed-up by modeled time series data of the sun's elevation (angle of the sun above the horizon, Fig. 3 B) during the time of sampling. Modeled data of sun altitude were obtained from the *United States Naval Observatory* (https://aa.usno.navy.mil/data/docs/AltAz.php, USNO, USA). To get insight into the seasonal dynamics of the light environment (Fig. 3 C), daily sun elevation data (observation time: 12:00 UTC+2) for the year 2018 at both stations have been obtained from the *keisan.casio* website (https://keisan.casio.com/exec/system/1224682331).

Besides the diel cycle in light intensity, both stations exhibit semidiurnal tidal oscillations, e.g. a rise and fall of the water level about every 12.4 hours (Fig 3 D). The amplitudes and phases of the tidal oscillations are quite similar between both stations, with amplitudes of about 0.5 m at JR85 and 0.3 m at B13, and peaks in the tidal height in the morning and evening hours, respectively. Information on the tidal dynamics (tidal height over time) at the two stations over the course of the samplings have been drawn from the *TPX08* model (Egbert & Erofeeva, 2002) by using the *OTPS* package (Tidal Prediction Software, http://www-po.coas.oregonstate.edu/~poa/www-

po/research/po/research/tide/index.html), through the environment of the *mbotps* program (MB-System; Caress & Chayes, 2016).

Another prominent feature of polar regions are the seasonal fluctuations in sea ice cover, which are an important factor influencing a wide range of physical and biological processes. In the Barents Sea, the seasonal maximum ice extend usually occurs in March/April, whereas a minimum is reached in September (Kvingedal, 2005). Within the last decades, the Barents Sea faced pronounced negative trends in sea ice extend throughout the whole year with increasing sea ice free periods during summer (Onarheim, Eldevik, Smedsrud, & Stroeve, 2018; Parkinson & Cavalieri, 2008). During sampling time at JR85, the ice edge was located at about 81° to 82° N, roughly following the shelf slope north of Svalbard, thus station JR85 (82.56 °N) was located well within the ice cover, whereas station B13 (74.5 °N) was ice free (Fig 3 A). Information on the location of the sea ice edge at the time of sampling at JR85 were obtained from ice concentration maps available from the *meereisportal* (meereisportal.de, Grosfeld et al., 2016).

To get information on the local physical properties of the water column at the time of sampling, vertical profiles of an SBE 911plus CTD (Sea-Bird Electronics, WA, USA) were used over the full depth of the water column. Besides sensors for temperature, pressure (depth) and conductivity (salinity), the CTD was additionally equipped with sensors measuring oxygen saturation (SBE 43, Sea-Bird Electronics) and Chlorophyll *a* (Chl *a*) fluorescence (Aquatracka III fluorometer, Chelsea Technologies Group, UK). CTD profiles at station JR85 have been taken on 18th June 15:45, and at B13 on 30th June 12:30 (all times in local time, i.e. UTC+2). Profiles of temperature, salinity, oxygen saturation, and Chlorophyll *a* from the surface to 200 m depth are shown in Fig. 4. Profiles are truncated at 200 m depth for higher resolution in the upper water column, as values remain largely constant below 200 m. Full depth profiles of the same parameters are shown in supplementary fig. 1. CTD data were provided by the British Oceanographic Data Centre (BODC, UK).

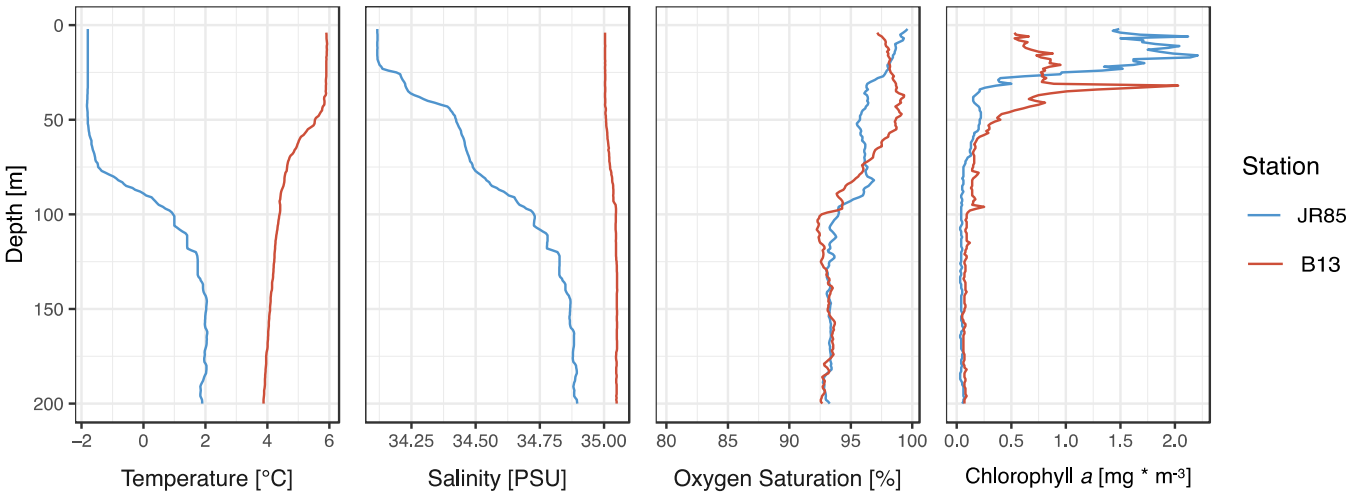

Figure 4: Vertical profiles of temperature, salinity, oxygen saturation and Chlorophyll a concentration at Station JR85 (blue) and B13 (red) for the top 200 m. Water depth at JR85 is 3700 m and at B13 360 m, full depth profiles are shown in suppl. Fig. 1.

The temperature profile at JR85 shows constant temperatures around -1.8°C for the top 50 m. With increasing depth, temperatures increase and reach about 2°C at 150 m and remain constant thereafter. At B13, temperatures are constant at close to 6°C for the upper 50 m and thereafter decrease to about 4°C at 150 m. Profiles of salinity show most pronounced changes at JR85, increasing from 34.1 in the upper 25 m to 34.8 practical salinity unit (PSU) at 150 m and remain constant thereafter. At B13, salinity remains constant at about 35 PSU throughout the water column. Temperature and salinity profiles indicate a distinct pycnocline between 75 and 100 m at JR85, separating cold and fresh surface waters from warmer and saltier underlying water masses. At B13, only a weak stratification with a thermocline at about 50 to 70 m is visible. Overall, both stations show a well-mixed water column below ~150 m, with lower temperatures and salinity at JR85, indicative of Arctic Water, and higher temperature and salinities at B13, indicative of Atlantic Water (Loeng, 1991). Profiles in Oxygen saturation show a similar pattern for both stations, with high values of 97-100 % oxygen saturation close to the surface, a decrease to 93 % at depth of 100 m and constant levels thereafter, indicating a well oxygenated water column. Chl *a* fluorescence shows peaks of about 2.2 $mg*m^{-3}$ for both stations, located at a depth of about 20 m at JR85 and 30 m at B13. Other data from measurements during the cruise both in the southern Barents Sea as well as at higher latitudes north of Svalbard, indicate that the southern Barents Sea region,

including station B13, may likely have already entered post-bloom conditions (Cottier, 2019). In contrast, other stations north of Svalbard showed pronounced phytoplankton bloom characteristics, especially in ice covered or recently ice-covered areas, indicative of an ongoing spring bloom condition further north.

2.2 Clock gene expression experiment

2.2.1 Sampling

Samples have been taken on 18th - 19th June 2018 at station JR85 (3 days prior Summer Solstice), and on 30th June - 1st July 2018 at station B13 (9 days after Summer Solstice) over a time course of 24 hours in 4-hour intervals, which resulted in seven timepoints per station. At JR85 sampling started at 18th June at 11:00 and ended with the last timepoint at 19th June at 11:00, sampling at B13 started at 30th June at 14:00 and ended at 1st July at 14:00. All times are noted in local time (UTC+2) which coincides with solar time (i.e. highest daily elevation of the sun at noon). Due to weather and logistical constraints on board, the actual time of sample fixation deviated from the targeted times for some timepoints, however, deviation was never more than 17 minutes, except for timepoint 5 at B13, which has been delayed for 28 minutes due to strong winds. A detailed table with sampling times is provided in the supplementary material (suppl. tab. 1).

At each timepoint the water column has been sampled from 200 m to the surface with vertical hauls of a WP2 plankton net (opening ⌀: 57 cm, net length: 236 cm, mesh size: 200 µm) with a meshed bucket cod end (mesh size: 200 µm) at a speed of 0.5 m*s^{-1}. After each haul, the content of the cod end was transferred to a bucket with seawater, which was immediately placed in a black bag and transferred into a dark cold room to reduce the disturbance of animals by bright light. In the cold room, the content of the bucket was carefully poured onto a 500 µm sieve to avoid small stage copepods and a spoon has been used, to transfer a fraction of the sample from the sieve into ~ 20 ml RNA*later* stabilization solution (Ambion, UK). Transferring the animals from the net into the stabilization solution has been done within less than 12 minutes for all samplings. A ~12 h period of incubation at 2 - 4˚C has been allowed to soak the samples thoroughly

with the stabilization solution before they were transferred to 80˚C for further transport and storage.

2.2.2 Sorting and RNA extraction

Before RNA extraction, copepods have been sorted from bulk samples in RNA*later* at 2˚C under a stereo microscope for species (*C. finmarchicus*) and stage (*CV*). To distinguish *C. finmarchicus* from its closely related congener *C. glacialis*, morphological indicators have been used, such as the redness of the antenna, which has been suggested to be a good indicator in the regions of sampling (Nielsen, Kjellerup, Smolina, Hoarau, & Lindeque, 2014). Moreover, in a recent study the geographic distribution of the Calanoid copepods occurring in the Arctic has been reassessed using species identification based on molecular markers (Choquet et al., 2017). The results confirmed the close association of *C. finmarchicus* with water masses of Atlantic origin and samples taken at a station in the Barents Sea, south of the polar front (similar to B13 in our study) showed a community of 100% *C. finmarchicus* and a station off the shelf north of Svalbard (similar to JR85) reported a large fraction of 91% to be *C. finmarchicus* and only 9% *C. glacialis* (detailed Supplementary Material 1 in (Choquet et al., 2017)). Irrespective of difficulties that may occur when distinguishing *C. finmarchicus* and *C. glacialis* by morphological characteristics, the study indicates that samples have been taken in today's core distribution area of *C. finmarchicus* where it makes up a major fraction of the copepod community.

For each timepoint and replicate, 15 *C. finmarchicus CV* copepods were distributed to a 2 ml Precellys® homogenization tube (Bertin Instruments, France), containing a mix of 1.4 mm and 2.8 mm ceramic beads and filled with 600 µl of TRIzol® reagent (ThermoFisher Scientific, USA), and homogenized with a Precellys® 24 Tissue Homogenizer (Bertin Instruments, France), using two times 15 sec. of homogenization at 5000 rpm with a 10 sec. break in between. In total, 3-5 replicates per timepoint have been used from Station JR85, dependent on the number of *CV* stage *C. finmarchicus* that were available from the bulk samples. At station B13, 5 replicates could be used for all timepoints (for details see supplementary tab. 1).

To efficiently extract total RNA from *C. finmarchicus* copepods, a combination of a Phenol/Chloroform based single-step extraction with a spin column based solid phase

extraction has been used. Therefore, after homogenization of the animals on TRIzol® reagent, RNA has been isolated using a chloroform induced phase separation (centrifugation for 15 min at 12000 g). To efficiently separate the RNA containing phase and thus increase the final yield, the phase separation step has been repeated by adding water instead of chloroform to the remaining sample, after the RNA containing phase has been removed.

The RNA containing phase was subsequently purified using the spin column system from the Direct-zol™ RNA MiniPrep Kit (Zymo Research, Irvine, CA, USA). During extraction of 1-2 replicates of each timepoint from station B13, instead of centrifugation, a QIAvac 24 plus system (Qiagen, Netherlands) was used to pass the sample through the spin column. This change in method is not expected to influence the results obtained. However, potential differences resulting from the method are controlled for by use of the QIAvac method in 1-2 replicates of each timepoint. The purified RNA has been eluted in a final volume of 35 µl of RNase free water and stored at -80˚C until further processing.

To quantify the extracted RNA, we used OD_{260} measurements from a NanoDrop 2000 spectrophotometer (ThermoFisher Scientific, USA). Additionally, $OD_{260/280}$ and $OD_{260/230}$ ratios were measured with the same instrument to check samples for purity. Furthermore, the integrity of the extracted RNA was checked on a 2100 Bioanalyzer system (Agilent Technologies, USA).

2.2.3 cDNA synthesis

After RNA extraction and purification, 2 µg of RNA have been reversely transcribed to cDNA. The total reaction volume was 40 µl, composed of 12 µl copepod RNA (final RNA concentration: 0.05 µg/µl), 2 µl pentadecamere primer (100 µM) and 26 µl of mastermix, containing 8 µl 5x reaction buffer, 1 µl RiboLock RNase inhibitor (40 U/µl), 2 µl RevertAid H Minus M-MuLV Reverse Transcriptase (200 U/µl; all ThermoFisher Scientific, USA), 4 µl dNTP (10 mM; Biolabs, USA), and 11 µl RNase free water. A “no template control” (NT) with RNase free water instead of sample has been used on each plate to test for contaminations of the reagents, and a “- reverse transcriptase control” (-RT) has been run on each plate for a subset of samples to test for DNA contamination of the RNA samples. The RNA has been reversely transcribed to cDNA using a T100

Thermal Cycler (Bio-rad Laboratories, USA) with the following program: 5 mins. at 25˚C, 60 mins. at 42˚C, 5 mins. at 70˚C, ∞ at 4˚C. Samples and replicates have been randomized between the single runs of reverse transcription. After completion of cDNA synthesis, cDNA was stored at -20˚C until further processing.

2.2.4 Quantitative real-time PCR

The expression of eight selected core clock genes (*clock* (*clk*), *cycle* (*cyc*), *period1* (*per*1), *timeless* (*tim*), *cryptochrome 2* (*cry2*), *doubletime 2* (*dbt2*), *vrille* (*vri*), *cryptochrome 1* (*cry1*)) and 3 candidate reference genes (*elongation factor 1-α* (*ef1*), *RNA polymerase* (*rna-poly*), *16s rRNA* (*16s*)) has been measured in *C. finmarchicus CV* copepods using a SYBRGreen based single gene assay. A table with primer details is presented in the Annex (suppl. tab. 2).

SYBRGreen primer for *C. finmarchicus* clock genes have already been designed, tested and successfully used in a previous study by Alexandra Schoenle (2015). For this study, Schoenle developed primer using the resources of putative *C. finmarchicus* core clock gene sequences identified by Christie et al. (Christie et al., 2013a) and candidate reference gene sequences from Lenz et al. (2014). Primer have been developed using the online software Primer3Plus and resulting primer sequences were checked subsequently for hetero dimers, self-dimers, hairpin structures and specificity, as well as folding and hybridization between primers. Also, primer efficiency tests have been conducted using serial dilutions of synthesized copepod cDNA, yielding good results.

Quantitative real-time PCR (qPCR) has been conducted in a total reaction volume of 20 µl, consisting of 8 µl copepod cDNA (initial concentration: 1.25 ng/µl; total amount in one reaction: 10 ng), 0.6 µl forward and reverse primer, respectively (10µM; final concentration in one reaction: 300nM), 10 µl PowerUp™ SYBR® Green Master Mix (ThermoFisher, USA), and 0.8 µl RNase free water. qPCR was done on a ViiA™ 7 system (Applied Biosystems, USA), using the following settings: 1 cycle of 2 min at 50˚C and 2 min. at 95˚C (DNA polymerase activation), 40 cycles of 15 s at 95˚C and 1 min. at 60˚C (amplification of target cDNA), 1 cycle of 15 s at 95˚C (1.6˚C/sec), 1 min. at 60˚C (1.6˚C/sec) and 15 s at 95˚C (0.15˚C/sec; all steps for melting curve analysis).

All samples have been run in technical duplicates and were randomly distributed between the different qPCR runs, to control for any differences between runs. NT

controls have been used regularly throughout the experiment, to test for contamination of the qPCR reagents.

2.2.5 Normalization and Statistics

Before normalizing the target genes mRNA expression levels, the three investigated reference genes (*ef1*, *rna-poly*, *16s*) were validated towards their expression stability throughout the sampled 24-hour cycle. Therefore, the online tool Reffinder (https://www.heartcure.com.au/reffinder/), developed by Xie et al. (2012), has been used. Reffinder is a program that combines the well-known and broadly used validation methods GeNorm (Vandesompele et al., 2002), NormFinder (Andersen, Jensen, & Ørntoft, 2004), Bestkeeper (Pfaffl, Tichopad, Prgomet, & Neuvians, 2004), and Delta-CT (Silver, Best, Jiang, & Thein, 2006), and subsequently ranks the investigated candidate reference genes by stability. To validate the Reffinder tool, the original versions of the GeNorm (R package "NormqPCR", Perkins et al., 2012), NormFinder (implementation into R function provided by Molecular Diagnostic Laboratory, Aarhus University Hospital (2015)) and Bestkeeper (Bestkeeper1, https://www.gene-quantification.de/bestkeeper.html) methods have been used in parallel. Further, the overall gene expression level of candidate reference genes compared to target gene expression levels have been investigated. Expression stability analysis revealed *16s* and *ef1* as most stable reference genes, both yielding good stability values. Therefore, the geometric mean of *ef1* and *16s* has been calculated to normalize the target gene expression level against, as has been suggested before (Vandesompele et al., 2002).

The normalization of the target gene expression levels to the reference gene expression levels was done using the $2^{-\Delta Ct}$ method (Livak & Schmittgen, 2001), where $\Delta Ct = Ct_{target\ gene} - Ct_{reference\ gene}$. The mean of the technical duplicates of the Ct values have been used as input Ct values for the normalization. The $2^{-\Delta Ct}$ values were used as a basis for all further statistics. mRNA expression profiles of *C. finmarchicus* clock genes have been checked for circadian and ultradian rhythms by the non-parametric method "RAIN" (**R**hythmicity **A**nalysis **I**ncorporating **N**onparametric methods, Thaben & Westermark, 2014) implemented in the R package "RAIN" and using the environment of the statistical software R (R Core Team, 2019). The RAIN software robustly detects rhythms in time series of predefined periods for a range of different wave forms and is especially suited

to work with non-normally distributed data and short timeseries (Thaben & Westermark, 2014). 24 h time series of mRNA expression levels of eight clock genes have been tested with RAIN for a range of periods and wave forms. Subsequently, significant rhythms with a period (τ) of 12 ± 4h were termed ultradian (U) and significant rhythms with a τ of 24 ± 4h were termed circadian (C), and the wave form yielding the most significant result has been chosen. As time series of genes at different stations have been tested individually and for different waveforms, the *false discovery rate* of the p-values has been corrected afterwards, using the Benjamini-Hochberg method (Benjamini & Hochberg, 1995), implemented in the *p.adjust* function in R (R Core Team, 2019).

Besides rhythm analysis, the overall expression level of each clock gene at each station has been calculated as the mean expression over all timepoints and replicates. Further, the amplitude (*A*) of the oscillation has been calculated for each gene at each Station after equation 1.

$$A = \frac{\max(t_{1,target},\ldots,t_{7,target}) - \min(t_{1,target},\ldots,t_{7,target})}{\min(t_{1,target},\ldots,t_{7,target})} \quad (1)$$

Due to a lack of normal distribution and homoscedasticity of the gene expression data, differences between genes and stations in amplitude and overall gene expression level have been tested using the Mann-Whitney-U test, a non-parametric version of the t-test (implemented in the R function *wilcox.test*, R Core Team, 2019). For all statistical tests a significance level of $p > 0.05$ has been assumed. For purposes of visualization, the fold change of the $2^{-\Delta Ct}$ values were calculated, by dividing each $2^{-\Delta Ct}$ value by the minimum value of the respective time series (i.e. fold change($2^{-\Delta Ct}_{tX}$) = $2^{-\Delta Ct}_{tX}$ / min($2^{-\Delta Ct}_{t1}$,…, $2^{-\Delta Ct}_{t7}$)).

2.3 Behavioral experiment

2.3.1 Sampling and sorting for behavioral experiments

Sampling of copepods for behavioral experiments has been conducted at the same stations and with the same sampling gear as described in 2.2.1. At JR85 animals for behavioral experiments have been sampled on 19th June 11:00, at B13 animals have been sampled on 30th June 17:30. The content of the cod end has been distributed to buckets with seawater and kept in the dark at 2˚C. Before the start of the experiment,

copepods have been sorted for species (*Calanus finmarchicus*) and stage (*CV*) under a stereo microscope and individuals were directly distributed to transparent acrylic test tubes (length: 10 cm, diameter: 1,2 cm), filled with cooled (2 - 4˚C) and 0.2 µm filtered seawater.

2.3.2 Experimental set up

To assess the behavior of individual copepods in relation to different photoperiods, filled test tubes were distributed to five modified *TriKinetics Drosophila activity monitors* (TriKinetics, MA, USA), subsequently termed *locomotor acivity monitors* (LAM), each monitor holding 32 test tubes (i.e. 32 individual copepods). The system is connected to a PC where the data acquisition software (DAMSystem3, TriKinetics) records each break of an infrared beam in the middle of the tube, and thus gives a measure of the behavioral activity of an individual copepod (see Fig. 5).

The LAMs have been set up under five photoperiods: two constant conditions, with one monitor under constant light (LL) and one under constant darkness (DD), and three different light dark (LD) cycles, mimicking a long day treatment with 18 h light/6 h dark (LD 18:6), a balanced treatment with 12 h light, 12 h dark (LD 12:12), and a short day treatment with 6 h light/18 h dark (LD 6:18). To provide a controlled light environment, the activity monitors were placed in a black box, where a LED bolt with a wavelength of 525 nm (Oznium.com, CO, USA) was attached to the ceiling. The hours of darkness in the LD cycles were spaced equally around local midnight. The experiments have been conducted in a temperature-controlled room at 2˚C (JR85) and 4˚C (B13), respectively, resembling ambient water temperatures in the field.

At station JR85 the experiment started at the 19th June at 14:00 and ended at the 24th June at 08:00. At station B13 the experiment ran from 30th June 20:30 to 5th July 11:00. After the end of the experiment, individual copepods from test tubes have been examined and photographed under a stereo microscope, to assess the general condition of the animals.

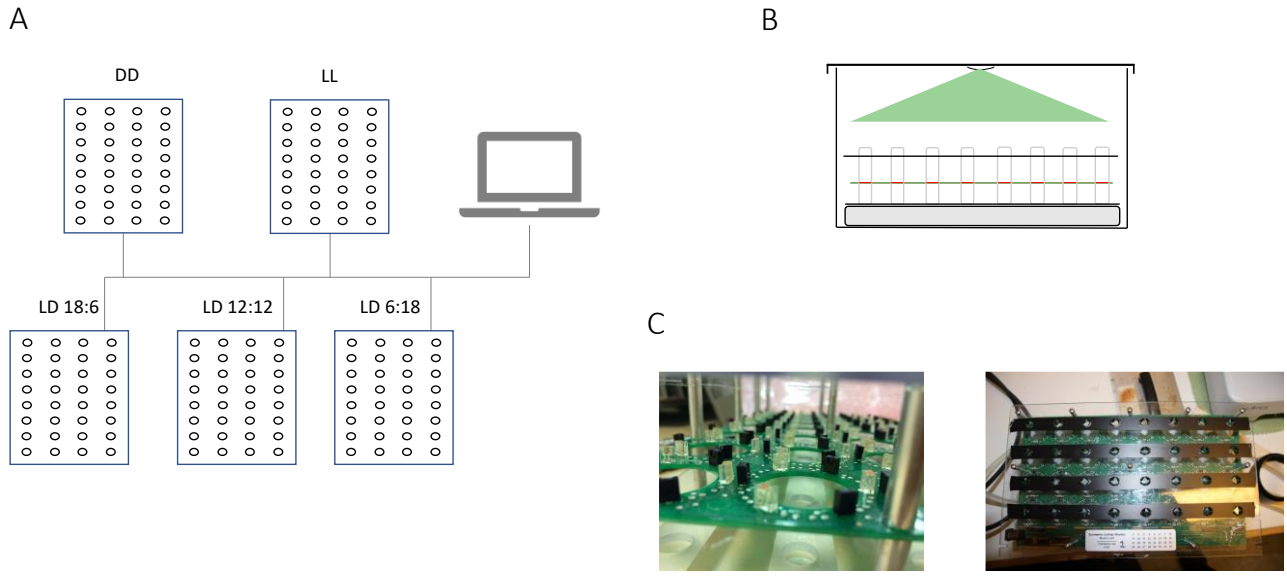

Figure 5: Figure 5: Design of behavioral experiments. A) Schematic overview of the experimental set-up. Five adapted Trikinetics locomotor activity monitors (LAM), each enclosed in dark box and supplied with a lighting system to create different photoperiodic treatments: constant darkness (DD), constant light (LL), and three different photoperiods with 18 h, 12 h and 6 h light, respectively. Data acquisition and light control is done by a PC with Trikinetics software. B) Schematic overview of one box, containing a LAM on top of vibration absorbing foam and an LED that provides the light cycle. C) Detailed photograph of the infrared beams and sensors, detecting the beam breaks (left) and top view of a LAM (own pictures).

2.3.3 Data handling and Statistics

Data on beam breaks during the behavioral experiments recorded from the LAMs data acquisition software were summed into bins of 60 mins, with the help of the "DAM File Scan" software (Version 1.10, TriKinetics). For further analysis, data have been truncated to four consecutive days, starting at 00:00 on the 20th and ending at 23:59 on the 24th of June for station JR85, and starting at 00:00 on the 1st July and ending at 23:59 on the 4th of July for station B13. The pictures of each individual after the experiments have been inspected to double check the individuals for species, stage and condition. Only data from *CV* stage *C. finmarchicus* in good condition have been kept for further data analysis. Moreover, the data have been checked for channels with absent activity (i.e. no beam breaks for ≥ 3 consecutive days) or obvious abnormal patterns (e.g. continuously increasing number of beam breaks) indicating technical errors, those channels were removed from the data set.

To detect rhythmic activity, the behavioral data were tested for rhythms of τ = 12 ± 4h (U) and $\tau = 24$ ± 4h (C) with the R package RAIN. The wave form settings have been kept at the default, and RAIN has been used in the "longitudinal" mode implemented for timeseries data that result from the same individual at each timepoint.

Subsequently, for each station and photoperiodic condition the number of days displaying rhythmic behavior have been summarized over the whole experiment and are interpreted as the *strength of rhythmicity*, with four out of four days rhythmic behavior considered as the strongest rhythmicity. Along with this measure, the percentage of copepods being rhythmic have been summarized for each photoperiodic condition and station.

3 Results

3.1 Results from the clock gene expression experiment

Considering the fact that a pronounced day night cycle was absent during the time of sampling, the terms “day” and “night”, that are further used for the ease of description, will here relate to phases of daily minimum (midnight) and maximum (noon) light intensity, as indicated by the sun angle data in Fig. 3 B.

Using rhythm analysis with RAIN, at station B13 seven out of eight clock genes were found to show a significant circadian oscillation (i.e. τ = 24 h ± 4 h; see Tab. 1). Expression patterns of *cycle, tim* and *cry2* were very similar at B13, all showing increasing mRNA transcription levels during the afternoon, reaching a maximum expression just before midnight (Fig. 6). Thereafter, expression levels of *cyc* and *cry2* decreased and reached lowest levels around noon of the following day, while *tim* decreased more rapidly reaching low values already in the morning hours. Similarly, *clk, vri* and *dbt2* expression levels increased over the afternoon but reached highest levels in the early morning. From there, expression levels dropped rapidly reaching minimal expression levels around midday. The expression of *per1* already peaked in the early evening (~18 h),

Table 1: Benjamini-Hochberg corrected p-values from rhythm analysis of clock gene expression profiles with RAIN. The expression profiles have been checked for ultradian (τ = 12 ± 4 h) and circadian (τ = 24 ± 4 h) periods. The level of significance is 0.05 and values higher than the significance level are not shown for the sake of clarity (ns).

	JR85		**B13**	
Target	Ultradian	Circadian	Ultradian	Circadian
clock	*ns*	**0.01**	*ns*	**> 0.0001**
cycle	**0.006**	**0.005**	**0.04**	**> 0.0001**
period 1	*ns*	**0.04**	*ns*	**> 0.0001**
timeless	*ns*	**0.05**	*ns*	**> 0.0001**
cryptochrome 2	**0.004**	*ns*	*ns*	**> 0.0001**
vrille	**0.002**	*ns*	*ns*	**0.001**
doubletime 2	**0.0007**	*ns*	*ns*	**> 0.0001**
cryptochrome 1	*ns*	**0.0009**	*ns*	*ns*

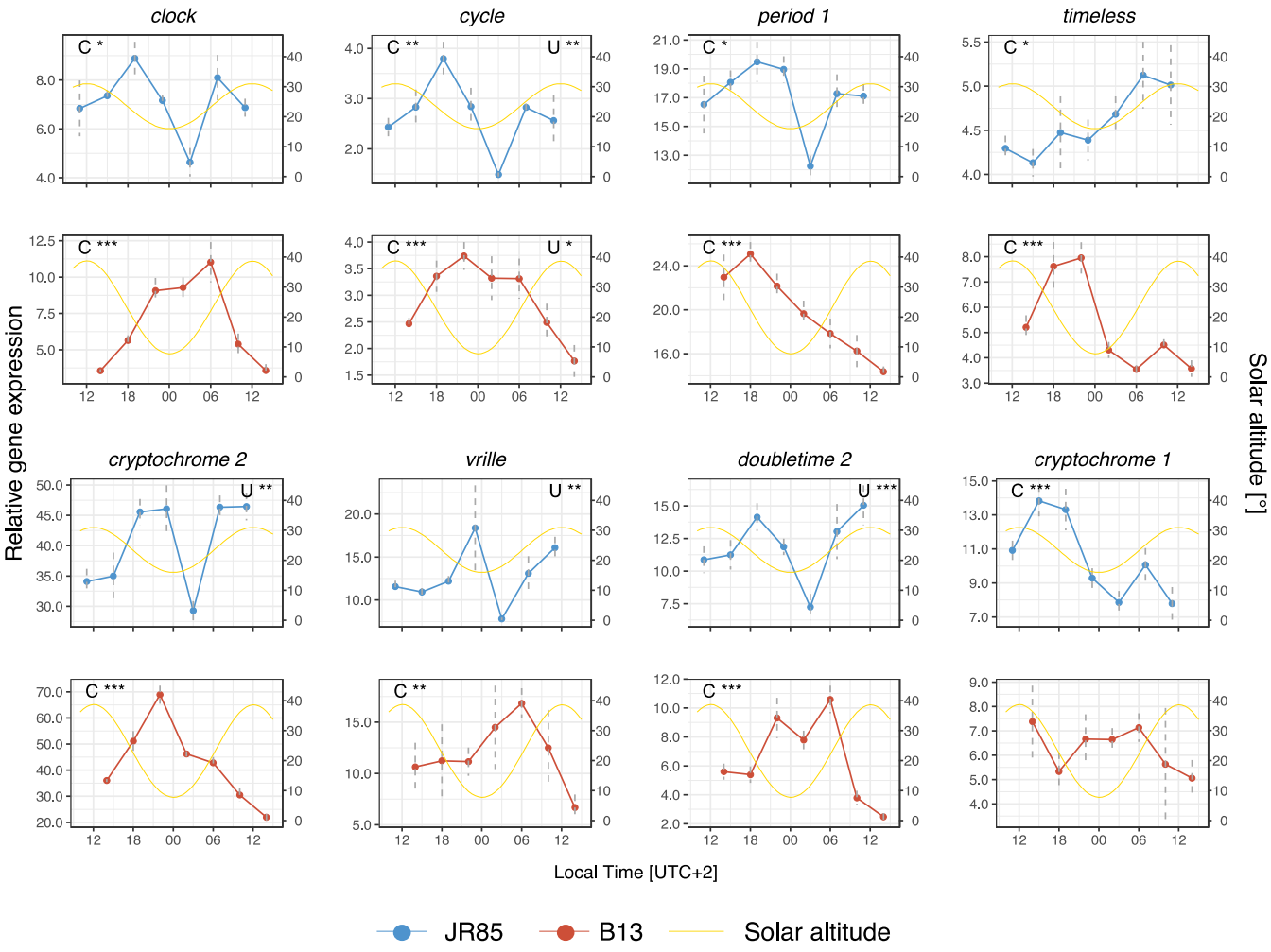

Figure 6: Temporal profiles of the relative gene expression of clock and clock-related genes in CV stage C. finmarchicus sampled during the period of Midnight Sun in the Arctic. Relative gene expression in animals sampled at the station JR85 (82.5˚ N, in the Nansen Basin) is shown in blue and gene expression in animals sampled at the station B13 (74.5˚ N, in the southern Barents Sea) is shown in red, as indicated for each target, respectively. Significance level of circadian (C, τ = 24 ± 4 h) and ultradian (U, τ = 12 ± 4 h) oscillations in relative gene expression as detected by rhythm analysis with RAIN are indicated with stars for each target gene at each station: "" p-value <0.05, "**" p-value <0.01, "***" p-value <0.001. The yellow line indicates the change of the sun's altitude above the horizon and thus fluctuations in light intensity over the course of sampling (also see Fig. 3 B).*

followed by a constant decrease that reached lowest levels around noon of the following day.

Only expression patterns of *cry1* did not show any significant oscillations over the 24 h cycle at station B13. In addition to a significant circadian oscillation, the rhythm analysis detected an ultradian oscillation for *cyc* at B13 (Tab. 1, Fig. 6).

At station JR85 five genes were rhythmically expressed in a circadian manner (*clk, cyc, per1*, *tim, cry1*; see Tab. 1) and showed an overall lower level of significance in the circadian oscillations of *clk*, *cyc*, *per1* and *tim* compared to those at station B13. In contrast, a circadian oscillation of *cry1* was not observed at station B13. Transcript levels

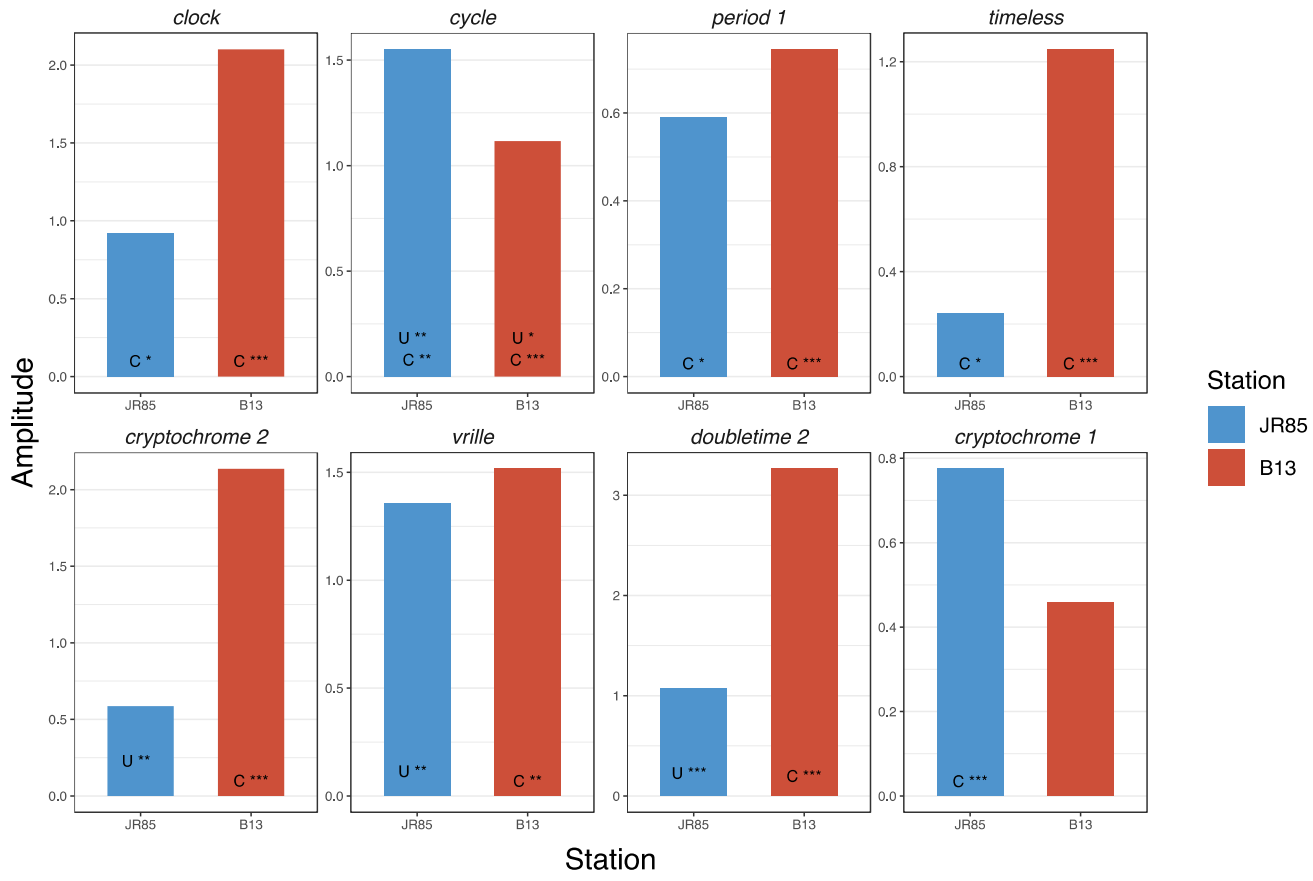

Figure 7: Amplitude of the clock gene oscillations shown in Fig. 6, calculated for each gene at each station over all timepoints, after eq. 1. Station JR85 is shown in blue and B13 in red. Significance levels of rhythmic clock gene oscillations, as already shown in Fig. 6, indicate for each amplitude, where a significant oscillation is associated.

of *tim* constantly increased from afternoon throughout the night, reaching peak expression in the morning, in contrast with the peak expression observed at station B13, where *tim* peaked before midnight.

Except for genes *tim* and *cry1*, the visual anlysis of gene expression indicated a shift to ultradian expression patterns at station JR85 with two peaks during the 24 h period (Fig. 6). This is reflected by the rhythm analysis, which showed significant ultradian oscillations for four genes at JR85 (*cyc, cry2, vri, dbt2*). Of these genes, *cyc* and *dbt2* showed a first peak in the evening (~ 19 h) and a second peak about 12 h later in the morning hours, in *dbt2* the second peak occurred slightly later, towards midday. In contrast, peak expressions of *vri* and *cry2* occurred around midnight and midday. Even though not detected by the rhythm analysis, the temporal patterns of *clk* and *per1* expression indicated an ultradian pattern at station JR85, with phases similar to *cyc* and *dbt2*.

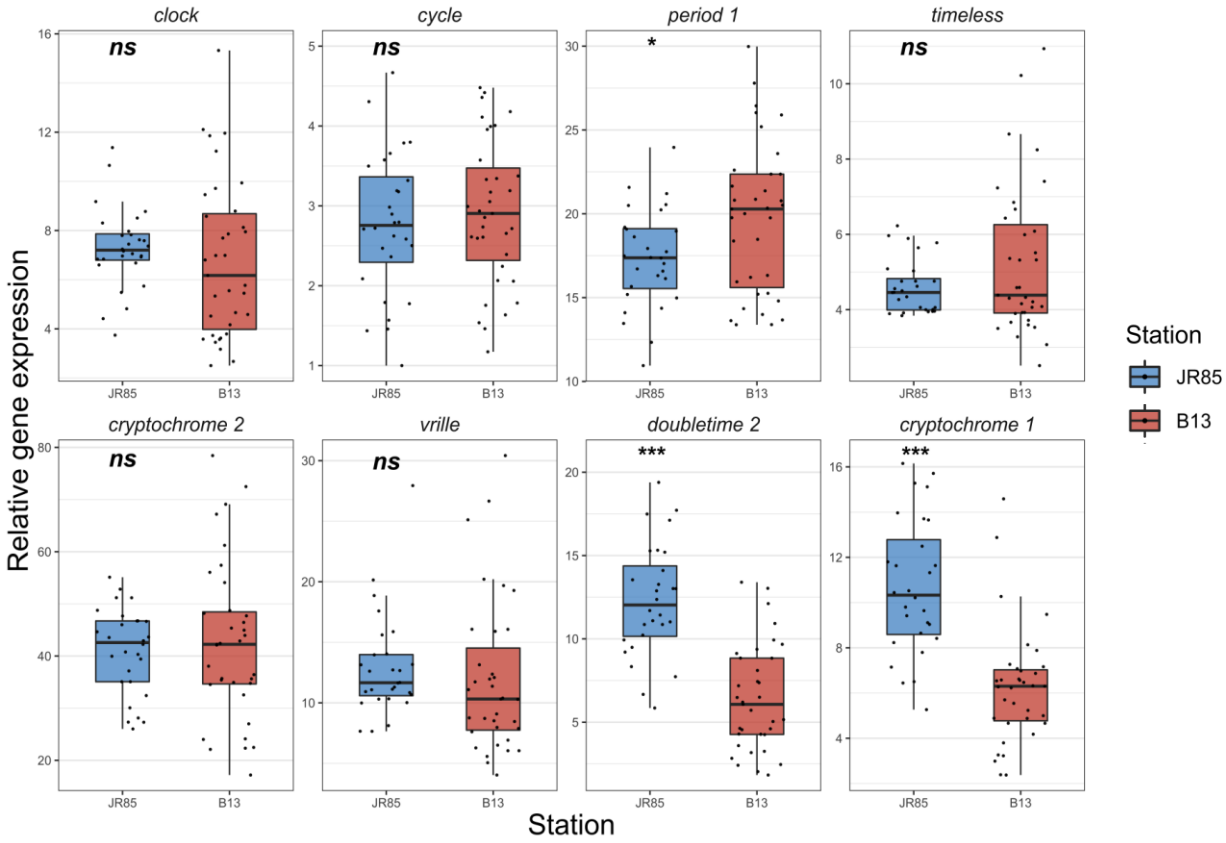

Figure 8: Visualization of the distribution of gene expression data over all timepoints per target and station. The lower and upper boundaries of the boxes indicate the first and third quartile (25th and 75th percentiles), respectively and the horizontal line the median. The whiskers span a maximum of 1.5 times the inter quartile range or until the lowest or highest value, respectively. The underlying data are shown as points. Significant differences between the stations for each target have been tested using a Mann-Whitney-U test, the results are shown in the top of each panel, with the significance levels as follows: "ns" p-value >0.05, "" p-value <0.05, "**" p-value <0.01, "***" p-value <0.001.*

In addition to the gene expression profile, the maximum amplitude of the oscillation of each target gene over the 24 h period has been calculated after equation 1 (Fig. 7). The amplitudes range from 0.2 to 1.5 at JR85, and from 0.4 to 3.2 at B13. It has to be considered that no significant oscillation is related to the expression profile of *cry1* at B13. Comparing the stations per target reveals that for *clk*, *per1*, *tim*, *cry2, vri* and *dbt2* the transcripts oscillate with higher amplitudes at B13, by a factor of 1.3, 0.3, 4.2, 2.6, 0.1, 2.0, respectively. For *cry1* and *cyc*, oscillations seem to have higher amplitudes at JR85, by a factor of 0.7 and 0.4, respectively. However, as only one amplitude value per target and station is available, no statistical analysis was performed. Comparing the stations by taking the amplitudes of all targets together does not indicate a significant station effect (Mann-Whitney-U test: *p-value* = 0.13, suppl. fig. 3 B).

To get information on the distribution, the gene expression data of all timepoints over the 24 h period are visualized with boxplots for each station and target (Fig. 8). Besides the distribution of the data, the boxplots and the underlying data that are plotted alongside, provide further information on the mean level of target gene expression. For five out of eight studied genes, no significant difference could be found in the level of gene expression between the stations B13 and JR85. However, significant differences were found for genes *per1*, *dbt2* and *cry1*. While *per1* was higher expressed at B13 (Mann-Whitney-U test: *p-value* = 0.04), *dbt2* and *cry1* where higher expressed at JR85 (*p-value dbt2* = <0.001; *p-value cry1* = <0.001). Moreover, a significant difference between the two stations was found, when data of all targets where analyzed together, with slightly higher expression for JR85 (*p-value* = 0.006, suppl. fig. 3 A).

3.2 Results from behavioral experiments

To assess the behavioral patterns of CV stage *C. finmarchicus* in response to different photoperiodic treatments, individuals (n = 11 - 26) have been screened for four consecutive days using an adapted LAM system (Fig. 5). Subsequently, behavioral data of each day have been checked for circadian (C, τ = 24 h ± 4 h) and ultradian (U, τ = 12 h ± 4 h) rhythms using RAIN and the number of days with rhythmic behavior has been assessed for each individual, which is interpreted as the *strength of rhythm*. Comparing the percentage of rhythmic copepods between stations under LD conditions reveals that a larger part of the copepods shows rhythmic behavior at station JR85, compared to B13 (Fig. 9). At JR85, about 20 % of the screened copepods in each treatment, except for ultradian rhythms under LD 18:6, showed significant rhythms, whereas for B13 values are at about 10-15 %, which holds true for both ultradian and circadian rhythms. The comparison of the copepods under constant conditions (DD, LL) indicates differences between stations considering ultradian rhythms, where a larger percentage of copepods is rhythmic with an higher strength at JR85, but almost no differences between stations for circadian rhythms. However, irrespective of the percentage, it needs to be considered that the ratio of numbers of rhythmic copepods

to total copepods used for these analysis (indicated in the top of each panel) is extremely low, with a maximum of 4 rhythmic copepods per treatment.

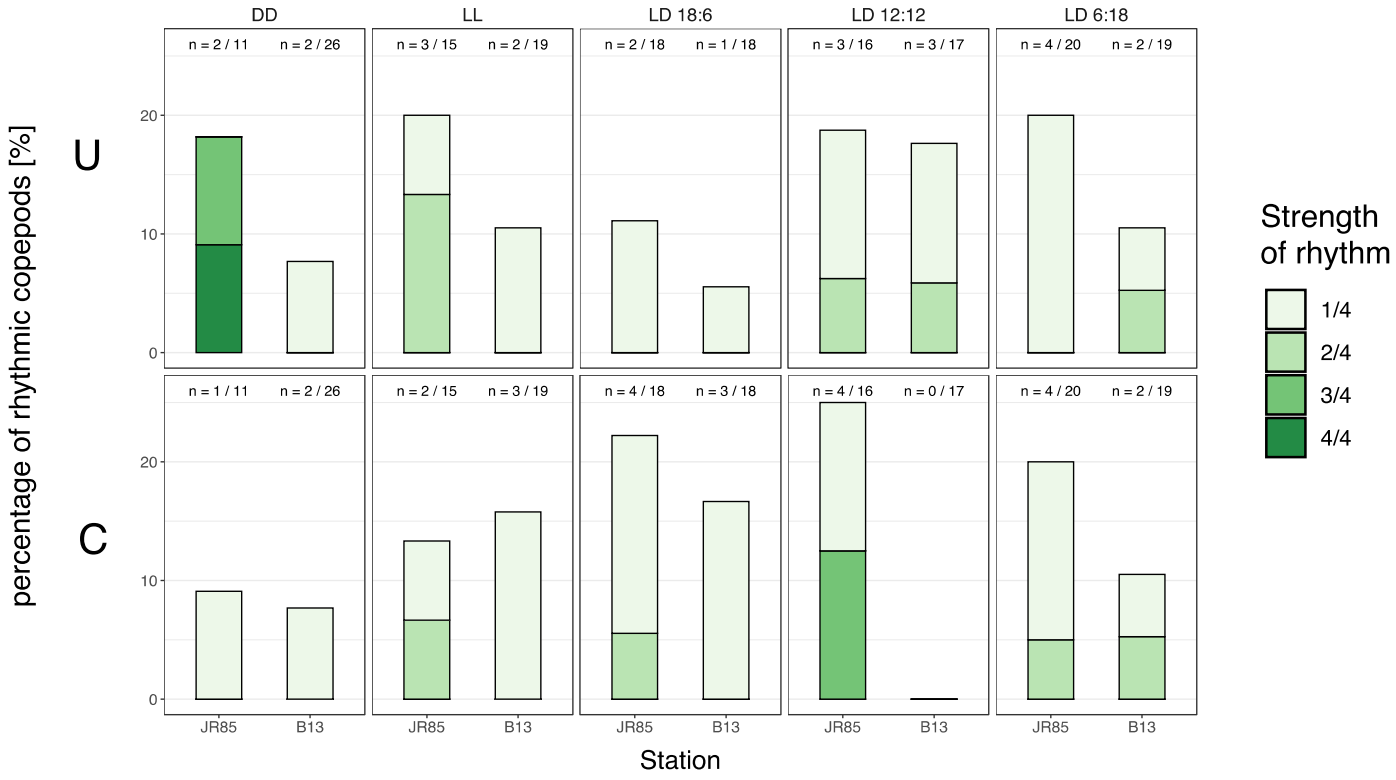

Figure 9: Percentage of C. finmarchicus individuals exhibiting significant ultradian (U, top row) or circadian (C, bottom row) rhythmic behavior in the onboard laboratory experiments at the two stations investigated. Each column shows the data from the respective photoperiodic treatment indicated at the top. The number of days an individual showed rhythmic behavior is interpreted as the "strength of the rhythm", indicated by the color shades. In addition to the percentage, the number of rhythmic copepods in relation to the total number of copepods considered for the analysis is shown at the top of each panel. Behavioral profiles of each individual considered for the rhythm analysis is shown in suppl. fig. 4.

4 Discussion

This study has generated first insights into the circadian rhythm of a key planktonic species, *Calanus finmarchicus*, during midnight Sun in the High Arctic. Biological clocks are central to all living systems providing an innate measure of time so that organisms can anticipate and adapt to cyclic changes in their environment (Jay C. Dunlap & Loros, 2016; Sandra J. Kuhlman et al., 2017; Tessmar-Raible et al., 2011). The main zeitgeber of the endogenous circadian clock is the daily light/dark cycle, leading to near 24 h biological rhythms. However, organisms living in the High Arctic are exposed to the absence of light/dark cycles during Midnight Sun. How the circadian clock of organisms is running in such conditions remains to be deciphered (Abhilash, Shindey, & Sharma, 2017; Williams, Barnes, & Buck, 2015). In previous studies it has been shown that *C. finmarchicus* possesses a robust circadian clock that is probably underpinning diel and seasonal rhythms (Häfker et al., 2017; Häfker, Teschke, Last, et al., 2018). Oscillations in clock gene expression existed under both LD and DD conditions in the laboratory as well as in the field in a *C. finmarchicus* population from a Scottish sea loch (56.5°N, photoperiod = 16h) and the clock gene expression patterns generally resembled those of terrestrial model species like *Drosophila* (Häfker et al., 2017; Mackey, 2007). Further, clock gene expression patterns from a high latitude fjord population (78.5˚N, photoperiod = ~ 24 h) sampled at the end of the Midnight Sun period showed that the *C. finmarchicus* circadian clock is able to maintain a robust rhythm under extremely long photoperiods (Häfker, Teschke, Hüppe, et al., 2018). Thus, the question remains, whether clock rhythmicity persists, or if clock gene oscillations become arrhythmic under Midnight Sun. Here we analyzed the clock gene expression in *C. finmarchicus* at two high latitude stations, JR85 (82.5°N) and B13 (74.5°N), 3 days before and 9 days after Summer Solstice (i.e. the day with the lowest oscillation in sun angle), respectively. Moreover, lab behavioral analyses have been conducted at the same two stations investigated.

4.1 A functional circadian clock during the period of Midnight Sun in the High Arctic

The analysis of clock gene expression patterns in *C. finmarchicus* from this study showed significant oscillations of clock genes at both stations (Tab. 1). This indicates that a functional circadian clock is present in *C. finmarchicus* sampled during the Midnight Sun period in the High Arctic. Interestingly, differences were apparent in the period of the oscillations between the northern (JR85) and southern station (B13). Clock gene expression data from organisms inhabiting high latitude regions are scarce (Williams et al., 2015). However, our findings contrast the few previous results of clock gene expression in Polar species under nearly LL conditions. Work on a field population of the Antarctic midge *Belgica antarctica* showed no cyclic clock gene expression during the Antarctic Summer (Kobelkova et al., 2015). Moreover, animals sampled from the field (~64 ˚N, photoperiod LD 21:3) as well as animals kept in the laboratory under LD 12:12 did not show oscillations in clock gene transcripts, which led to the author's suggestion that the circadian clock is "switched off" during the time of extremely long days or that the Antarctic midge lost its endogenous time keeping function and reacts solely to exogenous cues (e.g. temperature) in this harsh and variable environment. Studies on the Antarctic krill *Euphausia superba,* kept in the laboratory under different photoperiodic conditions showed that clock gene expression becomes arrhythmic and unsynchronized under constant light (LL), an indication that the circadian clock got disrupted under these extreme light conditions (Piccolin et al., 2018).

At station B13 in the Southern Barents Sea (74.5 ˚N), pronounced circadian oscillations were visible in all clock and clock-related genes investigated, except for *cry1* (Fig. 6). The expression patterns showed strong similarities with previous findings on the *C. finmarchicus* circadian clock which were obtained both in laboratory and field conditions under a natural photoperiod of 16 h (Häfker et al., 2017). Especially, while the peak expression of the core clock gene *clk* occurred in the morning in animals from the Scottish sea loch (Häfker et al., 2017), it occured at the phase of increasing light intensity in our results. Similarly, while the peak expression of *per1* and *tim* occured in the evening in the same study, it occured at the phase of decreasing light intensity in our results. Consequently, temporal expression patterns of *clk* and *per1* showed a clear

antiphase relationship, a common characteristic of functional circadian clock systems (Mackey, 2007). Moreover, the expression pattern of *cry2* was very similar to those of *per1* and *tim*, with higher expression before midnight (i.e. phase of lower light intensity) and a trough around midday (i.e. phase of higher light intensity). This suggests that PER, TIM and CRY2 form a heterotrimer to inhibit the transcriptional activity of the CLK/CYC heterodimer, as it is known from the honeybee *Apis mellifera* (Rubin et al., 2006) and has previously been suggested for *C. finmarchicus* (Häfker et al., 2017). Overall, the circadian clock gene oscillations of components present in all three feedback loops of the *Drosophila* circadian clock, strongly suggest that despite the absence of a light/dark cycle, the *C. finmarchicus* circadian clock is functional in animals sampled in the southern Barents Sea. As a daily light/dark cycle was absent during the time of sampling, it is likely that the small diel fluctuations in light properties, such as intensity or spectral composition, were sufficient to entrain the endogenous clock in *C. finmarchicus*. In fact, daily oscillations of the sun's altitude above the horizon persist throughout the period of Midnight Sun. Thus, in agreement with previous studies (Cottier et al., 2006; Wallace et al., 2010), diel oscillations in atmospheric PAR have been observed during the time of sampling at both stations (Fig. 3 B). According to the model, the solar altitude oscillated from 8˚ at midnight to 38˚ at midday during sampling at B13. Thus, it is likely that *C. finmarchicus* was able to detect these very low oscillations in light, which corroborate the previous report of very high light sensitivity for calanoid copepods (Båtnes, Miljeteig, Berge, Greenacre, & Johnsen, 2015). Moreover, it can be assumed that wavelength modifications also occur throughout the day, reinforcing the variations of light intensity in the transmission of the temporal information during Midnight Sun (Stelzer & Chittka, 2010). Interestingly, *cry1* did not exhibit a circadian expression pattern at station B13, suggesting that other light transduction pathways could be involved in entraining the circadian clock in *C. finmarchicus*.

Zooplankton DVM studies during the Arctic Midnight Sun have previously been performed, with contrasting results. On the one hand, some studies show ongoing DVM (Dale & Kaartvedt, 2000; Falkenhaug, Tande, & Semenova, 1997; Fortier, 2001) during the period of Midnight Sun (at 69-71 ˚N, Norwegian and Greenland sea; at 69 ˚N, Malangen fjord, Norway; at 74.5 ˚N Barrow Strait, Canadian Arctic). These results confirm that organisms seem able to detect low daily light oscillations. Further, Tran et

al. (2016) found persistent circadian rhythms in valve activity of the scallop *Chlamys islandica* throughout the Midnight Sun in the Arctic (78° 56 'N). On the other hand, studies reported disrupted zooplankton DVM (76-77.5 ˚N, Barents Sea; 79 ˚N, Kongsfjorden, Svalbard; 80 ˚N, Rijpfjorden, Svalbard) during this season (Blachowiak-Samolyk et al., 2006; Cottier et al., 2006; Darnis et al., 2017; Wallace et al., 2010), which could suggest that low light oscillations during Midnight Sun are not sufficient to temporally synchronize organisms. However, the absence of zooplankton DVM patterns could also result from a desynchronization between zooplankton species. Moreover, ongoing circadian rhythmicity throughout the Summer at high latitudes (68 - 78 °N) has been shown before on terrestrial organisms such as the Svalbard reindeer (*Rangifer tarandus platyrhynchus*), the Bumblebee (*Bombus terrestris*) or the Arctic ground squirrel (*Urocitellus parryii*; Arnold et al., 2018; Chittka, Stelzer, & Stanewsky, 2013; Williams, Barnes, & Buck, 2012; Williams et al., 2015; Williams, Barnes, Yan, & Buck, 2017), all suggesting that small ongoing fluctuations in light intensity, spectral composition or temperature are able to sustain circadian rhythmicity throughout the Midnight Sun period.

While these previous findings on ongoing circadian rhythmicity in high latitude inhabiting organisms suggests that their circadian clock is functional throughout the Arctic Summer, there is still a lack of proof for a functional endogenous timing system. Circadian rhythmicity in e.g. behavior, heart rate or body temperature as reported by the above-mentioned studies, represent measures of behavioral or physiological traits that are likely to be under the control of a circadian clock. However, the occurrence of diel rhythms of behavior or physiology does not necessarily imply a functional or entrained endogenous timing system, as organisms may directly react to external cues, a phenomenon known as "masking" (Aschoff, 1960; Bloch, Barnes, Gerkema, & Helm, 2013; Williams et al., 2015). Thus, to be able to comment on the functionality of the circadian clock, temporal gene expression patterns of the core clock components and their respective protein products need to be investigated, which is a complex, costly and time-consuming procedure, especially in polar regions. Therefore, this work presents a highly novel data set, which gives first time insights into the circadian rhythms of temporal clock gene expressions in a marine species inhabiting High Arctic regions during the period of Midnight Sun, revealing that the circadian clock of *C. finmarchicus*

is able to remain synchronized during this particular season. Further experiments using e.g. chemical clock disruption would be necessary to validate the functional aspect of the circadian clock of *C. finmarchicus* during Midnight Sun in the High Arctic.

4.2 A changing profile of oscillation along a latitudinal gradient

In contrast to the clear circadian expression patterns found at station B13, *C. finmarchicus* sampled at the very high latitudes of station JR85 (82.56˚N) exhibited significantly different temporal changes in clock gene transcription. While the rhythm analysis of core clock genes *clk*, *per1* and *tim*, as well as the blue light photoreceptor encoding *cry1* gene indicated significant circadian oscillations, core clock genes *cry2* and *vri*, showed significant ultradian oscillations with periods of ~12 h and rhythm analysis of the expression pattern of *cyc* showed both circadian and ultradian oscillations. It is noteworthy that this bimodal circadian/ultradian oscillation of *cyc* is also observed at station B13. Interestingly, an ultradian oscillation with a period of ~12 h, as well as an increase in the expression level is also observe in the clock associated *dbt2* gene at JR85, whose protein product is known to play a major role in posttranslational modification of PER and thus in the definition of period length (Muskus, Preuss, Fan, Bjes, & Price, 2007). This finding is complimented by a chemical clock disruption experiment conducted on *C. finmarchicus* sampled from a Scottish fjord population. The data from this experiment were not published but the experiment has been conducted and the data discussed as part of a Dissertation on the molecular basis of diel and seasonal rhythms in *C. finmarchicus* (Häfker, 2018). Within this experiment, temporal clock gene expression data have been obtained from animals treated with a chemical inhibitor of *casein kinase 1* proteins, which also targets the *dbt2* protein product DBT2. The chemical treatment resulted in a significant period lengthening of clock gene oscillations, thus pointing towards an important role of DBT in period definition.

Another peculiarity observed at station JR85 was the loss of the typical *clk* and *per1* antiphase expression, which has also been found in *E. superba* kept under LL in laboratory conditions (Piccolin et al., 2018) and sampled from the field under near LL conditions during the Antarctic Summer (Biscontin et al., 2017), as well as in

C. finmarchicus at high latitudes under near LL conditions (Häfker, Teschke, Hüppe, et al., 2018). Interestingly, the less pronounced circadian oscillations found at station JR85 are associated with lower daily oscillation of the solar altitude at this latitude. Indeed, the diel oscillations in solar altitude are reflected in diel oscillations of atmospheric PAR and thus light intensity at the respective day of sampling (Fig. 3 B). At JR85, the solar altitude oscillated of 15˚ (from 16˚ at midnight to 31˚ at midday) and of 31˚ at B13 (from 8˚ at midnight to 39˚ at midday; Fig. 3 B) throughout the course of a day, attributed to both the latitudinal position as well the smaller temporal deviation from Summer Solstice. Furthermore, sampling at JR85 was conducted within snow covered very close drift ice, which is known to strongly attenuate light (Wallace et al., 2010). In fact, comparing data from an ice-covered and an ice-free Arctic fjord, Wallace at al. found that closed snow covered sea ice decreased irradiance levels by a factor of 100 compared to ice free waters. Thus, potential attenuation of very small fluctuations in light by ice and snow could mitigate the periodic signal of light that can be perceived in the water column below and thus its potential to provide a reliable measure of time. However, circadian oscillations are still observed for four core clock genes (*clk*, *cyc*, *per*, *tim*), implying that organisms are still synchronized by the daily light cycles. Moreover, in contrast to station B13, a circadian expression pattern as well as an increased expression level has been found for *cry1* at JR85, a clock associated gene which is known to play a role in the transduction of photic signals from the environment. Interestingly, the decrease of circadian clock gene oscillation is not accompanied by a loss of rhythm but by an appearance of ultradian oscillations, which indicates that some sort of synchronization on the population level was present. The question remains what caused the synchronized ultradian oscillatory patterns in *C. finmarchicus* clock gene expression.

4.3 Switching to alternative *Zeitgebers* during a period of minimal fluctuations in light?

Rhythmic ultradian patterns with a period of ~12 h are probably most prominently known from organisms under the influence of semi-diurnal tidal cycles who synchronize to the 12.4 hour period of the flood and ebb flow (Tessmar-Raible, Raible, & Arboleda,

2011; Wilcockson & Zhang, 2008; Zhu, Dacso, & O'Malley, 2018). Circatidal rhythmicity has been found in a range of organisms inhabiting coastal and estuarine habitats, including several crustaceans such as the fiddler crab (*Uca pugnax*; Brown, Fingerman, Sandeen, & Webb, 1953), the green shore crab (*Carcinus maenas*; Naylor, 1958), the sea louse (*Eurydice pulchra*; Hastings, 1981; Zhang et al., 2013) or the mangrove cricket (*Apteronemobius asahinai* ;Satoh, Yoshioka, & Numata, 2008). Moreover, persistent circatidal rhythmicity in the absence of a tidal *Zeitgeber* (e.g. vibration or inundation) has been demonstrated in these organisms, strongly suggesting the existence of an endogenous circatidal rhythm. However, circatidal rhythms are not restricted to organisms inhabiting intertidal areas, as illustrated by tidal rhythms observed in the mollusk *Crassostrea gigas* or the crustacean *Limulus polyphemus* under subtidal conditions (Anderson, Watson, & Chabot, 2017; Tran et al., 2011). Indeed, it has been shown that cycles of current reversal (Bolliet & Labonne, 2008), hydrostatic pressure, food, agitation or turbulence (Forward, Thaler, & Singer, 2007; Hastings, 1981) are suitable to entrain circatidal rhythms. While it is still under debate how endogenous circatidal oscillations are produced, the discussion mainly focusses on three theories. The first suggests a separate circatidal oscillator that produces ~12.4 h endogenous oscillations independently to the circadian one (Palmer, 1995), which is supported by findings from studies on *E. pulchra* (Zhang et al., 2013) and *A. asahinai* (Takekata, Matsuura, Goto, Satoh, & Numata, 2012) that showed persistent circatidal rhythms even when the circadian clock has been disrupted experimentally. The second theory suggests the involvement of two circalunidian (24.8h lunar day cycle) oscillators coupled in anti-phase, whose common output results in the production of a circatidal rhythm (Naylor, 1996). The third one suggests a single bimodal oscillator that governs both circadian and circatidal patterns (Enright, 1976), which is supported by bimodal 12.4 / 24 h oscillations of the circadian clock machinery of *C. gigas* in the field under subtidal conditions (Tran et al., under review). Information on the tidal height over the course of sampling at JR85 indicate a semi-diurnal tidal cycle, with peak tidal heights in the "morning" and "evening" hours in phase with peak expression of most genes showing ultradian oscillations (also see suppl. fig 2). Further, Conover et al. (1986) were able to show cycles in ingestion rate of *Pseudocalanus spp.* that were related to the tidal cycle under sea ice in the Canadian Arctic. The findings were attributed to cyclic erosion of ice

algae by tidal currents and highest ingestion rates for the organisms at slack water, when current speeds are lowest, indicating that tidal flow could also provide cues indirectly through cyclic food availability. Even though the amplitude of the tidal height at the investigated stations was relatively small (± 0.2 m), the tidal fluctuations could be an indicator for the presence of horizontal tidal currents, which could cause periodic cycles of e.g. turbulence, agitation, change of current direction or food availability under sea ice at JR85. Thus, in a context of weak daily light intensity oscillation at the station JR85, tidal cues could function as an alternative *Zeitgeber* for the *C. finmarchicus* circadian clock and lead to both circadian and tidal oscillation of the circadian clock machinery, as proposed by the third hypothesis (Enright, 1976). However, longer sampling period and higher sample frequency would be necessary to distinguish the effect of the tidal cycle from a potential "morning" and "evening" effect.

4.4 Switch to a bimodal circadian pattern?

Besides an alternative Zeitgeber, that readily provides ultradian timing cues like the tidal cycle, it can also be hypothesized that the ultradian oscillations are the results of a simple daily light entrainment of the circadian clock. Indeed, ultradian oscillations have already been observed in some species in the laboratory under purely circadian entrainment. In a standard 12:12 light/dark cycle, *Drosophila* exhibits two peaks of activity: a morning peak and an evening peak, driven by two different types of neurons (Grima, Chélot, Xia, & Rouyer, 2004; Lamba, Bilodeau-Wentworth, Emery, & Zhang, 2014). Furthermore, studies on the mammalian circadian clock system in mice showed 12 h rhythms in NAD^+ levels in mouse liver (Ramsey et al., 2009), in the expression of core clock genes in mouse bone marrow, spleen and testis (Chen, Mantalaris, Bourne, Keng, & Wu, 2000; Liu, Cai, Sothern, Guan, & Chan, 2007; Yamamoto et al., 2004) or of enzymes associated with lipid metabolism (Kohsaka et al., 2007).

Recently, transcriptomic approaches allowed to discover groups of genes with ultradian expression rhythms under daily light/dark entrainments in mammals (Cretenet, Le Clech, & Gachon, 2010; El-Athman, Knezevic, Fuhr, & Relógio, 2019; Hughes et al., 2009, 2012; Vollmers et al., 2009) and in marine organisms such as the Antarctic krill or the

Pacific oyster (Biscontin et al., 2019; Payton et al., 2017). A potential explanation for the mechanisms underlying the presence of ~ 12 h oscillations is provided by the theory of "circadian harmonics" (Hughes et al., 2009), which states that the 12 h periods are produced by the interaction and/or modulation of ~24 h oscillations. The finding of highly dampened ~12 h oscillations *ex vivo*, which is also known from circadian outputs, further strengthens this hypothesis (Hughes et al., 2009). Westermark et al. (2013) further suggest that the interaction of two circadian transcription factors with an antiphase relationship are responsible for the occurrence of ~12 h rhythms. In contrast, a recent study identified a "12 h clock" in the mammalian timing system (Zhu et al., 2017). By analyzing data from a mouse liver transcriptome in both wild-type and knock-out mice (lacking *bmal1* or *clock*), the authors found persisting 12 h rhythms in knock-out mice where the circadian clock has been disturbed, pointing towards a separate mechanism that drives 12 h rhythms. While the presence of such a separate mechanism is under debate, it shows that the mechanisms that underly ~ 12 h rhythmicity on various organizational levels is far from clear and in light of the recent findings they should be taken more into focus in future studies. In our study, most of the observed ultradian oscillations at the station JR85 are not observed at the station B13, except for *cyc*. However, the reason why the unimodal circadian pattern at B13 would have switched to a bimodal circadian pattern (12 h ultradian rhythms) at station JR85 remains unclear.

4.5 A free running clock during Midnight Sun?

Alternatively, in light of studies discussed in the following, it can be hypothesized that the differences in expression patterns between the stations B13 and JR85 could reflect a situation where a robust *Zeitgeber* signal is totally absent at JR85, and where the clock is under free running conditions and would consequently exhibit its endogenous periodicity. In a study on the expression of putative clock genes in the Antarctic krill, *Euphausia superba*, Teschke et al. (2011) found significant circadian oscillations of the core clock gene component *cry2* with a 24 h period under LD conditions in the laboratory. Interestingly, under constant conditions, the period of expression significantly shortened to a period of ~18 h. Furthermore, in a recent study, Biscontin et

al. (2019) investigated the involvement of the *E. superba* circadian clock in the temporal orchestration of gene expression by analyzing transcriptome data from Antarctic krill also kept under both LD and DD conditions in the laboratory. While under LD a large part of the oscillating transcriptome showed significant oscillations with a period of 24 h, under DD conditions 77% of oscillating genes showed periods <24 h, and 42.4 % of them showed clear bimodal patterns (two peaks per day) with periods of 12-15 h. Moreover, the putative *E. superba* core clock gene components *clk* and *per* showed a period shortening from ~24 h to ~12 h under DD conditions, while *cry2* and *casein kinase ε* (*ckε*, the mammalian homologue to *Drosophila's doubletime*) showed bimodal oscillations under both LD and DD. In addition, DD conditions resulted in a complete loss of *clk*-*per* antiphase, which is in agreement with our results from JR85 as previously discussed. Even though the rhythm analysis did not detect ultradian rhythms in *clk* and *per1* in our study, the genes lost their typical antiphase relationship and patterns showed a clear transition from a unimodal distribution found at B13 towards a rather bimodal distribution found at JR85.

Ultradian oscillation of the circadian clock under free-running conditions could reveal an ancient adaptation of the clock system to a broad range of photoperiods, as suggested for *E. superba* (Biscontin et al., 2019; Teschke et al., 2011). It is known that the deviation of the free running period (FRP) from the 24 hour cycle is a common characteristic of endogenous circadian rhythms that helps to entrain to varying photoperiods throughout the seasonal cycle (Pittendrigh & Daan, 1976) and that diurnal organisms usually exhibit FRPs that are <24 h (Aschoff, 1960). A short FRP in Antarctic krill has therefore been interpreted as an adaptation to the extreme fluctuations in photoperiod experienced at polar latitudes (Teschke et al., 2011). This theory is further supported by several findings in the *Drosopholids D. littoralis* and *D. subobscura*, which reveal a trend of decreasing FRPs with increasing latitude (Hut, Paolucci, Dor, Kyriacou, & Daan, 2013). Moreover, it has been shown that transcripts with ultradian periods of ~12 h are more likely to be evolutionary conserved as they appear to be enriched in "ancient", highly conserved genes (Castellana et al., 2018), which could represent an adaptation to the shorter photoperiods that where present during the evolution of life on earth. In agreement with that, the identification of two *cryptochrome* genes (*cryptochrome1, cryptochrome2*) in the *C. finmarchicus* clock (Christie, Fontanilla, Nesbit, & Lenz, 2013b)

indicates similarities to the clock mechanism of the Antarctic krill or the monarch butterfly *D. plexippus* (Biscontin et al., 2017; Reppert, 2007), which are considered "ancient" clock systems.

One might argue that the period shortening has not been found in clock gene expression of *C. finmarchicus* kept under DD conditions in the laboratory (Häfker et al., 2017). However, in the laboratory study, animals have been well entrained to a clear light/dark cycle directly before transition into constant darkness. Moreover, gene expression was only monitored over two days under DD, thus showing the endogenous oscillations of a free running but recently well entrained clock. Therefore, it might take a longer time under the absence of a clear *Zeitgeber* until a transition to a putatively intrinsic FRP happens. For example, in *E. superba* a pronounced bimodal expression in *cry2* was only apparent on the third day under DD (Teschke et al., 2011). Furthermore, there might be large differences between the expression patterns from organisms sampled directly from the wild and those kept in a controlled environment in the laboratory (e.g. Biscontin et al., 2019; De Pittà et al., 2013; Häfker et al., 2017; Piccolin et al., 2018). As the ice edge of the polar ice cap usually reaches its minimum in September, it is likely that the region of sampling at JR85 has been ice covered since winter. Therefore, copepods might have been in this area for days or weeks prior to the sampling and thus not influenced by a clear *Zeitgeber* for a longer period. As a consequence, at the time of sampling the circadian clock might show its intrinsic oscillatory pattern, potentially evoked by complex interactions of circadian oscillators and posttranslational modifications.

However, while the discussion about a changing FRP in constant conditions in the light of evolution and adaptation to polar environments might be meaningful and applicable in studies where organisms are exposed to constant conditions in a controlled laboratory set up, a range of facts are challenging this discussion in the data presented in this work. First off all, the high light sensitivity that has been reported for calanoid copepods, which is in the range of $5 * 10^{-8}$ µmol photons m^{-2} s^{-1} (Båtnes et al., 2015), makes it highly unlikely that changes in light properties, apparent in the atmosphere, cannot be sensed by the animals in the water column, implying that even under sea ice habitats cannot be considered "constant environments" in terms of light. This is supported by the findings of significant circadian oscillations that have also been found

at JR85, suggesting that copepods are still synchronized by diel light oscillations. In addition, the detection of significant ultradian rhythms further indicates that individual animals are synchronized amongst one another. Moreover, each individual possesses its own internal rhythm, and a long-term free-running environment would have led to a desynchronization between organism and consequently to arrhythmic genes expression profiles. Therefore, even though ultradian patterns have been found in *C. finmarchicus* clock gene expression at station JR85 under low fluctuations in light properties, the theory of a free running clock is not applicable to our findings.

4.6 Reduced behavioral rhythmicity during the period of Midnight Sun at high latitudes

In parallel to gene expression studies, the behavioral patterns of CV stage *C. finmarchicus* individuals have been assessed at the two stations in an onboard laboratory experiment. To investigate the organism's responsiveness to different simulated daylengths, a photoperiodic treatment has been applied, mimicking a long day (LD 18:6), a short day (LD 6:18) and a balanced light dark cycle (LD 12:12), as well as two constant conditions (DD, LL) to test for a potential endogenous control of rhythmic behavioral patterns in *C. finmarchicus* inhabiting high latitude regions. Rhythm analysis with the RAIN software has been applied to the data of each individual, checking for ~12 h and ~24 h periods in behavioral activity and data have been subsequently summarized with a focus on differences between stations and photoperiodic treatment, as well as the period of rhythmic behavior (Fig. 9).

Overall, the results show that irrespective of the percentage, the total number of copepods displaying rhythmic behavior is extremely low under both LD and constant conditions in the laboratory (Fig. 9). This may indicate a cessation of rhythmic behavioral activity during the period of minimal fluctuations in light (e.g. intensity and/or spectral composition) in *C. finmarchicus* inhabiting high latitudes, which is in light with previous findings, showing a cessation of synchronized DVM during the Arctic Summer (Blachowiak-Samolyk et al., 2006; Cottier et al., 2006; Wallace et al., 2010). However, Cottier et al. proposed that while DVM during the time of continuous light becomes

desynchronized within a population, it might still be present on an individual level, with animals undertaking multiple migrations to the surface layer during a day, driven by hunger and satiation as suggested before (Pearre, 2003). However, as these migrations are thought to be strongly influenced by exogenous cues (i.e. food availability), they are likely not visible in a laboratory set up where food is absent. Besides the overall low number of rhythmic copepods, our experiments showed that even clear LD conditions did not trigger a bigger number of copepods to display rhythmic activity synchronized to the provided LD cycle. A previous study showed strong indications for the involvement of a circadian clock in the regulation *C. finmarchicus* DVM (Häfker et al., 2017). Furthermore, recent experiments that observed the behavior of individual copepods in the utilized setup using video technique, revealed that animals exhibited a pronounced light avoidance reaction (i.e. negative phototaxis) under LD conditions (personal comm. Dr. Kim Last). It has thus been suggested, that under LD conditions the data are indicative of the photo responsiveness of the animals. Consequently, considering that patterns of clock gene expression discussed previously strongly suggest that the *C. finmarchicus* clock stays functional, the weak behavioral rhythms suggest 1) that the behavior is uncoupled from the clock during Midnight Sun (i.e. not under the control of the circadian clock) and/or 2) that the behavioral light avoidance response is reduced during Midnight Sun.

Performing behavioral experiments in a laboratory setting is a rather challenging task, as laboratory experiments are conducted under controlled conditions which makes them highly artificial. This holds especially true for experiments onboard research vessels, where the common difficulties are further challenged by the constrains of limited space and technical infrastructure, as well as increased potential for disturbance by vibrations or ship movement. Nevertheless, the experimental set up using adapted *Drosophila* locomotor activity monitors has proven to produce meaningful data in previous experiments both on land and at sea (personal comm. Dr. Kim Last).

4.7 What is the adaptive significance of a functional clock under constant conditions?

As discussed below, our behavioral screenings of *C. finmarchicus,* suggest that rhythmic behavioral activity, such as DVM, could be uncoupled from the clock during the Midnight Sun period at high latitudes. It is known from other organisms, especially in polar regions, that the circadian clock may get partly uncoupled from functional output (e.g. behavioral or physiological functions) during the absence of a clear light/dark cycle, but the underlying mechanisms are diverse (Bloch et al., 2013). Some of these are based on disrupted, non-rhythmic oscillation on the transcriptional level, where either clock gene transcription is literally paused and thus no endogenous oscillation is produced in the pacemaker cells, or clock gene oscillations are highly damped in amplitude, so that the rhythmic information is not strong enough to drive rhythmic clock output. Even a robust oscillation on the single cell level can result in a highly dampened signal, when multiple pacemaker cells are not synchronized among one another. In cases, where synchronized rhythmic endogenous oscillations are present, overt daily rhythmicity can still be absent by literally uncoupling the pacemaker unit from the respective centers that regulate the output (i.e. the rhythmic information does not reach the regulatory units), or masking effects (i.e. exogenous cues) can override the rhythmic information (Bloch et al., 2013). When speculating on the mechanisms that could cause a separation of the circadian clock from the behavioral output in *C. finmarchicus* during Midnight Sun conditions, the ongoing synchronized clock gene oscillations would suggest that either an uncoupling of the clock from the centers of locomotor control or masking by external factors, such as food availability, are responsible for the lack in rhythmic behavioral output. However, further studies on the molecular level of the circadian clock as well as further insights into potential clock controlled behavioral and physiological functions in *C. finmarchicus* are needed, to get a better idea of the mechanisms that underly the interactions of the circadian clock and the behavioral output.

In contrast to the underlying mechanism, the adaptive advantage of uncoupling the circadian clock from rhythmic behavioral output during the absence of a light dark cycle seems clear. The cessation of DVM would allow the organisms to stay in the upper surface layer to feed on phytoplankton, which could be especially important in Arctic

regions, where the productive season is short and its timing highly variable (Leu et al., 2006; Søreide, Leu, Berge, Graeve, & Falk-Petersen, 2010). In addition, the advantage of avoiding predators (generally accepted as the ultimate reason for DVM; e.g. Ringelberg & van Gool, 2003) by migrating to the surface at nighttime, disappears under absence of a pronounced light dark cycle. Thus, it seems of advantage to pause the energetically costly migration and stay at the surface to feed. Furthermore, hunger and satiation driven small scale DVM might decrease the amount of time spent in the illuminated surface layer and thus may reduce overall predation risk by visually hunting predators (Cottier et al., 2006).

On the other hand, an endogenous clock that stays functional for other outputs even in the absence of a clear light/dark cycle allows the organism to temporally orchestrate physiological functions internally, which is thought to be of great importance (Mermet, Yeung, & Naef, 2017; Mohawk, Green, & Takahashi, 2012; Panda et al., 2002). From the findings of this work, it could also be hypothesized, that an increase in ultradian oscillations of clock gene transcripts at the northern station and under sea ice represents an adaptation to the specific environment these organisms inhabit. It could for example allow organisms to adapt to a more frequent or more variable food input by adjusting the production of e.g. digestive enzymes to more than one active feeding phase per day.

In addition, as the circadian clock might be involved in the timing of seasonal events (Goto, 2013), like diapause initiation or termination, it could be essential to keep a functional clock throughout the active phase during Summer, to be able to track the season and prepare for diapause in time. Moreover, seasonal investigations of circadian clock gene expression in a *C. finmarchicus* population in Scotland showed that circadian clock gene expression was present throughout the active phase (Spring/Summer) but did not show changes in diel expression patterns that coincided with the seasonal change in photoperiod (Häfker, Teschke, Last, et al., 2018). It has therefore been proposed, that seasonal timing via the circadian clock in *C. finmarchicus* could be achieved by the “external coincidence” model (Bünning, 1960; Pittendrigh, 1960). This model is based on the assumption that a photosensitive phase in the morning or evening hours is used to determine the photoperiod and thus the progression of the season. In our study, clock gene expression patterns at station B13 under extreme photoperiods

generally resembled the patterns known from *C. finmarchicus* under shorter photoperiods at lower latitudes (LD 16:8, Scotland), thus, supporting the presence of a seasonal timing mechanism similar to the external coincidence model in *C. finmarchicus*. Furthermore, the analysis of clock gene expression in *C. finmarchicus* from an Arctic fjord showed that the clock is functional in late Summer, during the active phase and in a phase of early Diapause or preparation for Diapause (Häfker, Teschke, Hüppe, et al., 2018). However, clock genes do not oscillate during the period of Diapause itself. The present work can now add to the seasonal picture of clock functioning in *C. finmarchicus* at high latitudes and suggests, that the circadian clock is functional throughout the whole active phase, from early spring to autumn, including periods of Midnight Sun. This may further point out the importance of the circadian clock as a tool to track the progression of the season and help to time seasonal events, which is of fundamental importance for *C. finmarchicus* to survive in the extreme conditions of the Arctic (Søreide et al., 2010).

5 Summary and Outlook

The findings of this work strongly suggest that the circadian clock in *C. finmarchicus* stays functional throughout the period of Midnight Sun in the Arctic, despite the absence of light/dark alternations. The observed circadian oscillations in clock gene expression patterns in copepods from the southern Barents Sea indicate that even small diel fluctuations in the intensity or spectral composition of light are sufficient to entrain the *C. finmarchicus* circadian clock. The observed period shortening in clock gene expression at the northern station are associated with lower diel fluctuations in light and a sea ice cover. Three hypothesizes have been advanced to explain this increase of ultradian oscillations: a switch to an alternative *Zeitgeber*, a switch of the circadian mode, and a display of a free running mode.

To get a better understanding of the underlying mechanisms that control behavioral and physiological functions in *C. finmarchicus*, further experiments using e.g. chemical clock disruption are needed. In addition, monitoring the temporal change in clock gene protein products over daily cycles, would allow for a more detailed insight into the molecular mechanisms underlying the circadian clock in *C. finmarchicus*.

6 Bibliography

Abhilash, L., Shindey, R., & Sharma, V. K. (2017). To be or not to be rhythmic? A review of studies on organisms inhabiting constant environments. *Biological Rhythm Research*, *48*(5), 677–691. https://doi.org/10.1080/09291016.2017.1345426

Allada, R., & Chung, B. Y. (2010). Circadian Organization of Behavior and Physiology in *Drosophila*. *Annual Review of Physiology*, *72*, 605–624. https://doi.org/10.1146/annurev-physiol-021909-135815

Andersen, C. L., Jensen, J. L., & Ørntoft, T. F. (2004). Normalization of real-time quantitative reverse transcription-PCR data: A model-based variance estimation approach to identify genes suited for normalization, applied to bladder and colon cancer data sets. *Cancer Research*, *64*(15), 5245–5250. https://doi.org/10.1158/0008-5472.CAN-04-0496

Anderson, R. L., Watson, W. H., & Chabot, C. C. (2017). Local tidal regime dictates plasticity of expression of locomotor activity rhythms of American horseshoe crabs, Limulus polyphemus. *Marine Biology*, *164*. https://doi.org/10.1007/s00227-017-3098-9

Archibald, K. M., Siegel, D. A., & Doney, S. C. (2019). Modeling the Impact of Zooplankton Diel Vertical Migration on the Carbon Export Flux of the Biological Pump. *Global Biogeochemical Cycles*, *33*(2), 181–199. https://doi.org/10.1029/2018GB005983

Arnold, W., Ruf, T., Loe, L. E., Irvine, R. J., Ropstad, E., Veiberg, V., & Albon, S. D. (2018). Circadian rhythmicity persists through the Polar night and midnight sun in Svalbard reindeer. *Scientific Reports*, *8*(1), 1–12. https://doi.org/10.1038/s41598-018-32778-4

Årthun, M., Eldevik, T., Smedsrud, L. H., Skagseth, Ø., & Ingvaldsen, R. B. (2012). Quantifying the Influence of Atlantic Heat on Barents Sea Ice Variability and Retreat. *Journal of Climate*, *25*(13), 4736–4743. https://doi.org/10.1175/JCLI-D-11-00466.1

Aschoff, J. (1954). Zeitgeber der tierischen Tagesperiodik. *Naturwissenschaften*, *41*(3), 49–56. Retrieved from http://www.springerlink.com/index/T1X1X43460N4152J.pdf

Aschoff, J. (1960). Exogenous and Endogenous Components in Circadian Rhythms. *Cold Spring Harbor Symposia on Quantitative Biology*, *25*, 11–28. https://doi.org/10.1101/SQB.1960.025.01.004

Aumont, O., Maury, O., Lefort, S., & Bopp, L. (2018). Evaluating the Potential Impacts of the Diurnal Vertical Migration by Marine Organisms on Marine Biogeochemistry. *Global Biogeochemical Cycles*. https://doi.org/10.1029/2018GB005886

Bae, K., & Edery, I. (2006). Regulating a circadian clock's period, phase and amplitude by phosphorylation: Insights from Drosophila. *Journal of Biochemistry*, *140*(5), 609–617. https://doi.org/10.1093/jb/mvj198

Båtnes, A. S., Miljeteig, C., Berge, J., Greenacre, M., & Johnsen, G. (2015). Quantifying the light sensitivity of Calanus spp. during the polar night: Potential for orchestrated migrations conducted by ambient light from the sun, moon, or aurora borealis? *Polar Biology*, *38*(1), 51–65. https://doi.org/10.1007/s00300-013-1415-4

Baumgartner, M. F., Cole, T. V. N., Campbell, R. G., Teegarden, G. J., & Durbin, E. G. (2003). Associations between North Atlantic right whales and their prey, *Calanus finmarchicus*, over diel and tidal time scales. *Marine Ecology Progress Series*, *264*, 155–166. Retrieved from http://www.int-res.com/abstracts/meps/v264/p155-166/

Baumgartner, M. F., & Tarrant, A. M. (2017). The Physiology and Ecology of Diapause in Marine Copepods. *Annual Review of Marine Science*, *9*(1), 387–411. https://doi.org/10.1146/annurev-marine-010816-060505

Beaugrand, G., & Kirby, R. R. (2010). Climate, plankton and cod. *Global Change Biology*, *16*(4), 1268–1280. https://doi.org/10.1111/j.1365-2486.2009.02063.x

Benjamini, Y., & Hochberg, Y. (1995). Controlling the False Discovery Rate: A Practical and Powerful Approach to Multiple Testing. *Journal of the Royal Statistical Society. Series B (Methodological)*, *57*(1), 289–300. Retrieved from https://www.jstor.org/stable/2346101

Biscontin, A., Martini, P., Costa, R., Kramer, A., Meyer, B., Kawaguchi, S., … Pittà, C. D. (2019). Analysis of the circadian transcriptome of the Antarctic krill Euphausia superba. *Scientific Reports*, *9*(1), 1–11. https://doi.org/10.1038/s41598-019-50282-1

Biscontin, A., Wallach, T., Sales, G., Grudziecki, A., Janke, L., Sartori, E., … Costa, R. (2017). Functional characterization of the circadian clock in the Antarctic krill, Euphausia superba. *Scientific Reports*, *7*(1), 1–13. https://doi.org/10.1038/s41598-017-18009-2

Blachowiak-Samolyk, K., Kwasniewski, S., Richardson, K., Dmoch, K., Hansen, E., Hop, H., … Mouritsen, L. (2006). Arctic zooplankton do not perform diel vertical migration (DVM) during periods of midnight sun. *Marine Ecology Progress Series*, *308*, 101–116. https://doi.org/10.3354/meps308101

Bloch, G. (2010). The social clock of the honeybee. *Journal of Biological Rhythms*, *25*(5), 307–317. https://doi.org/10.1177/0748730410380149

Bloch, G., Barnes, B. M., Gerkema, M. P., & Helm, B. (2013). Animal activity around the clock with no overt circadian rhythms: Patterns, mechanisms and adaptive value. *Proceedings of the Royal Society B: Biological Sciences*, *280*(1765), 20130019. https://doi.org/10.1098/rspb.2013.0019

Bolliet, V., & Labonne, J. (2008). Individual patterns of rhythmic swimming activity in Anguilla anguilla glass eels synchronised to water current reversal. *Journal of Experimental Marine Biology and Ecology*, *362*(2), 125–130. https://doi.org/10.1016/j.jembe.2008.06.017

Bradshaw, W. E., & Holzapfel, C. M. (2007). Evolution of Animal Photoperiodism. *Annual Review of Ecology, Evolution, and Systematics*, *38*(1), 1–25. https://doi.org/10.1146/annurev.ecolsys.37.091305.110115

Brown, F. A., Fingerman, M., Sandeen, M. I., & Webb, H. M. (1953). Persistent diurnal and tidal rhythms of color change in the fiddler crab, Uca pugnax. *Journal of Experimental Zoology*, *123*(1), 29–60. https://doi.org/10.1002/jez.1401230103

Bünning, E. (1960). Circadian Rhythms and the Time Measurement in Photoperiodism. *Cold Spring Harbor Symposia on Quantitative Biology*, *25*, 249–256. https://doi.org/10.1101/SQB.1960.025.01.026

Caress, D. W., & Chayes, D. N. (2016). MB-System Version 5.5.2284. Open source software distributed from the MBARI and L-DEO web sites (Version 5.5.2284).

Carmack, E., Polyakov, I., Padman, L., Fer, I., Hunke, E., Hutchings, J., … Winsor, P. (2015). Toward Quantifying the Increasing Role of Oceanic Heat in Sea Ice Loss in the

New Arctic. *Bulletin of the American Meteorological Society*, *96*(12), 2079–2105. https://doi.org/10.1175/BAMS-D-13-00177.1

Castellana, S., Mazza, T., Capocefalo, D., Genov, N., Biagini, T., Fusilli, C., … Mazzoccoli, G. (2018). Systematic Analysis of Mouse Genome Reveals Distinct Evolutionary and Functional Properties Among Circadian and Ultradian Genes. *Frontiers in Physiology*, *9*. https://doi.org/10.3389/fphys.2018.01178

Chen, Y.-G., Mantalaris, A., Bourne, P., Keng, P., & Wu, J. H. D. (2000). Expression of mPer1 and mPer2, Two Mammalian Clock Genes, in Murine Bone Marrow. *Biochemical and Biophysical Research Communications*, *276*(2), 724–728. https://doi.org/10.1006/bbrc.2000.3536

Chittka, L., Stelzer, R. J., & Stanewsky, R. (2013). Daily Changes in Ultraviolet Light Levels Can Synchronize the Circadian Clock of Bumblebees (Bombus terrestris). *Chronobiology International*, *30*(4), 434–442. https://doi.org/10.3109/07420528.2012.741168

Choquet, M., Hatlebakk, M., Dhanasiri, A. K. S., Kosobokova, K., Smolina, I., Søreide, J. E., … Hoarau, G. (2017). Genetics redraws pelagic biogeography of Calanus. *Biology Letters*, *13*(12), 20170588. https://doi.org/10.1098/rsbl.2017.0588

Christie, A. E., Fontanilla, T. M., Nesbit, K. T., & Lenz, P. H. (2013a). Prediction of the protein components of a putative *Calanus finmarchicus* (Crustacea, Copepoda) circadian signaling system using a de novo assembled transcriptome. *Comparative Biochemistry and Physiology Part D: Genomics and Proteomics*, *8*(3), 165–193. https://doi.org/10.1016/j.cbd.2013.04.002

Christie, A. E., Fontanilla, T. M., Nesbit, K. T., & Lenz, P. H. (2013b). Prediction of the protein components of a putative Calanus finmarchicus (Crustacea, Copepoda) circadian signaling system using a de novo assembled transcriptome. *Comparative Biochemistry and Physiology Part D: Genomics and Proteomics*, *8*(3), 165–193. https://doi.org/10.1016/j.cbd.2013.04.002

Conover, R. J. (1988). Comparative life histories in the genera Calanus and Neocalanus in high latitudes of the northern hemisphere. *Hydrobiologia*, (167/168), 127–142.

Conover, R. J., Herman, A. W., Prinsenberg, S. J., & Harris, L. R. (1986). Distribution of and Feeding by the Copepod Pseudocalanus Under Fast Ice During the Arctic

Spring. *Science*, *232*(4755), 1245–1247. https://doi.org/10.1126/science.232.4755.1245

Cottier, F. (2019). *JR17006 Cruise Report, RRS James Clark Ross, 11 June—6 July 2018, Changing Arctic Ocean* [Cruise Report]. Retrieved from British Oceanographic Data Centre website: https://www.bodc.ac.uk/resources/inventories/cruise_inventory/reports/jr17006.pdf

Cottier, F. R., Tarling, G. A., Wold, A., & Falk-Petersen, S. (2006). Unsynchronised and synchronised vertical migration of zooplankton in a high Arctic fjord. *Limnology and Oceanography*, *51*(6), 2586–2599. https://doi.org/10.4319/lo.2006.51.6.2586

Cretenet, G., Le Clech, M., & Gachon, F. (2010). Circadian Clock-Coordinated 12 Hr Period Rhythmic Activation of the IRE1α Pathway Controls Lipid Metabolism in Mouse Liver. *Cell Metabolism*, *11*(1), 47–57. https://doi.org/10.1016/j.cmet.2009.11.002

Dale, T., & Kaartvedt, S. (2000). Diel patterns in stage-specific vertical migration of Calanus finmarchicus in habitats with midnight sun. *ICES Journal of Marine Science: Journal Du Conseil*, *57*(6), 1800–1818. https://doi.org/10.1006/jmsc.2000.0961

Dalpadado, P., Ellertsen, B., Melle, W., & Dommasnes, A. (2000). Food and feeding conditions of Norwegian spring-spawning herring (Clupea harengus) through its feeding migrations. *ICES Journal of Marine Science: Journal Du Conseil*, *57*(4), 843–857. https://doi.org/10.1006/jmsc.2000.0573

Darnis, G., Hobbs, L., Geoffroy, M., Grenvald, J. C., Renaud, P. E., Berge, J., … Gabrielsen, T. (2017). From polar night to midnight sun: Diel vertical migration, metabolism and biogeochemical role of zooplankton in a high Arctic fjord (Kongsfjorden, Svalbard): Zooplankton migration and biogeochemical fluxes. *Limnology and Oceanography*, *62*(4), 1586–1605. https://doi.org/10.1002/lno.10519

De Pittà, C., Biscontin, A., Albiero, A., Sales, G., Millino, C., Mazzotta, G. M., … Costa, R. (2013). The Antarctic Krill *Euphausia superba* Shows Diurnal Cycles of Transcription under Natural Conditions. *PLoS One*, *8*(7), e68652. https://doi.org/10.1371/journal.pone.0068652

Doherty, C. J., & Kay, S. A. (2010). Circadian Control of Global Gene Expression Patterns. *Annual Review of Genetics*, *44*(1), 419–444. https://doi.org/10.1146/annurev-genet-102209-163432

Dunlap, Jay C. (1999). *Molecular Bases for Circadian Clocks*. *96*(2), 271–290. https://doi.org/10.1016/S0092-8674(00)80566-8

Dunlap, Jay C., & Loros, J. J. (2016). Yes, circadian rhythms actually do affect almost everything. *Cell Research*, *26*(7), 759–760. https://doi.org/10.1038/cr.2016.65

Durbin, E. G., Garrahan, P. R., & Casas, M. C. (2000). Abundance and distribution of *Calanus finmarchicus* on the Georges Bank during 1995 and 1996. *ICES Journal of Marine Science: Journal Du Conseil*, *57*(6), 1664–1685. https://doi.org/10.1006/jmsc.2000.0974

Egbert, G. D., & Erofeeva, S. Y. (2002). Efficient Inverse Modeling of Barotropic Ocean Tides. *Journal of Atmospheric and Oceanic Technology*, *19*(2), 183–204. https://doi.org/10.1175/1520-0426(2002)019<0183:EIMOBO>2.0.CO;2

El-Athman, R., Knezevic, D., Fuhr, L., & Relógio, A. (2019). A Computational Analysis of Alternative Splicing across Mammalian Tissues Reveals Circadian and Ultradian Rhythms in Splicing Events. *International Journal of Molecular Sciences*, *20*(16), 3977. https://doi.org/10.3390/ijms20163977

Emerson, K. J., Bradshaw, W. E., & Holzapfel, C. M. (2008). Concordance of the Circadian Clock with the Environment Is Necessary to Maximize Fitness in Natural Populations. *Evolution*, *62*(4), 979–983. https://doi.org/10.1111/j.1558-5646.2008.00324.x

Enright, J. T. (1976). Plasticity in an isopod's clockworks: Shaking shapes form and affects phase and frequency. *Journal of Comparative Physiology ? A*, *107*(1), 13–37. https://doi.org/10.1007/BF00663916

Falkenhaug, T., Tande, K., & Semenova, T. (1997). Diel, seasonal and ontogenetic variations in the vertical distributions of four marine copepods. *Marine Ecology Progress Series*, *149*, 105–119. https://doi.org/10.3354/meps149105

Falk-Petersen, S., Mayzaud, P., Kattner, G., & Sargent, J. R. (2009). Lipids and life strategy of Arctic Calanus. *Marine Biology Research*, *5*(1), 18–39. https://doi.org/10.1080/17451000802512267

Falk-Petersen, S., Pavlov, V., Timofeev, S., & Sargent, J. R. (2007). Climate variability and possible effects on arctic food chains: The role of *Calanus*. In *Arctic alpine ecosystems and people in a changing environment* (pp. 147–166). Retrieved from http://link.springer.com/chapter/10.1007/978-3-540-48514-8_9

Fortier, M. (2001). Visual predators and the diel vertical migration of copepods under Arctic sea ice during the midnight sun. *Journal of Plankton Research*, *23*(11), 1263–1278. https://doi.org/10.1093/plankt/23.11.1263

Forward, R. B., Thaler, A. D., & Singer, R. (2007). Entrainment of the activity rhythm of the mole crab Emerita talpoida. *Journal of Experimental Marine Biology and Ecology*, *341*(1), 10–15. https://doi.org/10.1016/j.jembe.2006.10.050

Goldman, B., Gwinner, E., Karsch, F. J., Saunders, D., Zucker, I., & Gall, G. F. (2004). Circannual Rhythms and Photoperiodism. In J. C. Dunlap, J. J. Loros, & P. J. DeCoursey (Eds.), *Chronobiology: Biological timekeeping* (pp. 107–142). Sunderland, MA: Sinauer.

Goto, S. G. (2013). Roles of circadian clock genes in insect photoperiodism. *Entomological Science*, *16*(1), 1–16. https://doi.org/10.1111/ens.12000

Grima, B., Chélot, E., Xia, R., & Rouyer, F. (2004). Morning and evening peaks of activity rely on different clock neurons of the Drosophila brain. *Nature*, *431*(7010), 869–873. https://doi.org/10.1038/nature02935

Grosfeld, K., Treffeisen, R., Asseng, J., Bartsch, A., Bräuer, B., Fritzsch, B., … Weigelt, M. (2016). *Online Sea-Ice Knowledge and Data Platform*. https://doi.org/10.2312/polfor.2016.011

Häfker, N. S. (2018). *The molecular basis of diel and seasonal rhythmicity in the copepod Calanus finmarchicus* (Dissertation). University of Oldenburg, Germany.

Häfker, N. S., Meyer, B., Last, K. S., Pond, D. W., Hüppe, L., & Teschke, M. (2017). Circadian Clock Involvement in Zooplankton Diel Vertical Migration. *Current Biology*, *27*(14), 2194-2201.e3. https://doi.org/10.1016/j.cub.2017.06.025

Häfker, N. S., Teschke, M., Hüppe, L., & Meyer, B. (2018). Calanus finmarchicus diel and seasonal rhythmicity in relation to endogenous timing under extreme polar photoperiods. *Marine Ecology Progress Series*, *603*, 79–92. https://doi.org/10.3354/meps12696

Häfker, N. S., Teschke, M., Last, K. S., Pond, D. W., Hüppe, L., & Meyer, B. (2018). *Calanus finmarchicus* seasonal cycle and diapause in relation to gene expression, physiology, and endogenous clocks: Calanus finmarchicus *seasonal rhythmicity*. *Limnology and Oceanography*. https://doi.org/10.1002/lno.11011

Harris, R. P., Irigoien, X., Head, R. N., Rey, C., Hygum, B. H., Hansen, B. W., … Carlotti, F. (2000). Feeding, growth, and reproduction in the genus *Calanus*. *ICES Journal of Marine Science*, *57*(6), 1708–1726. https://doi.org/10.1006/jmsc.2000.0959

Hastings, M. H. (1981). The entraining effect of turbulence on the circa-tidal activity rhythm and its semi-lunar modulation in Eurydice pulchra. *Journal of the Marine Biological Association of the United Kingdom*, *61*(1), 151–160. https://doi.org/10.1017/S0025315400045987

Hays, G. C. (2003). A review of the adaptive significance and ecosystem consequences of zooplankton diel vertical migrations. In *Migrations and Dispersal of Marine Organisms* (pp. 163–170). Springer.

Heath, M. R., Boyle, P. R., Gislason, A., Gurney, W. S. C., Hay, S. J., Head, E. J. H., … Speirs, D. (2004). Comparative ecology of over-wintering Calanus finmarchicus in the northern North Atlantic, and implications for life-cycle patterns. *ICES Journal of Marine Science*, *61*(4), 698–708. https://doi.org/10.1016/j.icesjms.2004.03.013

Hirche, Hans-Jürgen, & Kosobokova, K. (2007). Distribution of Calanus finmarchicus in the northern North Atlantic and Arctic Ocean—Expatriation and potential colonization. *Deep Sea Research Part II: Topical Studies in Oceanography*, *54*(23–26), 2729–2747. https://doi.org/10.1016/j.dsr2.2007.08.006

Hirche, H.-J. (1996a). Diapause in the marine copepod, Calanus finmarchicus—A review. *Ophelia*, *44*(1–3), 129–143.

Hirche, H.-J. (1996b). The reproductive biology of the marine copepod, Calanus finmarchicus—A review. *Ophelia*, *44*(1–3), 111–128.

Hirche, H.-J., & Kosobokova, K. (2007). Distribution of Calanus finmarchicus in the northern North Atlantic and Arctic Ocean—Expatriation and potential colonization. *Deep Sea Research Part II: Topical Studies in Oceanography*, *54*(23–26), 2729–2747. https://doi.org/10.1016/j.dsr2.2007.08.006

Hughes, M. E., DiTacchio, L., Hayes, K. R., Vollmers, C., Pulivarthy, S., Baggs, J. E., … Hogenesch, J. B. (2009). Harmonics of circadian gene transcription in mammals. *PLoS Genetics*, *5*(4), e1000442. https://doi.org/10.1371/journal.pgen.1000442

Hughes, M. E., Hong, H.-K., Chong, J. L., Indacochea, A. A., Lee, S. S., Han, M., … Hogenesch, J. B. (2012). Brain-Specific Rescue of Clock Reveals System-Driven Transcriptional Rhythms in Peripheral Tissue. *PLOS Genetics*, *8*(7), e1002835. https://doi.org/10.1371/journal.pgen.1002835

Hut, R. A., Paolucci, S., Dor, R., Kyriacou, C. P., & Daan, S. (2013). Latitudinal clines: An evolutionary view on biological rhythms. *Proceedings of the Royal Society B: Biological Sciences*, *280*(1765), 20130433–20130433. https://doi.org/10.1098/rspb.2013.0433

Ingvarsdóttir, A., Houlihan, D. f., Heath, M. r., & Hay, S. j. (1999). Seasonal changes in respiration rates of copepodite stage V *Calanus finmarchicus* (Gunnerus). *Fisheries Oceanography*, *8*, 73–83. https://doi.org/10.1046/j.1365-2419.1999.00002.x

Kobelkova, A., Goto, S. G., Peyton, J. T., Ikeno, T., Lee, R. E., & Denlinger, D. L. (2015). Continuous activity and no cycling of clock genes in the Antarctic midge during the polar summer. *Journal of Insect Physiology*, *81*, 90–96. https://doi.org/10.1016/j.jinsphys.2015.07.008

Kohsaka, A., Laposky, A. D., Ramsey, K. M., Estrada, C., Joshu, C., Kobayashi, Y., … Bass, J. (2007). High-Fat Diet Disrupts Behavioral and Molecular Circadian Rhythms in Mice. *Cell Metabolism*, *6*(5), 414–421. https://doi.org/10.1016/j.cmet.2007.09.006

Kraft, A., Berge, J., Varpe, Ø., & Falk-Petersen, S. (2013). Feeding in Arctic darkness: Mid-winter diet of the pelagic amphipods *Themisto abyssorum* and *T. libellula*. *Marine Biology*, *160*(1), 241–248. https://doi.org/10.1007/s00227-012-2065-8

Kuhlman, S. J., Mackey, S. R., & Duffy, J. F. (2007). *Biological Rhythms Workshop I: introduction to chronobiology*. *72*, 1–6. Cold Spring Harbor Laboratory Press.

Kuhlman, Sandra J., Craig, L. M., & Duffy, J. F. (2017). Introduction to Chronobiology. *Cold Spring Harbor Perspectives in Biology*, a033613. https://doi.org/10.1101/cshperspect.a033613

Kvile, K. Ø., Fiksen, Ø., Prokopchuk, I., & Opdal, A. F. (2017). Coupling survey data with drift model results suggests that local spawning is important for Calanus finmarchicus production in the Barents Sea. *Journal of Marine Systems*, *165*, 69–76. https://doi.org/10.1016/j.jmarsys.2016.09.010

Kvingedal, B. (2005). Sea-Ice Extent and Variability in the Nordic Seas, 1967—2002. *The Nordic Seas: An Integrated Perspective*, 39–49. https://doi.org/10.1029/158GM04

Lamba, P., Bilodeau-Wentworth, D., Emery, P., & Zhang, Y. (2014). Morning and Evening Oscillators Cooperate to Reset Circadian Behavior in Response to Light Input. *Cell Reports*, *7*(3), 601–608. https://doi.org/10.1016/j.celrep.2014.03.044

Lenz, P. H., Roncalli, V., Hassett, R. P., Wu, L.-S., Cieslak, M. C., Hartline, D. K., & Christie, A. E. (2014). De Novo Assembly of a Transcriptome for Calanus finmarchicus (Crustacea, Copepoda) – The Dominant Zooplankter of the North Atlantic Ocean. *PLOS ONE*, *9*(2), e88589. https://doi.org/10.1371/journal.pone.0088589

Leu, E., Falk-Petersen, S., Kwaśniewski, S., Wulff, A., Edvardsen, K., & Hessen, D. O. (2006). Fatty acid dynamics during the spring bloom in a High Arctic fjord: Importance of abiotic factors versus community changes. *Canadian Journal of Fisheries and Aquatic Sciences*, *63*(12), 2760–2779. https://doi.org/10.1139/f06-159

Lincoln, G. (2019). A brief history of circannual time. *Journal of Neuroendocrinology*, *31*(3), e12694. https://doi.org/10.1111/jne.12694

Lind, S., Ingvaldsen, R. B., & Furevik, T. (2018). Arctic warming hotspot in the northern Barents Sea linked to declining sea-ice import. *Nature Climate Change*, *8*(7), 634–639. https://doi.org/10.1038/s41558-018-0205-y

Liu, S., Cai, Y., Sothern, R. B., Guan, Y., & Chan, P. (2007). Chronobiological Analysis of Circadian Patterns in Transcription of Seven Key Clock Genes in Six Peripheral Tissues in Mice. *Chronobiology International*, *24*(5), 793–820. https://doi.org/10.1080/07420520701672556

Livak, K. J., & Schmittgen, T. D. (2001). Analysis of relative gene expression data using real-time quantitative PCR and the 2(-Delta Delta C(T)) Method. *Methods (San Diego, Calif.)*, *25*(4), 402–408. https://doi.org/10.1006/meth.2001.1262

Loeng, H. (1991). Features of the physical oceanographic conditions of the Barents Sea. *Polar Research*, *10*(1), 5–18. https://doi.org/10.3402/polar.v10i1.6723

Mackey, S. R. (2007). *Biological Rhythms Workshop IA: Molecular Basis of Rhythms Generation*. *72*, 7–19. https://doi.org/10.1101/sqb.2007.72.060

MDL. (2015). *Documentation for running Normfinder in R* [Online]. Retrieved from Molecular Diagnostic Laboratory, Dept. Of Molecular Medicine, Aarhus University Hospital website: https://moma.dk/files/newDocOldStab_v5.pdf

Melle, W., Runge, J., Head, E., Plourde, S., Castellani, C., Licandro, P., … Chust, G. (2014). The North Atlantic Ocean as habitat for Calanus finmarchicus: Environmental factors and life history traits. *Progress in Oceanography*, *129*, 244–284. https://doi.org/10.1016/j.pocean.2014.04.026

Merlin, C., Gegear, R. J., & Reppert, S. M. (2009). Antennal circadian clocks coordinate sun compass orientation in migratory monarch butterflies. *Science*, *325*(5948), 1700–1704. https://doi.org/10.1126/science.1176221

Mermet, J., Yeung, J., & Naef, F. (2017). Systems Chronobiology: Global Analysis of Gene Regulation in a 24-Hour Periodic World. *Cold Spring Harbor Perspectives in Biology*, *9*(3), a028720. https://doi.org/10.1101/cshperspect.a028720

Mohawk, J. A., Green, C. B., & Takahashi, J. S. (2012). Central and Peripheral Circadian Clocks in Mammals. *Annual Review of Neuroscience*, *35*(1), 445–462. https://doi.org/10.1146/annurev-neuro-060909-153128

Muskus, M. J., Preuss, F., Fan, J.-Y., Bjes, E. S., & Price, J. L. (2007). Drosophila DBT lacking protein kinase activity produces long-period and arrhythmic circadian behavioral and molecular rhythms. *Molecular and Cellular Biology*, *27*(23), 8049–8064. https://doi.org/10.1128/MCB.00680-07

Naylor, E. (1958). Tidal and diurnal rhythms of locomotory activity in Carcinus maenas. *Journal of Experimental Biology*, *35*, 602–610.

Naylor, E. (1996). Crab Clockwork: The Case for Interactive Circatidal and Circadian Oscillators Controlling Rhythmic Locomotor Activity of Carcinus Maenas. *Chronobiology International*, *13*(3), 153–161. https://doi.org/10.3109/07420529609012649

Niehoff, B., & Hirche, H.-J. (2000). The reproduction of Calanus finmarchicus in the Norwegian Sea in spring. *Sarsia*, (85), 15–22.

Niehoff, Barbara, Klenke, U., Hirche, H.-J., Irigoien, X., Head, R., & Harris, R. (1999). A high frequency time series at Weathership M, Norwegian Sea, during the 1997 spring bloom: The reproductive biology of Calanus finmarchicus. *Marine Ecology Progress Series*, *176*, 81–92. https://doi.org/10.3354/meps176081

Nielsen, T. G., Kjellerup, S., Smolina, I., Hoarau, G., & Lindeque, P. (2014). Live discrimination of Calanus glacialis and C. finmarchicus females: Can we trust phenological differences? *Marine Biology*, *161*(6), 1299–1306. https://doi.org/10.1007/s00227-014-2419-5

Onarheim, I. H., Eldevik, T., Smedsrud, L. H., & Stroeve, J. C. (2018). Seasonal and Regional Manifestation of Arctic Sea Ice Loss. *Journal of Climate*, *31*(12), 4917–4932. https://doi.org/10.1175/JCLI-D-17-0427.1

Palmer, J. D. (1995). Review of the Dual-Clock Control of Tidal Rhythms and the Hypothesis that the Same Clock Governs Both Circatidal and Circadian Rhythms. *Chronobiology International*, *12*(5), 299–310. https://doi.org/10.3109/07420529509057279

Panda, S., Antoch, M. P., Miller, B. H., Su, A. I., Schook, A. B., Straume, M., … Hogenesch, J. B. (2002). Coordinated Transcription of Key Pathways in the Mouse by the Circadian Clock. *Cell*, *109*(3), 307–320. https://doi.org/10.1016/S0092-8674(02)00722-5

Parkinson, C. L., & Cavalieri, D. J. (2008). Arctic sea ice variability and trends, 1979–2006. *Journal of Geophysical Research: Oceans*, *113*(C7). https://doi.org/10.1029/2007JC004558

Payton, L., Perrigault, M., Hoede, C., Massabuau, J.-C., Sow, M., Huvet, A., … Tran, D. (2017). Remodeling of the cycling transcriptome of the oyster Crassostrea gigas by the harmful algae Alexandrium minutum. *Scientific Reports*, *7*(1). https://doi.org/10.1038/s41598-017-03797-4

Pearre, S. (2003). Eat and run? The hunger/satiation hypothesis in vertical migration: history, evidence and consequences. *Biological Reviews*, *78*(01), 1–79. https://doi.org/10.1017/S146479310200595X

Perkins, J. R., Dawes, J. M., McMahon, S. B., Bennett, D. L., Orengo, C., & Kohl, M. (2012). ReadqPCR and NormqPCR: R packages for the reading, quality checking and

normalisation of RT-qPCR quantification cycle (Cq) data. *BMC Genomics*, *13*(1), 296. https://doi.org/10.1186/1471-2164-13-296

Pfaffl, M. W., Tichopad, A., Prgomet, C., & Neuvians, T. P. (2004). Determination of stable housekeeping genes, differentially regulated target genes and sample integrity: BestKeeper – Excel-based tool using pair-wise correlations. *Biotechnology Letters*, *26*(6), 509–515. https://doi.org/10.1023/B:BILE.0000019559.84305.47

Piccolin, F., Meyer, B., Biscontin, A., De Pittà, C., Kawaguchi, S., & Teschke, M. (2018). Photoperiodic modulation of circadian functions in Antarctic krill Euphausia superba Dana, 1850 (Euphausiacea). *Journal of Crustacean Biology*, *38*(6), 707–715. https://doi.org/10.1093/jcbiol/ruy035

Pittendrigh, C. S. (1960). Circadian Rhythms and the Circadian Organization of Living Systems. *Cold Spring Harbor Symposia on Quantitative Biology*, *25*, 159–184. https://doi.org/10.1101/SQB.1960.025.01.015

Pittendrigh, C. S., & Daan, S. (1976). A Functional Analysis of Circadian Pacemakers in Nocturnal Rodents. IV. Entrainment: Pacemaker as Clock. *Journal of Comparative Physiology A*, *106*(3), 291–331. https://doi.org/10.1007/BF01417856

R Core Team. (2019). *R: A language and environment for statistical computing.* Retrieved from https://www.R-project.org/

Ramsey, K. M., Yoshino, J., Brace, C. S., Abrassart, D., Kobayashi, Y., Marcheva, B., … Bass, J. (2009). Circadian Clock Feedback Cycle Through NAMPT-Mediated NAD+ Biosynthesis. *Science*, *324*(5927), 651–654. https://doi.org/10.1126/science.1171641

Rensing, L., & Ruoff, P. (2002). Temperature Effect on Entrainment, Phase Shifting, and Amplitude of Circadian Clocks and Its Molecular Bases. *Chronobiology International*, *19*(5), 807–864. https://doi.org/10.1081/CBI-120014569

Reppert, S. M. (2007). The ancestral circadian clock of monarch butterflies: Role in time-compensated sun compass orientation. *Cold Spring Harbor Symposia on Quantitative Biology*, *72*, 113–118. https://doi.org/10.1101/sqb.2007.72.056

Reygondeau, G., & Beaugrand, G. (2011). Future climate-driven shifts in distribution of Calanus finmarchicus. *Global Change Biology*, *17*(2), 756–766. https://doi.org/10.1111/j.1365-2486.2010.02310.x

Ringelberg, J., & van Gool, E. (2003). On the combined analysis of proximate and ultimate aspects in diel vertical migration (DVM) research. *Hydrobiologia*, *491*, 85–90.

Rubin, E. B., Shemesh, Y., Cohen, M., Elgavish, S., Robertson, H. M., & Bloch, G. (2006). Molecular and phylogenetic analyses reveal mammalian-like clockwork in the honey bee (*Apis mellifera*) and shed new light on the molecular evolution of the circadian clock. *Genome Research*, *16*(11), 1352–1365. https://doi.org/10.1101/gr.5094806

Saikkonen, K., Taulavuori, K., Hyvönen, T., Gundel, P. E., Hamilton, C. E., Vänninen, I., … Helander, M. (2012). Climate change-driven species' range shifts filtered by photoperiodism. *Nature Climate Change*, *2*(4), 239–242. https://doi.org/10.1038/nclimate1430

Satoh, A., Yoshioka, E., & Numata, H. (2008). Circatidal activity rhythm in the mangrove cricket Apteronemobius asahinai. *Biology Letters*, *4*(3), 233–236. https://doi.org/10.1098/rsbl.2008.0036

Schoenle, A. (2015). *Time to (dia)pause—Clock gene expression patterns in the calanoid copepod Calanus finmarchicus during early and late diapause* (Master Thesis). University of Bremen.

Silver, N., Best, S., Jiang, J., & Thein, S. L. (2006). Selection of housekeeping genes for gene expression studies in human reticulocytes using real-time PCR. *BMC Molecular Biology*, *7*, 33. https://doi.org/10.1186/1471-2199-7-33

Skaret, G., Dalpadado, P., Hjøllo, S. S., Skogen, M. D., & Strand, E. (2014). Calanus finmarchicus abundance, production and population dynamics in the Barents Sea in a future climate. *Progress in Oceanography*, *125*, 26–39. https://doi.org/10.1016/j.pocean.2014.04.008

Søreide, J. E., Leu, E., Berge, J., Graeve, M., & Falk-Petersen, S. (2010). Timing of blooms, algal food quality and Calanus glacialis reproduction and growth in a changing Arctic. *Global Change Biology*, *16*(11), 3154–3163. https://doi.org/10.1111/j.1365-2486.2010.02175.x

Steen, H., Vogedes, D., Broms, F., Falk-Petersen, S., & Berge, J. (2007). Little auks (*Alle alle*) breeding in a High Arctic fjord system: Bimodal foraging strategies as a

response to poor food quality? *Polar Research*, *26*(2), 118–125. https://doi.org/10.1111/j.1751-8369.2007.00022.x

Stelzer, R. J., & Chittka, L. (2010). Bumblebee foraging rhythms under the midnight sun measured with radiofrequency identification. *BMC Biology*, *8*(1), 93. https://doi.org/10.1186/1741-7007-8-93

Sundby, S. (2000). Recruitment of Atlantic cod stocks in relation to temperature and advection of copepod populations. *Sarsia*, *85*, 277–298. Retrieved from http://bio.uib.no/sarsia/PDF/85(4)1.pdf

Takahashi, J. S. (2017). Transcriptional architecture of the mammalian circadian clock. *Nature Reviews Genetics*, *18*(3), 164–179. https://doi.org/10.1038/nrg.2016.150

Takekata, H., Matsuura, Y., Goto, S. G., Satoh, A., & Numata, H. (2012). RNAi of the circadian clock gene period disrupts the circadian rhythm but not the circatidal rhythm in the mangrove cricket. *Biology Letters*, *8*(4), 488–491. https://doi.org/10.1098/rsbl.2012.0079

Tande, K. S., & Slagstad, D. (1982). Ecological investigation on the zooplankton community of Balsfjorden, northern Norway. *Sarsia*, *67*(1), 63–68.

Tataroglu, O., Zhao, X., Busza, A., Ling, J., O'Neill, J. S., & Emery, P. (2015). Calcium and SOL Protease Mediate Temperature Resetting of Circadian Clocks. *Cell*, *163*(5), 1214–1224. https://doi.org/10.1016/j.cell.2015.10.031

Teschke, M., Wendt, S., Kawaguchi, S., Kramer, A., & Meyer, B. (2011). A Circadian Clock in Antarctic Krill: An Endogenous Timing System Governs Metabolic Output Rhythms in the Euphausid Species Euphausia superba. *PLoS ONE*, *6*(10), e26090. https://doi.org/10.1371/journal.pone.0026090

Tessmar-Raible, K., Raible, F., & Arboleda, E. (2011). Another place, another timer: Marine species and the rhythms of life. *BioEssays*, *33*(3), 165–172. https://doi.org/10.1002/bies.201000096

Thaben, P. F., & Westermark, P. O. (2014). Detecting Rhythms in Time Series with RAIN. *Journal of Biological Rhythms*, *29*(6), 391–400. https://doi.org/10.1177/0748730414553029

Tomioka, K., & Matsumoto, A. (2010). A comparative view of insect circadian clock systems. *Cellular and Molecular Life Sciences*, *67*(9), 1397–1406. https://doi.org/10.1007/s00018-009-0232-y

Tomioka, K., & Matsumoto, A. (2015). Circadian molecular clockworks in non-model insects. *Current Opinion in Insect Science*, *7*, 58–64. https://doi.org/10.1016/j.cois.2014.12.006

Torgersen, T., & Huse, G. (2005). Variability in retention of Calanus finmarchicus in the Nordic Seas. *ICES Journal of Marine Science*, *62*(7), 1301–1309. https://doi.org/10.1016/j.icesjms.2005.05.016

Tran, D., Nadau, A., Durrieu, G., Ciret, P., Parisot, J.-P., & Massabuau, J.-C. (2011). Field Chronobiology of a Molluscan Bivalve: How the Moon and Sun Cycles Interact to Drive Oyster Activity Rhythms. *Chronobiology International*, *28*(4), 307–317. https://doi.org/10.3109/07420528.2011.565897

Tran, D., Sow, M., Camus, L., Ciret, P., Berge, J., & Massabuau, J.-C. (2016). In the darkness of the polar night, scallops keep on a steady rhythm. *Scientific Reports*, *6*, 32435. https://doi.org/10.1038/srep32435

Vandesompele, J., De Preter, K., Pattyn, F., Poppe, B., Van Roy, N., De Paepe, A., & Speleman, F. (2002). Accurate normalization of real-time quantitative RT-PCR data by geometric averaging of multiple internal control genes. *Genome Biology*, *3*(7), research0034.1-research0034.11. Retrieved from https://www.ncbi.nlm.nih.gov/pmc/articles/PMC126239/

Vera, L. M., Negrini, P., Zagatti, C., Frigato, E., Sánchez-Vázquez, F. J., & Bertolucci, C. (2013). Light and feeding entrainment of the molecular circadian clock in a marine teleost (*Sparus aurata*). *Chronobiology International*, *30*(5), 649–661. https://doi.org/10.3109/07420528.2013.775143

Vollmers, C., Gill, S., DiTacchio, L., Pulivarthy, S. R., Le, H. D., & Panda, S. (2009). Time of feeding and the intrinsic circadian clock drive rhythms in hepatic gene expression. *Proceedings of the National Academy of Sciences*, *106*(50), 21453–21458. https://doi.org/10.1073/pnas.0909591106

Walkusz, W., Kwasniewski, S., Petersen, S. F., Hop, H., Tverberg, V., Wieczorek, P., & Weslawski, J. M. (2009). Seasonal and spatial changes in the zooplankton community of Kongsfjorden, Svalbard. *Polar Research*, *28*(2), 254–281. https://doi.org/10.1111/j.1751-8369.2009.00107.x

Wallace, M. I., Cottier, F. R., Berge, J., Tarling, G. A., Griffiths, C., & Brierley, A. S. (2010). Comparison of zooplankton vertical migration in an ice-free and a seasonally ice-

covered Arctic fjord: An insight into the influence of sea ice cover on zooplankton behavior. *Limnology and Oceanography*, *55*(2), 831–845. https://doi.org/10.4319/lo.2010.55.2.0831

Westermark, P. O., & Herzel, H. (2013). Mechanism for 12 hr rhythm generation by the circadian clock. *Cell Reports*, *3*(4), 1228–1238. https://doi.org/10.1016/j.celrep.2013.03.013

Wilcockson, D., & Zhang, L. (2008). Circatidal clocks. *Current Biology*, *18*(17), R753–R755. https://doi.org/10.1016/j.cub.2008.06.041

Williams, C. T., Barnes, B. M., & Buck, C. L. (2012). Daily body temperature rhythms persist under the midnight sun but are absent during hibernation in free-living arctic ground squirrels. *Biology Letters*, *8*(1), 31–34. https://doi.org/10.1098/rsbl.2011.0435

Williams, C. T., Barnes, B. M., & Buck, C. L. (2015). Persistence, Entrainment, and Function of Circadian Rhythms in Polar Vertebrates. *Physiology*, *30*(2), 86–96. https://doi.org/10.1152/physiol.00045.2014

Williams, C. T., Barnes, B. M., Yan, L., & Buck, C. L. (2017). Entraining to the polar day: Circadian rhythms in arctic ground squirrels. *Journal of Experimental Biology*, *220*(17), 3095–3102. https://doi.org/10.1242/jeb.159889

Xie, F., Xiao, P., Chen, D., Xu, L., & Zhang, B. (2012). miRDeepFinder: A miRNA analysis tool for deep sequencing of plant small RNAs. *Plant Molecular Biology*. https://doi.org/10.1007/s11103-012-9885-2

Yamamoto, T., Nakahata, Y., Soma, H., Akashi, M., Mamine, T., & Takumi, T. (2004). Transcriptional oscillation of canonical clock genes in mouse peripheral tissues. *BMC Molecular Biology*, *5*(1), 18. https://doi.org/10.1186/1471-2199-5-18

Yerushalmi, S., & Green, R. M. (2009). Evidence for the adaptive significance of circadian rhythms. *Ecology Letters*, *12*(9), 970–981. https://doi.org/10.1111/j.1461-0248.2009.01343.x

Zhang, L., Hastings, M. H., Green, E. W., Tauber, E., Sladek, M., Webster, S. G., … Wilcockson, D. C. (2013). Dissociation of Circadian and Circatidal Timekeeping in the Marine Crustacean Eurydice pulchra. *Current Biology*, *23*(19), 1863–1873. https://doi.org/10.1016/j.cub.2013.08.038

Zhu, B., Dacso, C. C., & O'Malley, B. W. (2018). Unveiling "Musica Universalis" of the Cell: A Brief History of Biological 12-Hour Rhythms. *Journal of the Endocrine Society*, *2*(7), 727–752. https://doi.org/10.1210/js.2018-00113

Zhu, B., Zhang, Q., Pan, Y., Mace, E. M., York, B., Antoulas, A. C., … O'Malley, B. W. (2017). A Cell-Autonomous Mammalian 12 hr Clock Coordinates Metabolic and Stress Rhythms. *Cell Metabolism*, *25*(6), 1305-1319.e9. https://doi.org/10.1016/j.cmet.2017.05.004

Acknowledgement

This work has been greatly supported by several people that I would like to thank.
First of all, I would like to thank Prof. Dr. Bettina Meyer for giving me the possibility to keep on working on this exciting topic and a once more instructive time in her working group. Another special thanks goes to my second supervisor Dr. Kim Last, for great support during the past cruises, one of which has resulted in this thesis, interesting, long and fun discussions and for taking the time and effort to be the second supervisor on my thesis.
I have to express my very special thanks to Dr. Laura Payton who patiently guided me through every step from the initial preparations of the laboratory work to the end of the writing process and who took the scientific supervision of this work. Moreover, I like to thank the whole working group at the AWI, for great support during the preparation of the sampling campaigns and for always taking the time to answer countless questions. I would also like to thank Dr. David Wilcockson for his support during the sampling campaign and for valuable discussions on my data.
Finally, I am very grateful to all the people, who supported me in any way during the past years of my studies in Oldenburg and especially to my family, for simply always being there.

Annex

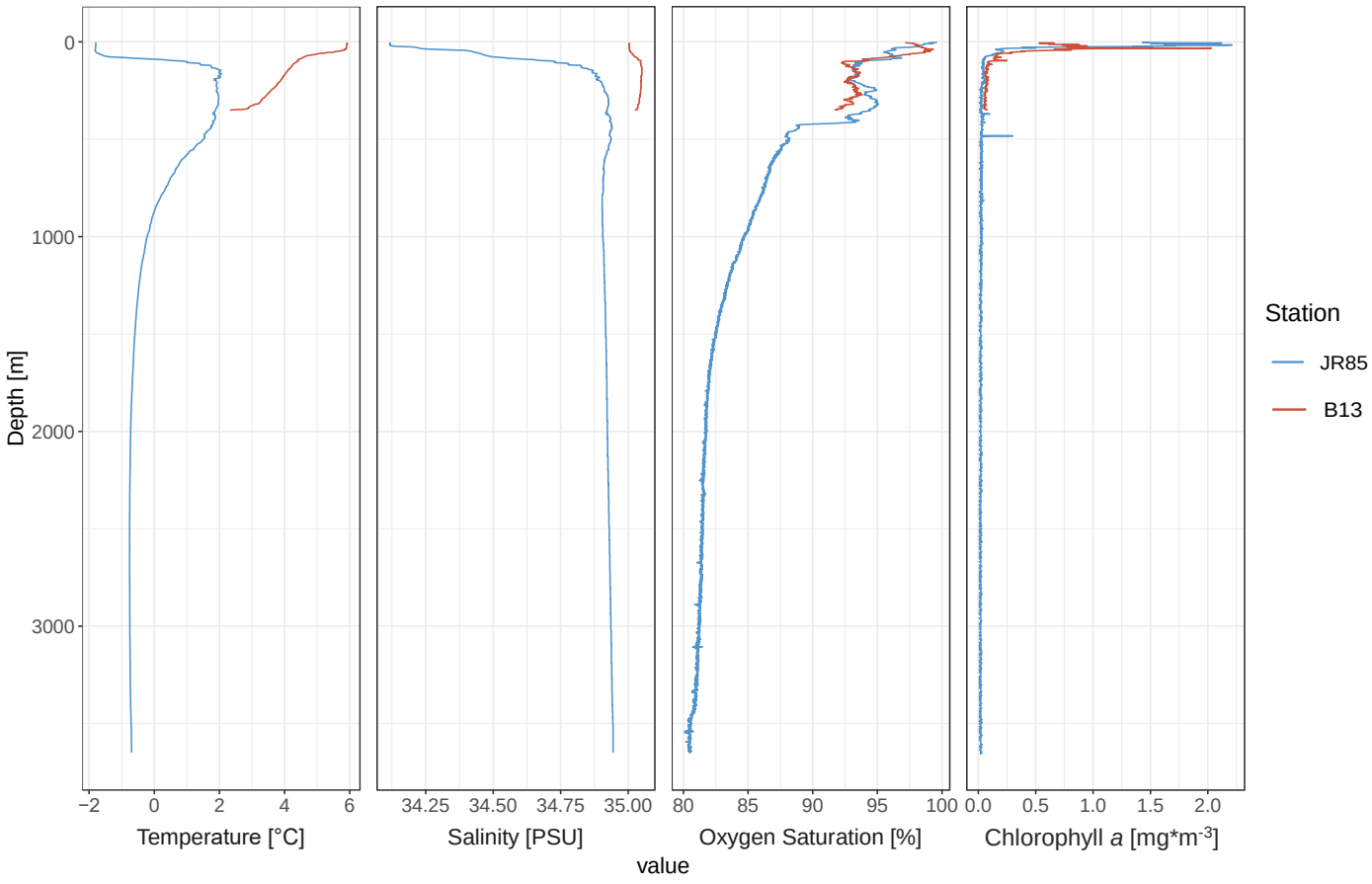

Supplementary figure 1: Full depth vertical profiles of temperature, salinity, oxygen saturation and Chlorophyll a concentration at Station JR85 (blue) and B13 (red).

Supplementary table 1: Sampling details for the two Stations investigated.

		Sampling			
Station	Timepoint	Date	Targeted Time	Time sample fixed	Replicates
JR85	T1	18.06.2018	11:00	10:43	3
	T2	18.06.2018	15:00	15:00	5
	T3	18.06.2018	19:00	18:59	5
	T4	18.06.2018	23:00	23:15	3
	T5	19.06.2018	03:00	03:00	3
	T6	19.06.2018	07:00	07:00	4
	T7	19.06.2018	11:00	11:03	5
B13	T1	30.06.2018	14:00	13:54	5
	T2	30.06.2018	18:00	18:01	5
	T3	30.06.2018	22:00	22:00	5
	T4	01.07.2018	02:00	01:57	5
	T5	01.07.2018	06:00	06:28	5
	T6	01.07.2018	10:00	10:00	5
	T7	01.07.2018	14:00	14:10	5

Supplementary table 2: Details on C. finmarchicus clock gene primer used in this study. Primer design has been conducted by A. Schoenle in the course of a previous study (2015), as described in section 2.2.4

Target	Target (abbr)	Function	Direction	Sequence (5' - 3')	Tm (˚C)	CG (%)	Source
clock	*clk*	core clock	forward	ACTCGGATTGGCTTTGATGG	65.6	50.0	comp76772 c1 seq1 (Christie et al., 2013b)
			reverse	TTCTCAGGTGCAACGTTTCC	64.7	50.0	
cycle	*cyc*		forward	CAGAGCAGGAAGGATAATGAGC	63.5	50.0	comp160482 c0 seq1 (Christie et al., 2013b)
			reverse	TGTAAGCATTGGCACTCAGC	63.6	50.0	
period 1	*per1*		forward	ACATTGTCACAAGCCCTTGG	64.4	50.0	comp171214 c0 seq1 (Christie et al., 2013b)
			reverse	ACAGATGCTCCTTGTGATGC	62.5	50.0	
timeless	*tim*		forward	CCTAACCTGTTACCGTTGACC	61.8	52.4	comp88114 c0 seq1 (Christie et al., 2013b)
			reverse	ATCGCTCACCAATGACTTCC	63.6	50.0	
cryptochrome 2	*cry2*		forward	AGCAACCACCGAATATGACC	63.2	50.0	comp181328 c0 seq1 (Christie et al., 2013b)
			reverse	AACTGACCTTGTGGCATTCC	63.5	50.0	
vrille	*vri*		forward	TGCAGCCTCACAACATTACC	63.3	50.0	comp71844 c0 seq1 (Christie et al., 2013b)
			reverse	AAACACGCAGGGATTTCACG	66.6	50.0	
doubletime 2	*dbt2*	clock associated	forward	CAATGATACAGACTGGGACTGG	62.9	50.0	comp126103 c3 seq2 (Christie et al., 2013b)
			reverse	TGGTTGCATCTGACAGAACC	63.4	50.0	
cryptochrome 1	*cry1*	light input pathway	forward	GGGTTTCAACTGGCTTTGG	63.9	52.6	comp37700 c0 seq1 (Christie et al., 2013b)
			reverse	CCTCTCACTTACCAGAAGATGC	61.4	50.0	
elongation factor 1-α	*ef1*	Reference	forward	AGTTGCTGGCTTGTTCTTGG	63.8	50.0	comp8 c1 seq1 (Lenz et al., 2014)
			reverse	GGTTAAGTCCGTGGAGATGC	63.0	55.0	
RNA polymerase	*rna-poly*		forward	TCAATGACGAGGTTCTCAGG	62.5	50.0	comp19535 c1 seq1 (Lenz et al., 2014)
			reverse	ATCAACTGTTGCCACTCTCG	62.5	50.0	
16s rRNA	*16s*		forward	CCGCGTTAGTGTTAAGGTAGC	62.1	52.4	comp2 c0 seq1 (Lenz et al., 2014)
			reverse	CTTCTCGTCCTAGTACAACTGC	59.3	50.0	

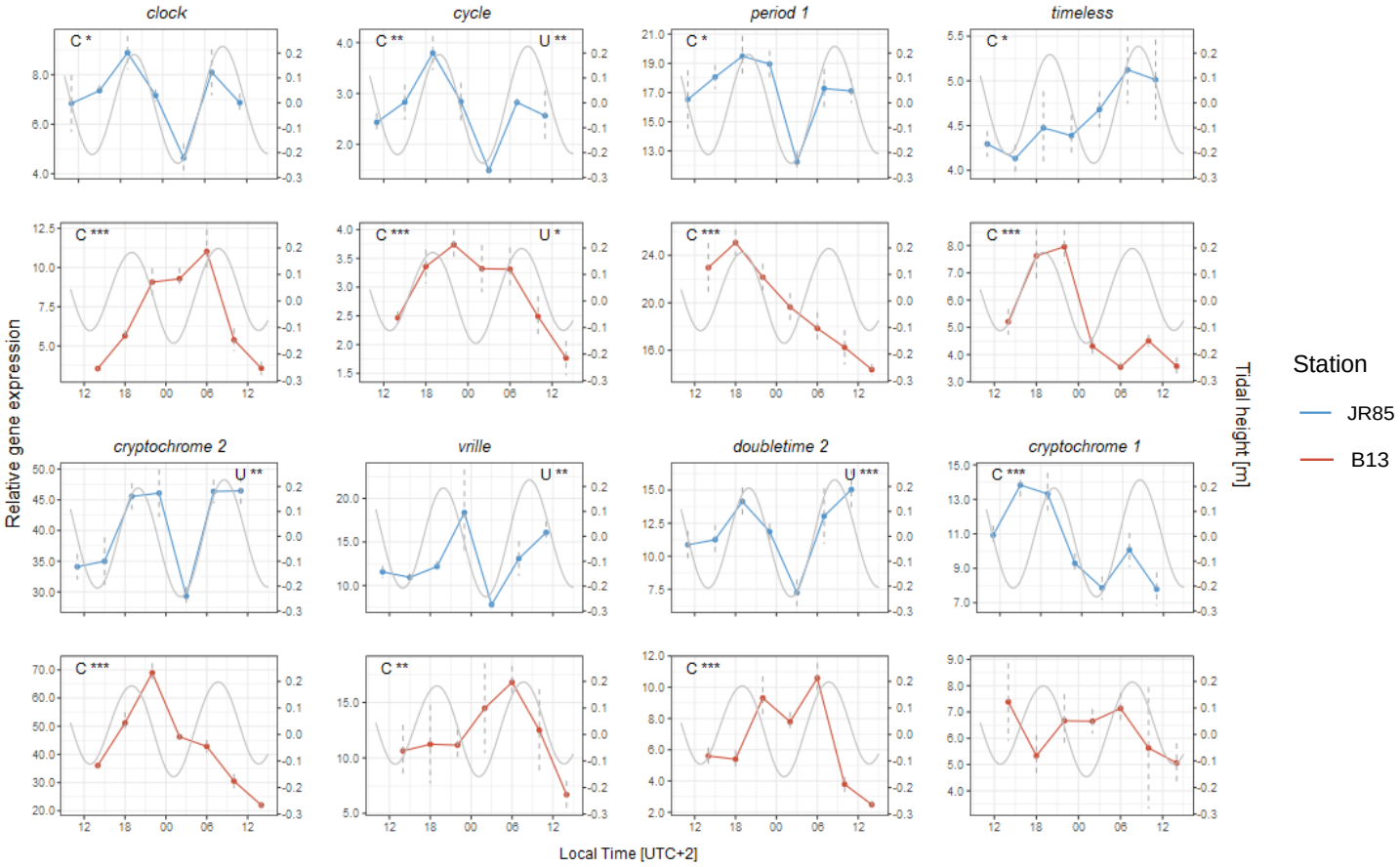

Supplementary figure 2: Temporal profiles of the relative gene expression of clock and clock-related genes in CV stage C. finmarchicus sampled during the period of Midnight Sun in the Arctic. Relative gene expression in animals sampled at the station JR85 (82.5˚ N, in the Nansen Basin) is shown in blue and gene expression in animals sampled at the station B13 (74.5˚ N, in the southern Barents Sea) is shown in red, as indicated for each target, respectively. Significance level of circadian (C, τ = 24 ± 4 h) and ultradian (U, τ = 12 ± 4 h) oscillations in relative gene expression as detected by rhythm analysis with RAIN are indicated with stars for each target gene at each station: "" p-value <0.05, "**" p-value <0.01, "***" p-value <0.001. The grey line indicates the change of the tidal height over the course of sampling (also see Fig. 3 D).*

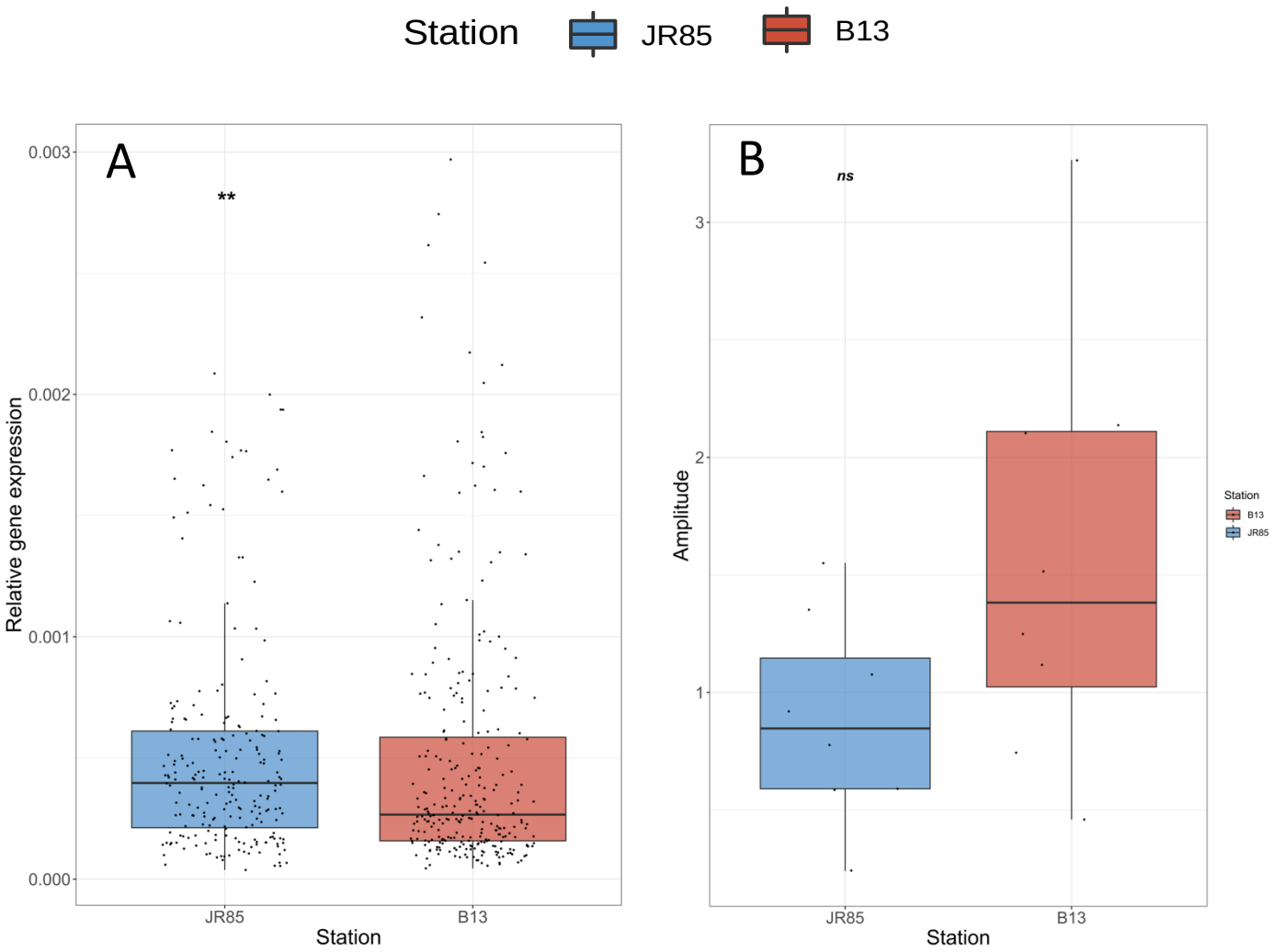

Supplementary figure 3: Visualization of the distribution of A) gene expression data and B) the amplitudes of the oscillations over all targets per station. The lower and upper boundaries of the boxes indicate the first and third quartile (25th and 75th percentiles), respectively and the horizontal line the median. The whiskers span a maximum of 1.5 times the inter quartile range or until the lowest or highest value, respectively. The underlying data are shown as points. Significant differences between the stations have been tested using a Mann-Whitney-U test, the results are shown in the top of each panel. A significant difference in expression level at the two stations was found with p-value = 0.006. No significant difference was found between the two stations in terms of amplitude (p-value = 0.13).

Supplementary figure 4 (continued on the following pages): Behavioral activity of individual CV stage C. finmarchicus used for the rhythm analysis in this study (Fig. 9). The number of infrared beam breaks per 30 mins is shown over the analyzed period of the experiment (four consecutive days). Plots in blue color show animals from station JR85, plots in red show animals from B13. Each plot represents one photoperiodic treatment, indicated at the top of the plot and each panel shows the beam breaks of one individual. Grey bars in the background indicate darkness. Dashed vertical lines mark midnight. The results of the rhythm analysis with RAIN are shown by letters C (circadian rhythm) and U (ultradian rhythm), and level of significance is indicated by stars as follows: "" p-value <0.05, "**" p-value <0.01, "***" p-value <0.001.*

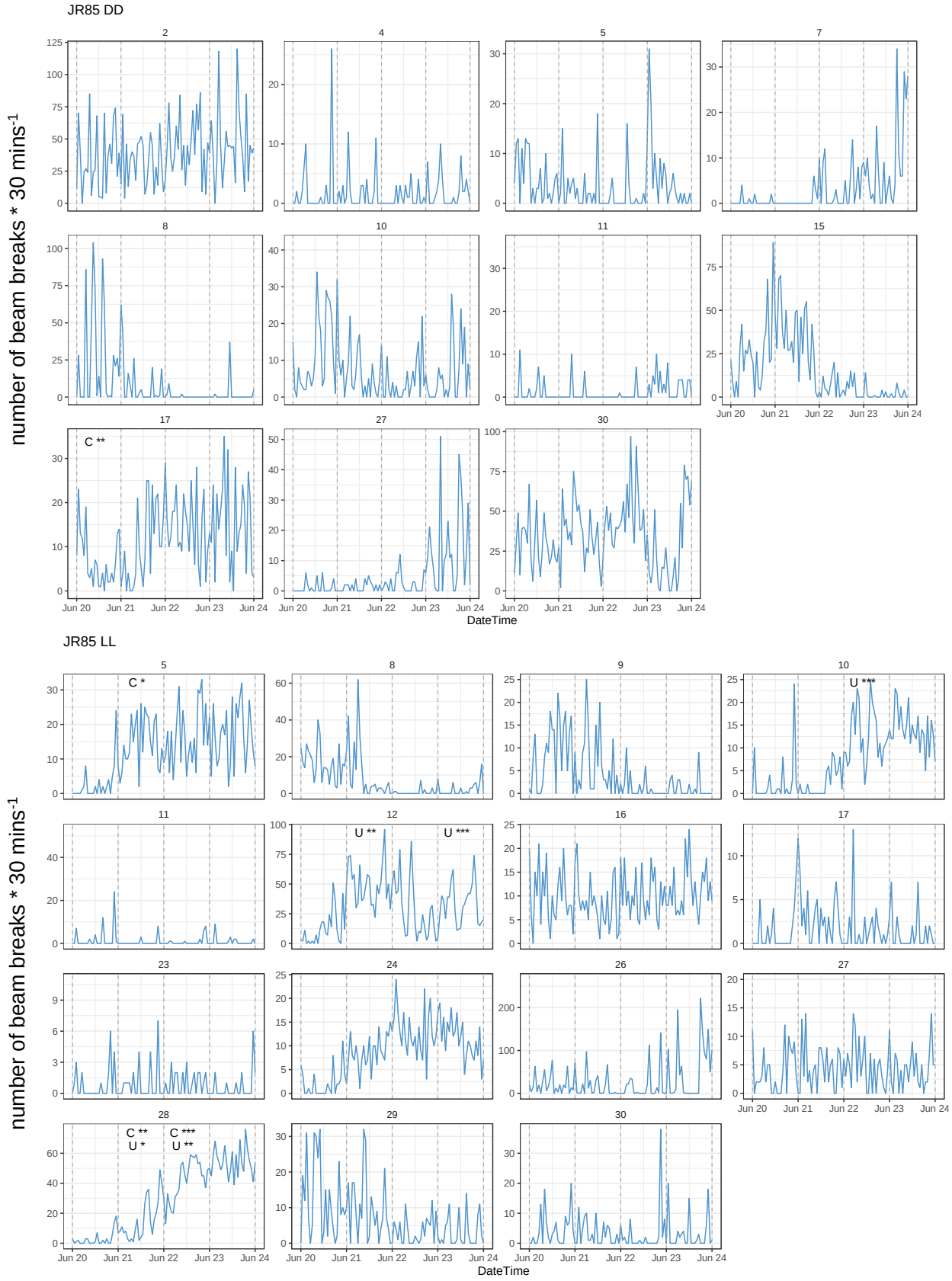

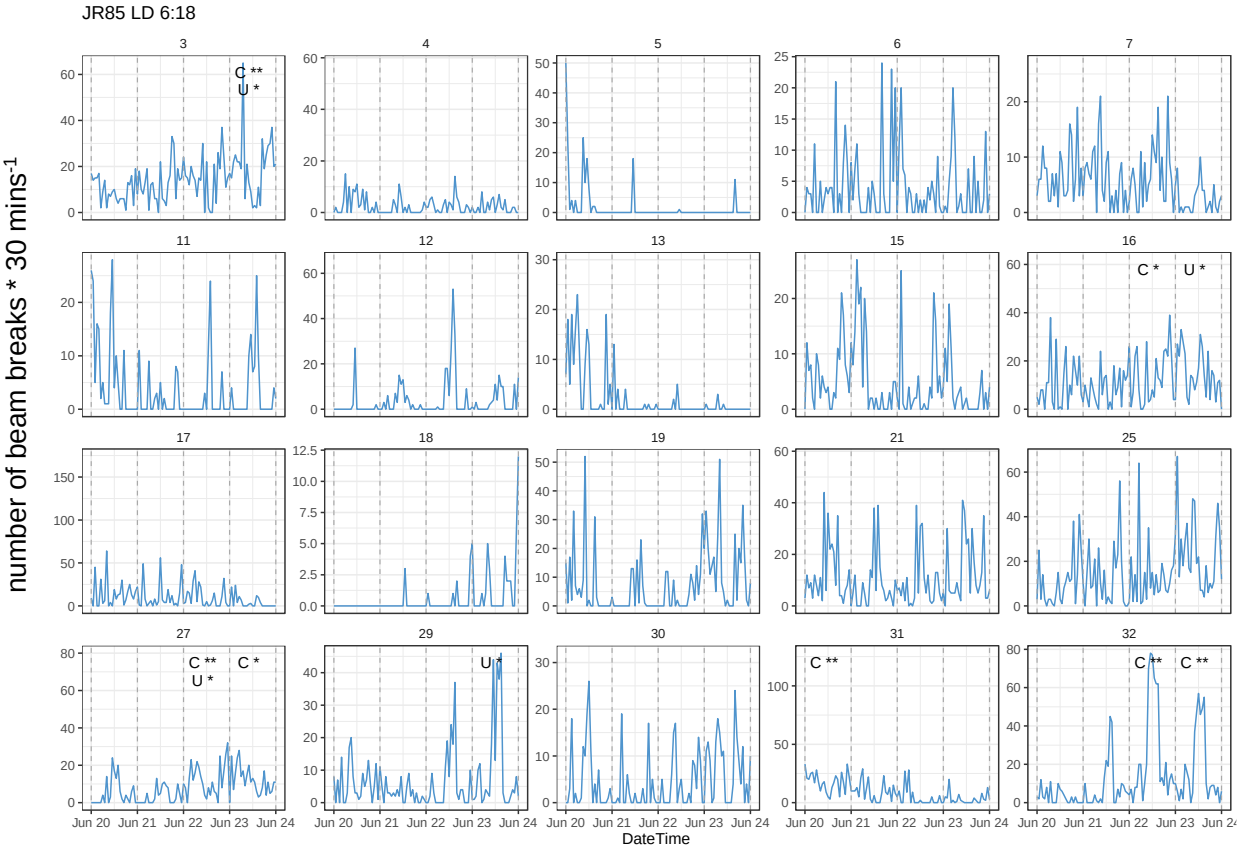
JR85 LD 6:18
number of beam breaks * 30 mins-1
DateTime
Jun 20
Jun 21
Jun 22
Jun 23
Jun 24

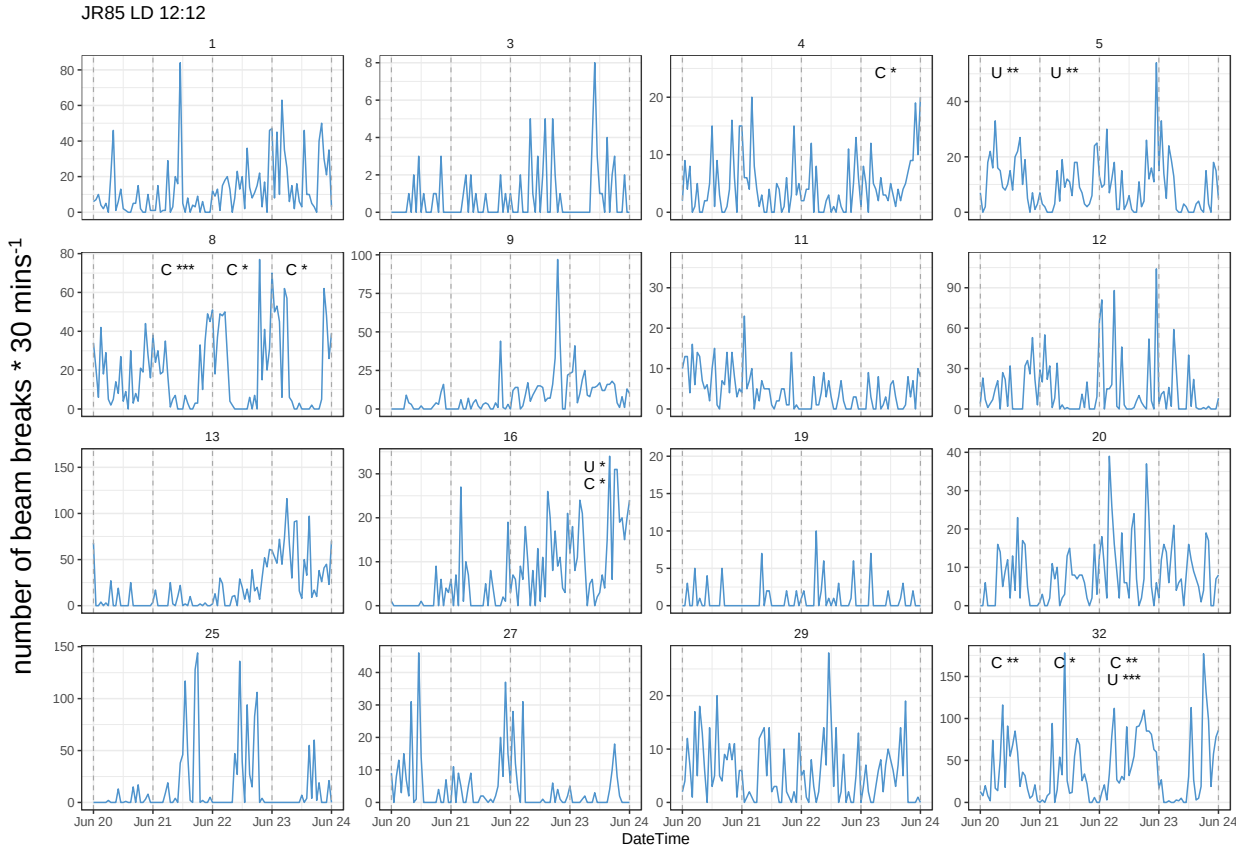
JR85 LD 12:12
number of beam breaks * 30 mins-1
DateTime
Jun 20
Jun 21
Jun 22
Jun 23
Jun 24

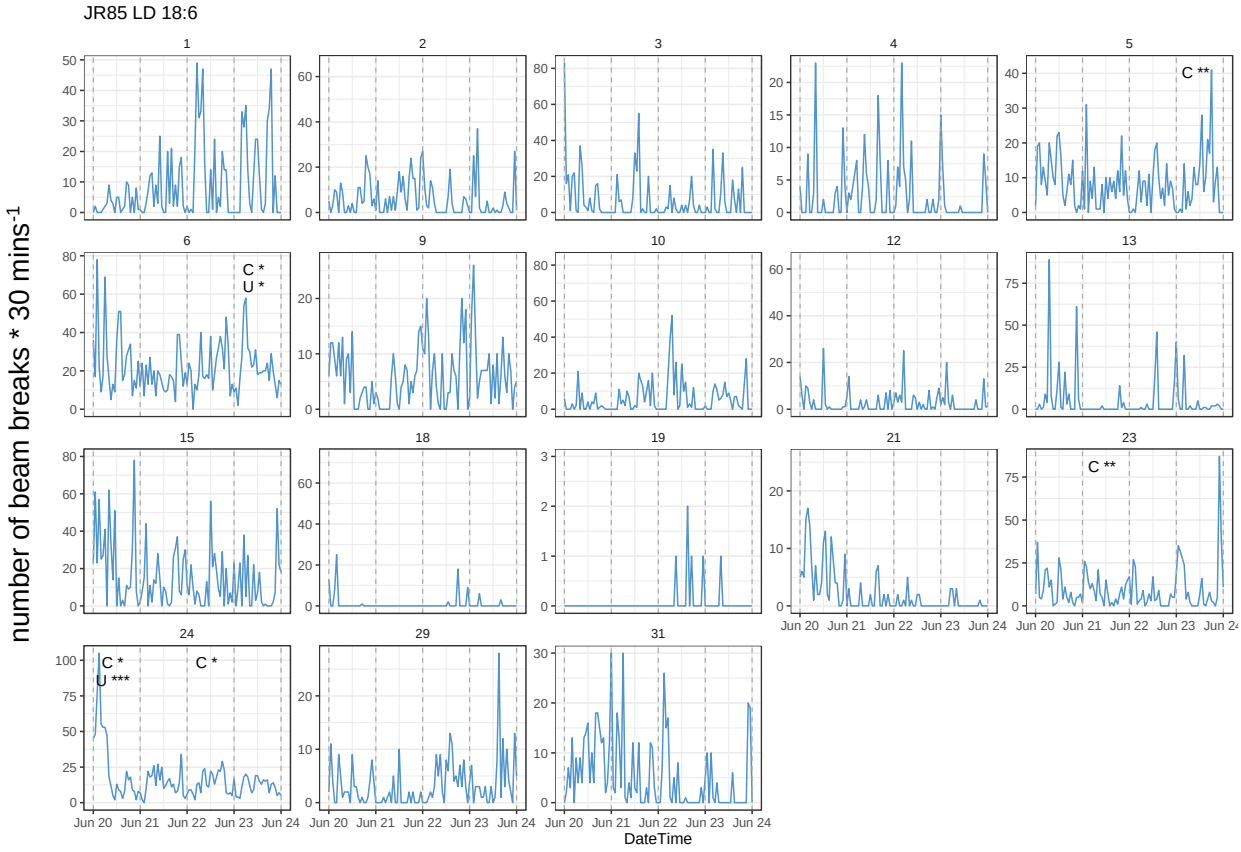
JR85 LD 18:6
number of beam breaks * 30 mins-1
DateTime
C **
C *
U *
C *
U ***
C *
C **

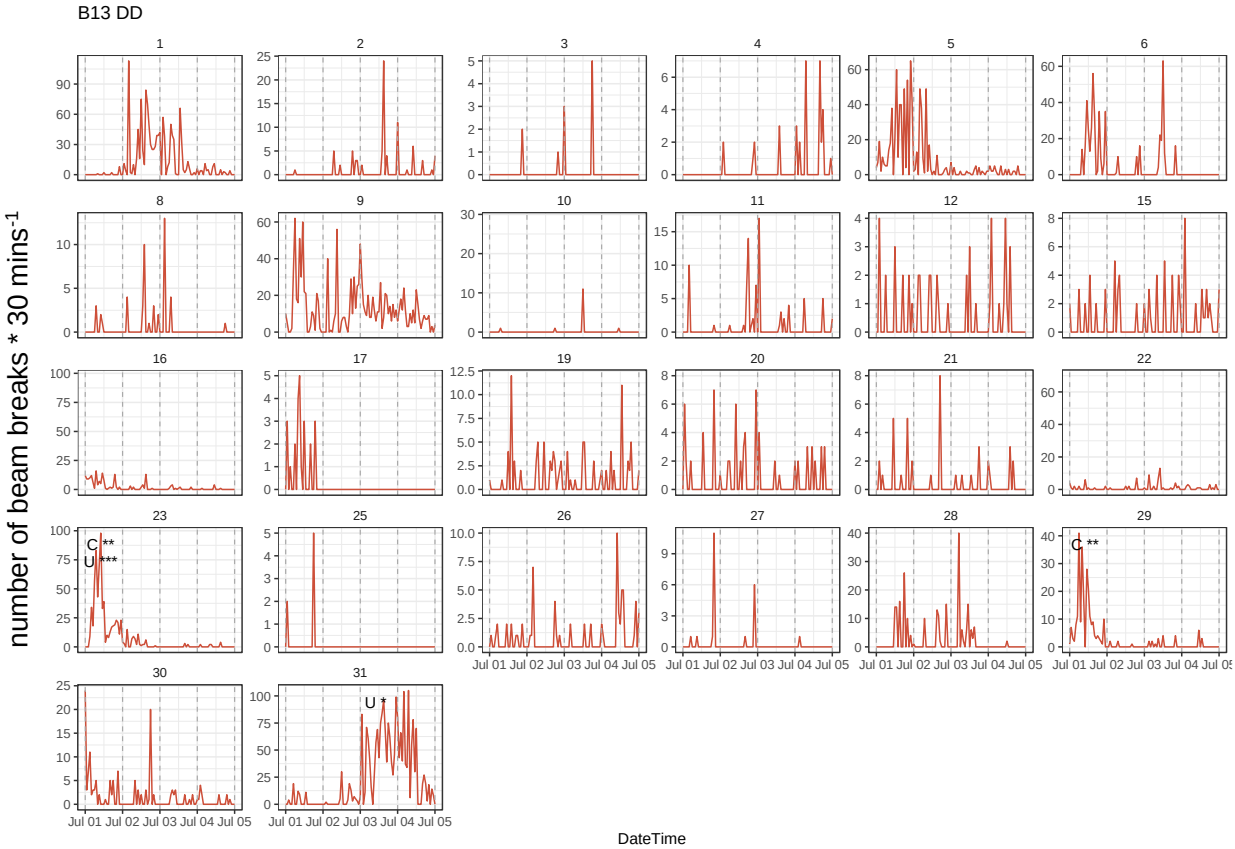
B13 DD
number of beam breaks * 30 mins-1
DateTime
C **
U ***
U *
C **

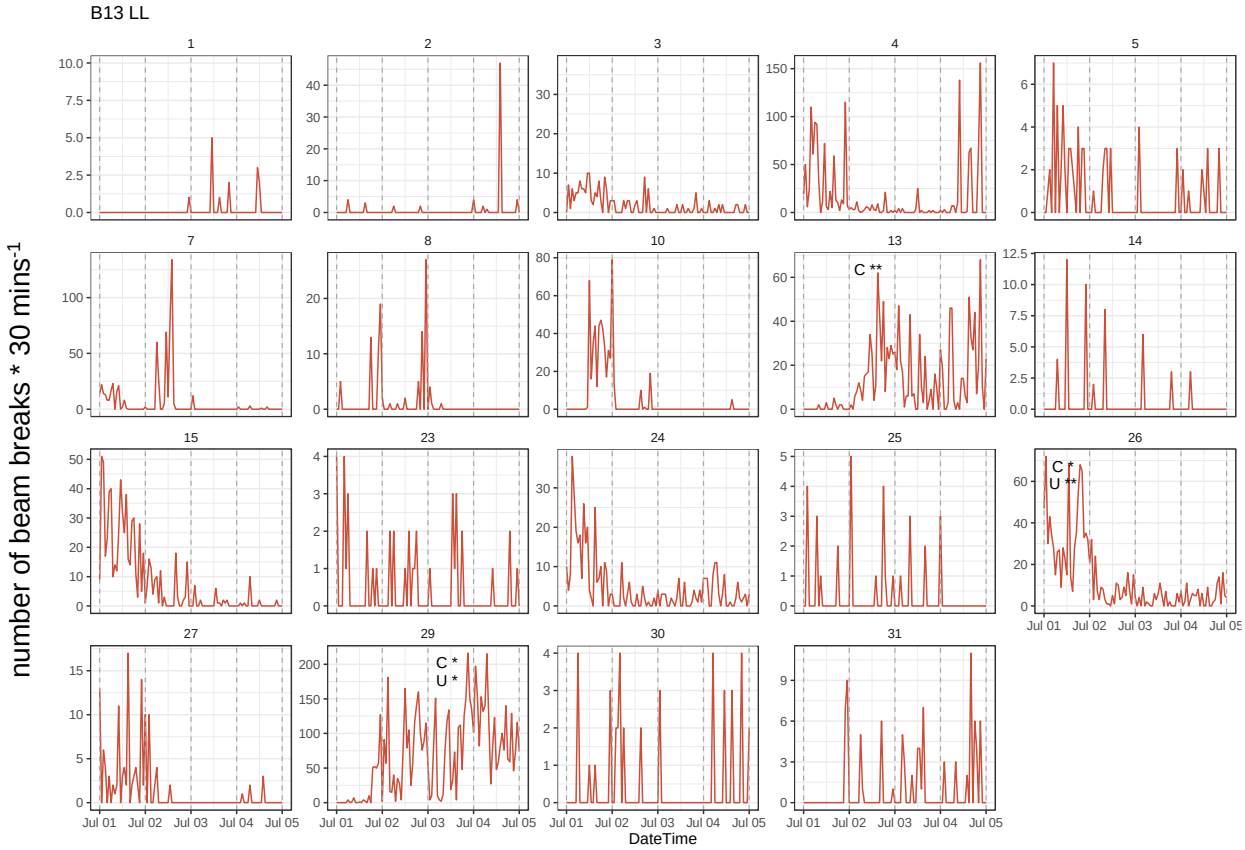
B13 LL
number of beam breaks * 30 mins-1
1
2
3
4
5
7
8
10
13
C **
14
15
23
24
25
26
C *
U **
27
29
C *
U *
30
31
Jul 01
Jul 02
Jul 03
Jul 04
Jul 05
DateTime

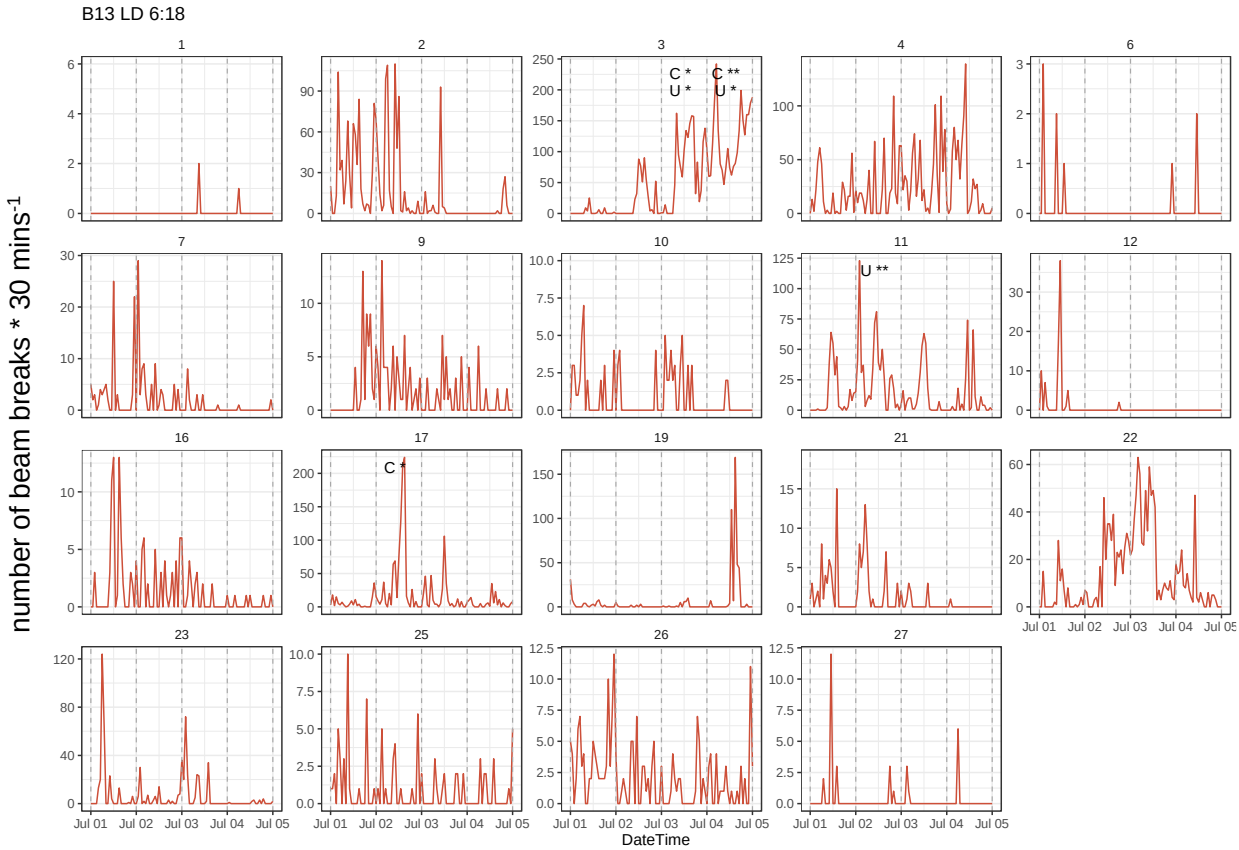
B13 LD 6:18
number of beam breaks * 30 mins-1
1
2
3
C *
U *
C **
U *
4
6
7
9
10
11
U **
12
16
17
C *
19
21
22
23
25
26
27
Jul 01
Jul 02
Jul 03
Jul 04
Jul 05
DateTime

B13 LD 12:12

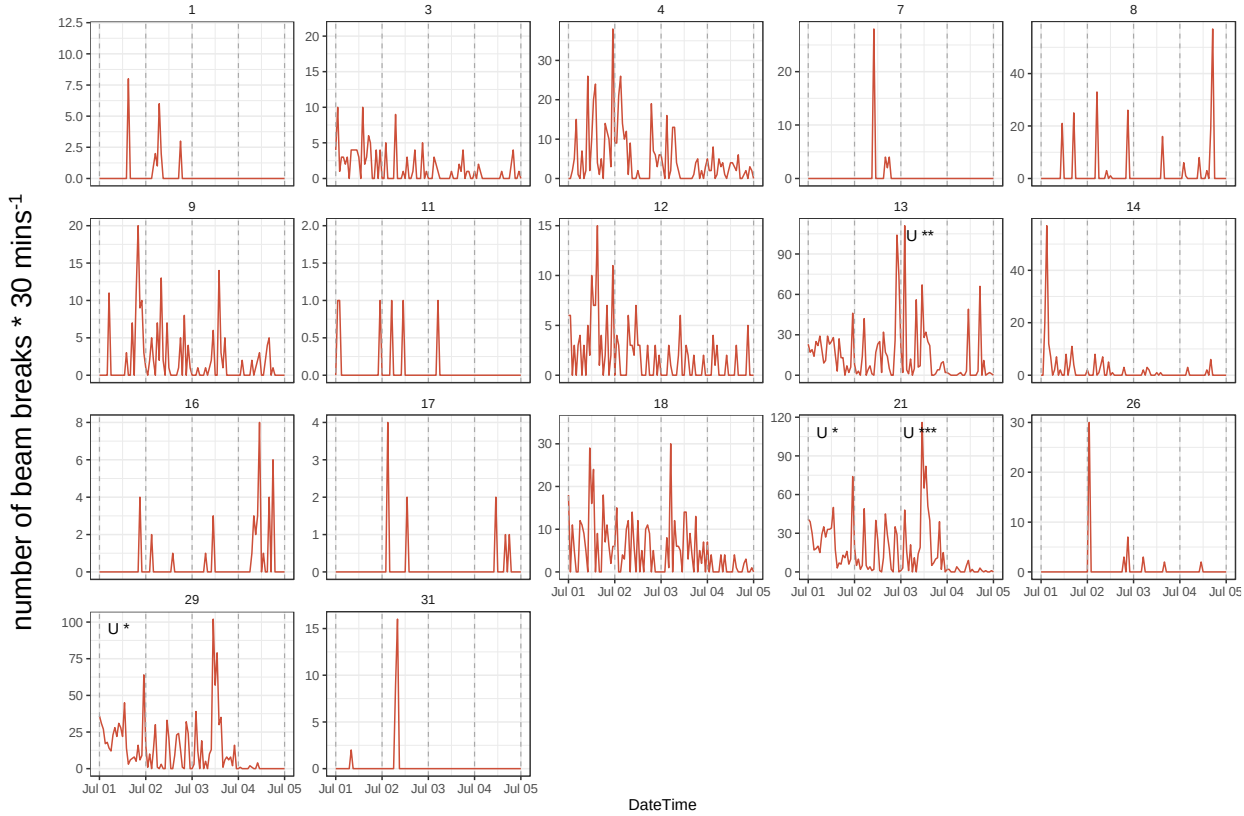

B13 LD 18:6

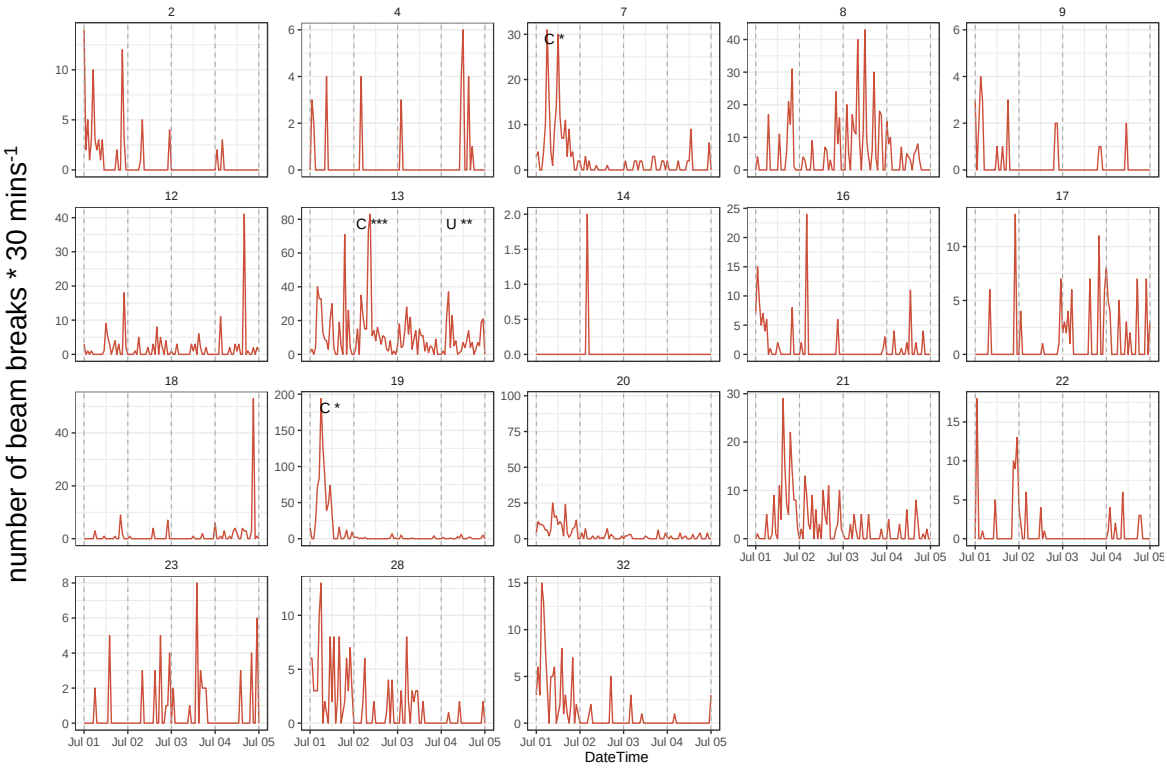

X

Statutory Declaration

I declare that I have developed and written the enclosed master-thesis entitled

Clock gene oscillation in the copepod *Calanus finmarchicus* in the Arctic: the effect of latitude and season

entirely by myself and have not used sources or means without declaration in the text. Any thoughts or quotations which were inferred from these sources are clearly marked as such. Furthermore, I assure that I have followed the general principles of scientific work and publication as defined in the guidelines of good scientific practice of the University of Oldenburg.

Lukas Hüppe

Oldenburg, 27.11.2019